INFLATION AND BB-MODE ANGULAR SPECTRUM OF CMB

A thesis submitted in partial fullfillment for the degree of

DOCTOR OF PHILOSOPHY IN PHYSICS

BY

N. MALSAWMTLUANGI

SCHOOL OF PHYSICS

UNIVERSITY OF HYDERABAD

HYDERABAD 500 046

INDIA

July 2017

INFLATION AND BB-MODE ANGULAR SPECTRUM OF CMB

Declaration

I hereby declare that this thesis entitled "Inflation and BB-mode Angular Spectrum of CMB" is a record of the work done by me during August 2012 to July 2017 under the supervision of Prof. P.K. Suresh at the School of Physics, University of Hyderabad in partial fulfillment of the requirements for the award of the degree of Doctor of Philosophy in Physics. No part of this thesis has been previously published nor submitted for a degree or diploma or any other qualification at University of Hyderabad or anywhere else to the best of my knowledge.

N. Malsawmtluangi
Regn. no: 12PHPH15
School of Physics
University of Hyderabad
Date:

CERTIFICATE

This is to certify that the thesis entitled "Inflation and BB-mode Angular Spectrum of CMB" submitted by Ms. N. Malsawmtluangi bearing registration number 12PHPH15 in partial fulfillment of the requirements for award of Doctor of Philosophy in the School of Physics is a bonafide work carried out by her under my supervision and guidance.

This thesis is free from plagiarism and has not been submitted previously in part or in full to this or any other University or Institution for award of any degree or diploma.

Parts of this thesis have been:

A. published in the following publications:

1. N. Malsawmtluangi and P.K. Suresh, *European Physical Journal C* **76**, 240 (2016), ISSN: 1434-6052 (online), Chapter 5.

B. presented in the following conferences:

1. "International Conference on Celestial Mechanics and Dynamical Astronomy", December 15-17, 2015, organized by Maulana Azad National Urdu University, Hyderabad, held at Maulana Azad National Urdu University, Hyderabad (International).

2. "IF-YITP GR+HEP+Cosmo International Symposium VI", August 3-5, 2016, organized jointly by The Institute for Fundamental Study and Yukawa Institute for Theoretical Physics, held at The Institute for Fundamental Study, Naresuan University, Thailand (International).

3. "The 13th International Symposium on Cosmology and Particle Astrophysics" (CosPA2016), November 28 - December 2, 2016, organized by School of Physics, The University of Sydney, held at The University of Sydney, Australia (International).

C. published as conference proceedings presented in:

1. "IF-YITP GR+HEP+Cosmo International Symposium VI", (accepted) (International).

Further, the student has passed the following courses towards fulfillment of coursework requirement for Ph.D:

Course Code	Name	Credits	Pass/Fail
PY801	Advanced Quantum Mechanics	4	Pass
PY803	Advanced Statistical Mechanics	4	Pass
PY804	Advanced Electromagnetic Theory	4	Pass
PY821	Research Methodology	4	Pass

Prof. P.K. Suresh
Thesis Supervisor
School of Physics
University of Hyderabad
Date:

Dean
School of Physics
University of Hyderabad

Preface

The thesis is mainly dedicated to study the BB-mode correlation angular power spectrum of cosmic microwave background radiation by placing the massless as well as massive primordial gravitational waves in the squeezed vacuum state and thermal vacuum state for various slow-roll inflationary models with the recent joint data of the BICEP2/Keck Array and Planck missions.

Gravitational waves are one of the finest predictions of the theory of general relativity and finally its first direct detection was made on September 14^{th}, 2015, thus confirming its existence in the universe. It is believed that gravitational waves carry vital information about their source and the surrounding dynamics almost unimpeded, hence they are believed to open up a new window to understand the universe. Gravitational waves which were generated in the very early universe especially during inflationary period, known as primordial gravitational waves, are also expected to help in understanding the dynamics of the very early universe.The existence of the primordial gravitational waves is still elusive, however its presence can be realized through its effect on the cosmic microwave background radiation. The primordial gravitational waves are capable of polarizing the cosmic microwave background radiation at a small level and thus, left their own signatures called B-modes with swirling pattern. The density perturbations also left their imprint on the cosmic microwave background radiation due to the Thomson scattering of primordial photons off of free electrons called the E-modes with radial pattern. Further, the primordial gravitational waves seeded from inflation are believed to be in a specific quantum state called the squeezed vacuum state. The primordial gravitational waves are expected to form a stochastic background of standing waves. Hence the primordial gravitational waves in the squeezed vacuum state form a non-stationary background. This leads to oscillatory features in the angular spectrum of the cosmic microwave background anisotropy. Therefore it is expected that the existence of the primordial gravitational waves in the squeezed vacuum state and existence of the waves itself and the inflation also can be realized through the study of BB-mode cor-

relation angular power spectrum of cosmic microwave background radiation. Also, the primordial gravitational waves after the decoupling may remain in thermal state after the recombination. Therefore, due to these thermalized gravitons, the gravitational waves generated during inflation are believed to be amplified by stimulated emission into the existing thermal background of gravitational waves. This thermal effect is also expected to be reflected on the B-mode angular power spectrum of cosmic microwave background.

As mentioned, the inflation predicts the presence of primordial gravitational waves and there are several inflation models which have been proposed. Some of these models are based on a single scalar field which drove the inflationary process while some models are based on multiple scalar fields. Single field models predict an almost Gaussian distribution of temperature and density perturbations that are adiabatic while multiple scalar field leads to non-Gaussian distribution of temperature and density perturbations. Some of the observational results on the cosmic microwave background radiation anisotropy support the predictions of the single field models. On the other hand, the recent observations of the cosmic microwave background anisotropy show hemispherical asymmetry across the cosmic microwave background radiation sky. This feature attracts several explanations, one of which is that it could originate from multiple field inflation while this is impossible from a single scalar field without violating homogeneity and isotropy. These results show that discriminating the inflationary models in terms of the Gaussianity or non-Gaussianity test alone is not sufficient. Hence an alternative mechanism is also needed to validate these models. Therefore the present study also makes an attempt to validate the inflationary models with the BB-mode correlation angular power spectrum of cosmic microwave background radiation along with the recent joint data of the BICEP2/Keck Array and Planck mission.

The theory of general relativity is a well established theory, however attempts have been made to modify it. One of these is the theory of massive gravity which endows a non-zero mass to the graviton which is commonly believed to be massless. If the graviton indeed has mass, then the corresponding primordial massive gravitational waves are expected to have an observable effect on the temperature and polarization anisotropies of the cosmic microwave background radiation. Thereby the effect would also be reflected on the BB-mode correlation angular power spectrum of cosmic microwave background radiation and can be studied with the recent joint data of the BICEP2/Keck Array and Planck mission.

Therefore the thesis is to study the effect of primordial gravitational waves on the BB-mode angular power spectrum of cosmic microwave background for various slow-roll inflation models by placing the primordial gravitational waves in the squeezed vacuum and/or thermal states, and also to explore the existence of massive primordial gravitational waves for various slow-roll inflation models with the recent joint analysis data of Planck and BICEP2/Keck Array missions. Further, the study is also extended to validate and discriminate the various inflationary modes with the BB-mode angular power spectrum of cosmic microwave background radiation with the joint data of the BICEP2/Keck Array and Planck missions.

The organization of this thesis is as follows: In the first chapter, the background of the work is introduced followed by the standard model of cosmology, the inflationary scenario, the cosmological perturbations and gravitational waves are briefly discussed.

The second chapter contains the discussion on the origin of cosmic microwave background radiation, its anisotropy and polarizations. Various angular power spectra of cosmic microwave background, especially the BB-mode correlation angular power spectrum of cosmic microwave background are also presented.

The third chapter is to study the primordial gravitational waves in the squeezed vacuum state for the expanding Friedmann-Lemaitre-Robertson-Walker universe for several inflation models. Various slow-roll inflationary models under the present study are discussed briefly and computations of their tensor spectral index and initial value of the tensor amplitude are also provided. Also the thermal effect on the primordial gravitational waves and its effect on the BB-mode angular power spectrum of cosmic microwave background radiation for various inflation models are considered. The obtained results are compared with the joint analysis data of BICEP2/Keck Array and Planck.

The fourth chapter is to study the effect of massive primordial gravitational waves on the BB-mode correlation angular power spectrum of cosmic microwave background radiation for several inflation models, then compare them to their massless counterparts as well as with the BICEP2/Keck and Planck joint data thereby providing constraint on the mass of the graviton from the cosmological consideration.

In the fifth chapter, the BB-mode angular power spectrum of cosmic microwave background radiation from massive gravitational waves is considered in the squeezed vacuum and thermal states. The analysis for several inflation models are compared to see the existence of the primordial massive gravitational waves in the squeezed

as well as in the thermal states with the joint BICEP2/Keck and Planck data.

Summary and conclusions of the work are presented in chapter 6.

Notations and Units

Throughout the thesis, we use the following notations and units:
Partial derivative $\partial_\alpha = \frac{\partial}{\partial x^\alpha}$.
Covariant derivative ∇_α.
Greek indices $\alpha, \beta, \gamma, ...$ correspond to $0, 1, 2, 3$.
Latin indices i, j, k correspond to $1, 2, 3$.

We follow Einstein's summation convention
Sign convention (-, +, +, +).

We take $c = \hbar = k_B = 1$.

We use the following energy equivalence throughout the thesis
$1\ \mathrm{m}^{-1} = 299792458$ Hz.
1 eV $= 2.41798826(72) \times 10^{14}$ Hz.
1 kg $= 1.35639140(81) \times 10^{50}$ Hz.
1 Hz $= 1.0293 \times 10^{14}\ \mathrm{Mpc.}^{-1}$

Acknowledgment

I would like to express my heartfelt gratitude to my supervisor Prof. P.K. Suresh for giving me the chance and support to study Cosmology which has always been my dream, and for introducing me to the very interesting field of gravitational waves and guiding me since my project during my M.Sc and then throughout my Ph.D. I am extremely grateful for his patience and encouragements and upliftments through my ups and downs during my research. I am very grateful to him for showing me the bright side of whatever impediment I encountered during my studies and showing me positive approach to everything and for his unending support through and through. I am also very thankful to him for giving me the opportunity to co-guide project students which is invaluable for my experience.

I would like to thank my committee members Dr. Soma Sanyal, Prof. E. Harikumar and Prof. Bindu A. Bambah for their valuable suggestions, advice and recommendations.

I would also like to thank the current Dean of School of Physics, Prof. Bindu A. Bambah and the former Deans Prof. R. Singh and Prof. S. Chaturvedhi for their supports and recommendations whenever I ask for one.

I am grateful to Dr. Soma Sanyal and Prof. G. Rajaram under whom I had teaching assistant duties for three semesters each and to School of Physics for giving me the chance to do so.

Special thanks to School of Physics, University of Hyderabad for giving me the opportunity to pursue what I have always wanted to study.

I would like to extend my gratitude to Dr. Rizwan Ul Haq Ansari, Maulana Azad National Urdu University, Hyderabad who was the external invigilator for both my upgradation from Junior Research Fellow to Senior Research Fellow and extension of my Senior Research Fellowship for his comments, advice and suggestions.

I am grateful to the BICEP2/Keck Array and Planck Collaborations for providing their data, and I also acknowledge the use of online CAMB (Code for Anisotropies in the Microwave Background) tool.

I would like to thank Council for Scientific and Industrial Research (CSIR), New Delhi for financial support through JRF/SRF scheme throughout my research. I would also like to acknowledge University with Potential for Excellence (UPE), University of Hyderabad for their partial financial support for my travel to The University of Sydney, Australia for "The 13th International Symposium on Cosmology and Particle Astrophysics (CosPA2016)". I also thank Asia Pacific Centre for Theoretical Physics (APCTP), Korea for their financial support for both my travels to Naresuan University, Thailand for "IF-YITP GR+HEP+Cosmo International Symposium VI" and to the University of Sydney, Australia for CosPA2016.

I thank my family back home for their undying support towards everything especially my studies, and for their understandings, acceptance and prayers with every stubborn step I take and every decision I make.

I would also like to thank my friends back home and in Hyderabad for their encouraging words and moral support, and also my colleagues and the office staffs in School of Physics for helping me out in whatever way I required and requested.

Last, but not least, I would like to thank the current and past members of the Mizo Post-Graduate Students Union (MPGSU-UoH), University of Hyderabad, who are like family to me, for their encouragements and making my stay in this university more fun and enjoyable.

Contents

Chapter 1

Introduction

Predicted by Albert Einstein in 1916 in his general relativity theory, gravitational waves are the disturbances in the curvature of spacetime which travel with the speed of light in the spacetime. According to the theory of general relativity, matter/energy cause the gravity and can be understood in terms of the curvature of spacetime [1, 2]. The gravitational waves can carry vital information about their source and the surrounding dynamics almost impartially, hence they are the new window to explore the universe. Gravitational waves (GWs) are transverse-traceless and are quadrupolar in nature. The GWs, as they propagate, stretch and squeeze the surrounding space in the direction orthogonal to it. Thus, any object or body in the path of the gravitational waves would experience a tidal force acting perpendicularly to its the direction of propagation; thus such object or body, if placed on a plane orthogonal to the propagation direction, would oscillate as long as the gravitational waves pass through them. Astrophysical sources like supernova explosions, neutron star or pulsar binaries, black hole mergers can generate gravitational waves. Indirect observational evidence of the GWs came from the PSR B1913+16, which is a pulsar-neutron star binary system, in 1974 [3] and PSR J0737-3039, a binary system of two pulsars, in 2003 [4], while both the first and second direct detections of GWs, GW150914 and GW151226 respectively, both in 2015, came from black hole mergers [5, 6, 7]. The third direct detection of gravitational waves, QW170104 in 2017 also resulted from black hole mergers [8].

Gravitational waves are also believed to have been induced in the very early evo-

lution stage of the universe by the variable and strong gravitational field. These are called primordial or sometimes, relic gravitational waves. The primordial gravitational waves are believed to be able to provide vital information about their source almost unimpeded, hence they are very important tool to understand the very early universe. The primordial GWs have traversed the universe since its generation till the current time and hence, its wavelength is believed to have increased significantly such that it has become extremely weak to the point that its direct detection would be extremely difficult. However, primordial gravitational waves along with the primordial density perturbations are believed to have left their signatures known as the B-mode and E-mode polarizations respectively. These distinct patterns can be observed on the cosmic microwave background (CMB) radiation. Gravitational lensing effect on the CMB can also lead to the E-mode pattern being changed to the B-mode pattern at late times. The Degree Angular Scale Interferometer (DASI) detected the E-mode polarization in 2002 [9, 10]. Observation of B-modes would confirm the existence of GWs and also would help test the various models of inflationary scenario. While the B-modes produced from lensing of E-modes have been detected in 2013 by the South Pole Telescope [11], B-modes from relic gravitational waves have not yet been observed and probes to detect them are currently going on actively [12, 13, 14, 15, 16]. Its detection can unravel many mysteries of the universe.

The primordial gravitational waves produced during the inflationary period are believed to exist in a specific quantum state, known as squeezed vacuum state. This is due to the fact that the inflationary quantum vacuum field fluctuations generated non-zero variance for quantum fluctuations which, due to parametric amplification by the background curvature, transformed the initial vacuum state with no particle into a quantum state with multiple particles, a state known as the squeezed vacuum state. Due to the parametric amplification of the primordial GWs, the phase variance of the wave mode is being strongly squeezed while there is strong increase in the variance of its amplitude at the same time so that the uncertainty product is being held. The effect of primordial GWs being in the squeezed vacuum state is expected to be reflected on the BB-mode auto-correlation angular spectrum of the

CMB anisotropy.

There are several inflation models, most of which propose that the inflation is due to single scalar field while there are some models which assume more than one scalar field for it. Single scalar field inflation models predict structure formation from adiabatic fluctuations of density perturbations and hence statistics of CMB anisotropy is Gaussian in nature. Inflation models with multiple field, on the other hand, predict structure formation due to isocurvature perturbations and it gives rise to non-Gaussian nature of the CMB anisotropy. However, observations of the CMB anisotropy indicate a negligible amount of non-Gaussianity and severe constraints on the amplitude of the isocurvature perturbations due to the anisotropy level of the CMB. These results tend to favor single field models. However there is observed hemispherical asymmetry in the power level of CMB at large angular scales. This may arise due to multiple scalar fields as a single scalar field cannot produce such asymmetry without violating the homogeneity and isotropy. There have been several studies on single and multiple scalar field inflation models and several constraints have been imposed on them based on theoretical and observational considerations. These indicate that discriminating and validating the inflationary models require alternative tests rather than the Gaussianity alone.

In the field theory framework pertaining to gravity, the force of gravity is believed to be mediated by a particle with spin-2 called graviton which is expected to have zero mass. However, starting with the idea of a spin-2 particle with non-zero mass, several approaches have been taken to endow the graviton with mass. There are also several attempts to estimate the bounds on the mass of graviton both from theoretical and observational approaches with the help of astrophysical sources. If the speed of propagation of gravitational waves is found to be slower than that of light, this would imply that graviton possesses a small but non-zero mass. This small mass of graviton is also expected to be reflected through the signature of the massive primordial GWs on the CMB polarization and anisotropy. It is believed that if the graviton mass is comparable to the Hubble parameter, then it can provide repulsive effects at cosmological distances thus leading to late time cosmic acceleration in the universe which provides an alternative theory to explain the accelerating expansion

of the universe rather than the popular belief that the expansion is due to the dark energy.

The thesis is written on the aforementioned background and is mainly dedicated to study the BB-mode correlation angular spectrum of the CMB by placing the massless as well as massive relic GWs in the squeezed as well as thermal vacuum states for various slow-roll inflation models and comparing the results with the analysis data from BICEP2/Keck and Planck mission collaboration.

1.1 The standard model of cosmology

Cosmology involves the scientific study of the origin, evolution and dynamics of the universe. The most generally accepted model of cosmology is based on both the general relativity theory and the cosmological principle, which assumes the notion of isotropy and homogeneity of the universe on large scales, known as the standard model of cosmology. The standard model has successfully given good accounts on the origin and abundance of light elements, the expansion of the universe and the origin of the CMB. At the same time, it has some shortcomings as it fails to explain some problems like the cosmological singularity, the spatial flatness of the universe and galaxy formation etc. To attend to some of its shortcomings, the cosmic inflationary scenario was proposed according to which the universe expanded exponentially in its early stage for a brief period of time. The inflation also generated metric perturbations known as tensor perturbations or primordial GWs. The standard model is built on the cosmological principle and the Einstein's general theory of relativity.

1.1.1 Einstein field equations

The Einstein field equations form the fundamental equation of general theory of relativity. It describes the gravity in terms of the curvature of spacetime with appropriate source for it. These equations specify the relation of the spacetime

curvature to the source of gravity and can be written as

$$G_{\alpha\beta} = R_{\alpha\beta} - \frac{1}{2} g_{\alpha\beta} R = 8\pi G T_{\alpha\beta} \tag{1.1}$$

where $G_{\alpha\beta}$ defines the Einstein tensor, $R_{\alpha\beta}$ denotes the Ricci tensor and $g_{\alpha\beta}$ denotes the symmetric metric tensor, R is the Ricci curvature scalar, G is the Newtonian gravitational constant, $T_{\alpha\beta}$ is the energy-momentum tensor which acts as the source of gravity.

The Ricci tensor can be obtained as

$$R_{\alpha\beta} = \partial_\beta \Gamma^\gamma{}_{\alpha\gamma} - \partial_\gamma \Gamma^\gamma{}_{\alpha\beta} + \Gamma^\delta{}_{\alpha\gamma} \Gamma^\gamma{}_{\delta\beta} - \Gamma^\delta{}_{\alpha\beta} \Gamma^\gamma{}_{\delta\gamma} \tag{1.2}$$

where each index Γ is the Christoffel symbol of the second kind related to the derivative of the covariant fundamental metric tensor $g_{\alpha\beta}$ as

$$\Gamma^\gamma{}_{\alpha\beta} = \frac{1}{2} g^{\gamma\delta} \left(\partial_\beta g_{\delta\alpha} + \partial_\alpha g_{\delta\beta} - \partial_\delta g_{\alpha\beta} \right) \tag{1.3}$$

and the Ricci scalar can be described as the trace of the Ricci tensor with respect to the metric tensor as

$$R = g^{\alpha\beta} R_{\alpha\beta}. \tag{1.4}$$

The Friedmann-Lemaitre-Robertson-Walker (FLRW) metric describes an isotropic and homogeneous universe. This metric can be written as

$$ds^2 = -dt^2 + a^2(t) \left(\frac{dr^2}{1 - Kr^2} + r^2 d\theta^2 + r^2 \sin^2 \theta d\phi^2 \right) \tag{1.5}$$

where a represents the scale factor which characterizes the expansion of the universe. $K = -1, 0, +1$ indicates the curvature parameter and correspondingly describes open, flat and closed universe respectively. Here r, θ, ϕ represent the comoving spherical coordinates.

The Einstein equations can be solved by choosing perfect fluid as a source for gravity. The energy-momentum tensor pertaining to a perfect fluid can be represented as

$$T_{\alpha\beta} = (p + \rho) U_\alpha U_\beta + p g_{\alpha\beta}, \tag{1.6}$$

where p and ρ are the pressure and density of the fluid respectively and $U^\alpha = (1, 0, 0, 0)$ is the four-velocity of the fluid.

Therefore the non-zero components of the Einstein field equations are:

$$\frac{\dot{a}^2}{a^2} + \frac{K}{a^2} = \frac{8\pi G}{3}\rho, \tag{1.7}$$

and,

$$2\frac{\ddot{a}}{a} + \frac{\dot{a}^2}{a^2} + \frac{K}{a^2} = -8\pi G p, \tag{1.8}$$

where *dot* indicates the time t derivative, eq.(1.7) and eq.(1.8) are called the first and second Friedmann equations respectively. These equations are not independent but are related through the continuity equation as,

$$\dot{\rho} = -3H(p + \rho), \tag{1.9}$$

where $H = \frac{\dot{a}}{a}$ represents the Hubble parameter.

The Friedmann equations lead to the following acceleration condition of the FLRW universe

$$\frac{\ddot{a}}{a} = -\frac{4\pi G}{3}(3p + \rho). \tag{1.10}$$

The general description for the equation of state can be written in the form of the equation of state parameter

$$w = \frac{p}{\rho}. \tag{1.11}$$

The continuity equation eq.(1.9) can be rewritten using the equation of state parameter

$$\frac{d\ln\rho}{d\ln a} = -3(1 + w), \tag{1.12}$$

and it leads to,

$$\rho \propto a^{-3(1+w)}. \tag{1.13}$$

Using eq.(1.13) with eq.(1.7) gives the evolution of the scale factor as,

$$a \propto t^{\frac{2}{3}(1+w)}. \tag{1.14}$$

For radiation, $\rho = 3p$, hence, $w = 1/3$ and eq.(1.9) becomes,

$$\rho_r = a^{-4}, \tag{1.15}$$

where ρ_r represents energy density in radiation. The scale factor corresponding to radiation dominated flat universe is,

$$a \propto t^{1/2}. \tag{1.16}$$

For dust, pressure is negligible, $w = 0$, hence eq.(1.9) becomes,

$$\rho_m \simeq a^{-3}, \tag{1.17}$$

where ρ_m represents the dust energy density, and the scale factor corresponding to dust in the flat matter dominated universe is,

$$a \propto t^{2/3}. \tag{1.18}$$

For vacuum energy, $\rho = -p$, hence the equation of state parameter is $w = -1$. From eq.(1.9), we get

$$\rho \simeq constant, \tag{1.19}$$

and the corresponding scale factor is,

$$a \propto \exp(Ht). \tag{1.20}$$

Hence, on characterizing the expansion of the universe with the help of the scale factor, the energy densities of the different stages of the universe scale differently. During radiation domination, the wavelength of radiation expands with the expansion of the universe and hence, its energy is redshifted, thus causing rapid decrease in its energy density. For matter domination, pressure is nearly negligible and all the energy is in the mass. Thus the mass density dilutes with the volume of the scale factor. For vacuum dominated era, the energy density remains constant.

1.1.2 Successes and shortcomings

The standard model of cosmology is very successful in describing the evolution and some of the observed features of the universe. It is successful in describing the

existence and the abundance of light elements like hydrogen, deuterium, helium, lithium etc., the expansion of the universe and the origin of the cosmic microwave background which are in turn confirmed by various observations. However, despite these successes, there are several shortcomings related to the standard model [17]. Some of the major problems are:

Singularity problem: Extrapolating backward the expansion of the universe to the time $t = 0$ leads to the cosmological singularity which is a state of infinite temperature and energy density and the classical general relativity breaks down in this regime.

Flatness problem: The total energy density in the universe is close to unity which implies an almost spatially flat universe for which it requires extreme fine tuning of the energy density initially.

Horizon problem: Why the regions in the CMB sky which are causally disconnected look the same in all directions?

Monopole problem: The phase transitions during the early universe were predicted to give rise to topological defects including magnetic monopole which, once created, cannot be destroyed and would persist to the present universe as relics.

In order to resolve the problems associated with the standard model of cosmology, the cosmic inflationary scenario was proposed [18, 19].

1.2 Inflationary scenario

In the first few seconds after the big bang event, the universe briefly underwent a period of sudden exponential expansion of space itself, called inflation. In the simplest and most common inflationary scenario, a homogeneous and canonical scalar field called inflaton drives the accelerated expansion of very early stage of the universe.

The action for an inflaton ϕ minimally coupled to gravity can be written as,

$$S_\phi = \int d^4x\sqrt{-g}\left(\frac{1}{2}g^{\alpha\beta}\nabla_\alpha\phi\nabla_\beta\phi - V(\phi)\right). \tag{1.21}$$

The inflaton equation of motion in the FLRW metric is,

$$\ddot{\phi}(t) + 3H\dot{\phi}(t) + V'(\phi) = 0, \tag{1.22}$$

where dot and prime respectively indicate the time and the field derivatives. The respective energy density and pressure of the scalar field can be written as

$$\rho_\phi = \frac{\dot{\phi}^2}{2} + V,$$

$$p_\phi = \frac{\dot{\phi}^2}{2} - V.$$

Therefore the first Friedmann equation becomes,

$$H^2 = \frac{1}{3m_{pl}^2}\left(\frac{\dot{\phi}^2}{2} + V(\phi)\right), \tag{1.23}$$

where $m_{pl} = \frac{1}{8\pi G}$ denotes the reduced Planck mass.

For exponential expansion, the energy density of the scalar field is dominated by its potential energy, i.e., $V \gg \dot{\phi}^2/2$, known as the slow-roll condition, hence the energy density becomes $\rho_\phi \simeq V$, thus the Friedmann equation in terms of the scalar field potential becomes,

$$H^2 \approx \frac{V(\phi)}{3m_{pl}^2}. \tag{1.24}$$

The slow-roll condition is characterized by a set of parameters called the slow-roll parameters which are often defined in terms of the scalar potential V along with its derivatives,

$$\begin{aligned}
\epsilon &\equiv \frac{m_{pl}^2}{2}\left(\frac{V'(\phi)}{V(\phi)}\right)^2, \\
\eta &\equiv m_{pl}^2\left(\frac{V''(\phi)}{V(\phi)}\right), \\
\xi^2 &\equiv m_{pl}^4\left(\frac{V'(\phi)V'''(\phi)}{V^2(\phi)}\right), \\
\sigma^3 &\equiv m_{pl}^6\left(\frac{V''(\phi)V''''(\phi)}{V^3(\phi)}\right),
\end{aligned} \tag{1.25}$$

and so on. Slow-roll condition demands that ϵ and the absolute values of the higher derivatives of these parameters should be less than unity, i.e., $\epsilon \ll 1$, $|\eta| \ll 1$, $|\xi^2| \ll 1$, etc. The higher order slow-roll parameters ensure a prolonged inflation as the potential would not be flat enough for the scalar field to roll unless the curvature of the scalar potential itself is small. Hence the slow-roll conditions ensure that the scalar potential has a curvature but which is, at the same time, smaller than the instantaneous value of the Hubble parameter so that the inflaton slowly rolls down its own potential for a long enough time to allow for sufficient expansion of space such that the initial problems plaguing the standard model are resolved. Inflation ends as soon as the slow-roll conditions are violated.

During the period of inflation, the scale factor a increases by a factor $Z \approx 10^{29}$. This resolves the fine-tuning in the flatness problem by reducing the curvature by a factor Z^2 while the expansion term (Hubble parameter) remains effectively constant; it also blows up the homogeneous space linearly by a factor Z and smoothens out the space, thus resolving the horizon problem and leads to a homogeneous and isotropic universe; and also resolves the monopole problem by separating the monopoles, thus lowering their density by a factor Z^3 and effectively diluting them as the universe expands. The theory of inflation also gives explanation to the amplification of primordial quantum fluctuations and the large scale structure formation in the universe.

The amount of inflation can be characterized by the e-folding number N, which is simply the logarithm of the amount of expansion given by

$$N \simeq \frac{1}{m_{pl}^2} \int_{\phi_{end}}^{\phi} \frac{V(\phi)}{V'(\phi)} d\phi. \tag{1.26}$$

At least $N = 55$ e-folds are required to resolve the horizon problem.

1.2.1 Quantum fluctuations of scalar field

Homogeneous scalar field alone cannot provide perturbation, therefore the perturbation of scalar field is essential to seed the large scale structure formation in the

universe. The perturbed scalar field in the flat FLRW background can be given as,

$$\phi(\tau, \mathbf{x}) = \phi(\tau) + \delta\phi(\tau, \mathbf{x}), \tag{1.27}$$

where $\phi(\tau)$ represents the inflaton field and $\delta\phi(\tau, \mathbf{x})$ denotes the scalar field fluctuation, $d\tau = dt/a$ defines the conformal time.

The scalar perturbation can be rescaled in terms of the mode function $f(\tau, \mathbf{x})$ as,

$$\delta\phi(\tau, \mathbf{x}) = \frac{f(\tau, \mathbf{x})}{a(\tau)}, \tag{1.28}$$

and its equation of motion in the Fourier space is,

$$f_k'' + \left(k^2 - \frac{a''}{a}\right) f_k = 0, \tag{1.29}$$

called the Mukhanov-Sasaki equation, here prime indicates conformal time derivative and k is the wave number. In the subhorizon limit, $k^2 \gg \frac{a''}{a}$, the above equation becomes

$$f_k'' + k^2 f_k = 0, \tag{1.30}$$

which shows that the mode functions satisfy the equation of motion of a simple harmonic oscillator.

For de-Sitter background, $a''/a \approx 2/\tau^2$. For slow-roll inflation, the Mukhanov-Sasaki equation in the de-Sitter space can be written as,

$$f_k'' + \left(k^2 - \frac{2}{\tau^2}\right) f_k = 0. \tag{1.31}$$

which has the exact solution given by,

$$f_k(\tau) = b\frac{e^{-ik\tau}}{\sqrt{2k}}\left(1 - \frac{i}{k\tau}\right) + d\frac{e^{ik\tau}}{\sqrt{2k}}\left(1 + \frac{i}{k\tau}\right). \tag{1.32}$$

The initial condition sets $b = 1$, and $d = 0$ which gives the resulting equation of motion for the mode function,

$$f_k(\tau) = b\frac{e^{-ik\tau}}{\sqrt{2k}}\left(1 - \frac{i}{k\tau}\right). \tag{1.33}$$

The scalar field fluctuations are basically the quantum fluctuations, hence in the quantum language the mode function can be treated as an operator. Therefore the

operator $\hat{f}(\tau, \mathbf{x})$ can be decomposed in the Fourier space,

$$\hat{f}(\tau, \mathbf{x}) = \int \frac{d^3k}{(2\pi)^{3/2}} \left[f_k(\tau)\hat{a}_{\mathbf{k}} + f_k^*(\tau)\hat{a}_{\mathbf{k}}^\dagger \right] e^{i\mathbf{k}.\mathbf{x}}, \tag{1.34}$$

where $\hat{a}$ denotes the annihilation operator and $\hat{a}^\dagger$ is the creation operator. The expectation value of $\hat{f}(\tau, \mathbf{x})$ vanishes while its variance is,

$$\begin{aligned} \langle 0|\hat{f}^\dagger(\tau, \mathbf{0})\hat{f}(\tau, \mathbf{0})|0\rangle &= \int d\ln k \frac{k^3}{2\pi^2}|f_k(\tau)|^2, \\ &= \int d\ln k P_f(k, \tau), \end{aligned} \tag{1.35}$$

where $P_f(k, \tau) \equiv \frac{k^3}{2\pi^2}|f_k(\tau)|^2$ is dimensionless and is called the power spectrum. Therefore the power spectrum for the scalar field fluctuations can be expressed as,

$$P_{\delta\phi}(k) \approx \left(\frac{H}{2\pi}\right)^2 \Big|_{k=aH}, \tag{1.36}$$

where $k = aH$ indicates that the power spectrum is computed at horizon crossing.

1.3 Cosmological perturbations

The cosmological perturbation theory can relate the inflation to the large scale structure formation in the universe and the CMB anisotropy [20]. To discuss the cosmological perturbation, consider the metric perturbation in the following form:

$$g_{\alpha\beta} = \bar{g}_{\alpha\beta} + \delta g_{\alpha\beta}, \tag{1.37}$$

where $\bar{g}_{\alpha\beta}$ represents the background metric. The perturbed metric $\delta g_{\alpha\beta}$ is taken to be the first order fluctuation. It can be decomposed into 10 independent components which can be parametrized by scalar, vector and tensor functions as:

$$\begin{aligned} \delta g_{00} &= 2a^2\varphi, \\ \delta g_{0i} &= a^2(Q_i - \partial_i B), \\ \delta g_{ij} &= a^2[-h_{ij} - \partial_i F_j - \partial_j F_i + 2(\psi\delta_{ij} - \partial_i\partial_j E)], \end{aligned} \tag{1.38}$$

satisfying the conditions,

$$\begin{aligned} \partial_i Q^i &= \partial_i F^i = 0, \\ h_i^i &= \partial_i h_j^i = 0. \end{aligned} \tag{1.39}$$

The parameters φ, ψ, B, E are functions of scalar fluctuations called Bardeen variables. The parameters Q_i and F_i are transverse functions which describe the vector fluctuations in three dimensions thus leading to 4 independent degrees of freedom. The parameter h_{ij} is the rank-2 transverse-traceless tensor which describes the tensor fluctuations in three dimensions thus leading to 2 independent components.

The scalar perturbations and vector perturbations transform under rotation in the coordinates of the background spacetime while tensor perturbations behave like a spin-2 field under rotation and are gauge-invariant; vector perturbations behave like a spin-1 field under rotation and the scalar perturbations are spin-0 under spatial rotation. In the linear scale, the evolution of the scalar, vector and tensor perturbations are independent of each other and therefore they do not couple to each other, hence they can be treated separately. The evolution of the full perturbation is simply the linear superposition of the independent evolution of these perturbations. The scalar perturbations couple to pressure and density perturbations which grow and lead to structure formation via gravitational instability. Vector perturbations tend to decay as the universe expands. Tensor perturbations are sensitive to the evolution of spacetime curvature and physically, they represent the primordial gravitational waves for which the two degrees of freedom correspond to two polarization states.

The Einstein field equations can be perturbed and considered to first order to acquire the equations of evolution of the tensor, scalar and vector modes:

$$\delta^{(1)}R^{\beta}_{\alpha} - \frac{1}{2}\delta^{\beta}_{\alpha}\delta^{(1)}R = 8\pi G\delta^{(1)}T^{\beta}_{\alpha}, \tag{1.40}$$

where $\delta^{(1)}$ gives the first order perturbation relative to any of the modes. However, from now on, only the tensor mode perturbation will be discussed. From eq.(1.38), one gets the two polarizations of the tensor perturbations as,

$$\begin{aligned} \delta g_{ij} &= -a^2 h_{ij}, \\ \delta g^{ij} &= \frac{h^{ij}}{a^2} \end{aligned} \tag{1.41}$$

Then the first order Christoffel symbols of the second kind are,

$$\begin{aligned}
\delta\Gamma^{0}{}_{ij} &= \frac{1}{2}(h'_{ij} + 2Hh_{ij}), \\
\delta\Gamma^{j}{}_{i0} &= \frac{1}{2}h_i^{j\prime}, \\
\delta\Gamma^{k}{}_{ij} &= \frac{1}{2}(\partial_j h_i^k + \partial_i h_j^k - \partial^k h_{ij}),
\end{aligned} \tag{1.42}$$

where prime ($'$) indicates conformal time τ derivative. The perturbed Ricci tensors can then be expressed as,

$$\begin{aligned}
\delta R_{ij} &= \frac{1}{2}[h''_{ij} + 2Hh'_{ij} + 2(H' + 2H^2)h_{ij} - \nabla^2 h_{ij}], \\
\delta R_i^j &= -\frac{1}{2a^2}[h_i^{j\prime\prime} + 2Hh_i^{j\prime} - \nabla^2 h_i^j],
\end{aligned} \tag{1.43}$$

where $\nabla^2 = \partial_i\partial^i$ is the Laplacian, and the fluctuation of the Ricci tensor with mixed indices has been obtained using,

$$\delta R_i^j = \delta(g^{jk}R_{ki}) = \delta g^{jk}\bar{R}_{ki} + \bar{g}^{jk}\delta R_{ij},$$

the background Ricci tensor being given by,

$$\bar{R}_{ij} = (H' + 2H^2)\delta_{ij}.$$

Since neither the scalar fields nor the fluid sources contribute to the tensor modes, the evolution of the field h_i^j in the Fourier space becomes,

$$h_i^{j\prime\prime} + 2Hh'_i + k^2 h_i^j = 0. \tag{1.44}$$

Then using the conditions in eq.(1.39), one can obtain the two physical polarizations of the gravitational waves which are transverse and traceless,

$$\begin{aligned}
h_1^1 &= -h_2^2 = h_+, \\
h_1^2 &= h_2^1 = h_\times.
\end{aligned} \tag{1.45}$$

These are known as plus polarization and cross polarization respectively and these two polarization states obey the same evolution equation.

1.4 Scalar perturbations

During the inflationary expansion, the scalar field perturbations exit the horizon. On super-horizon scales, these perturbations are frozen and re-enter the horizon at later times. At horizon re-entry, the scalar field fluctuation changes to the scalar perturbation also known as density perturbation. Thus one can relate the scalar field perturbation $\delta\phi$ to the density perturbation $\mathcal{R}$ in the spatially flat gauge which can be written as,

$$\mathcal{R} = -\frac{H}{\dot{\phi}}\delta\phi, \tag{1.46}$$

and the variance of $\mathcal{R}$ is then given by,

$$\langle|\mathcal{R}|^2\rangle = \left(\frac{H}{\dot{\phi}}\right)^2 \langle|\delta\phi|^2\rangle, \tag{1.47}$$

where $\delta\phi$ are the scalar field fluctuations and the two-point correlation functions of $\mathcal{R}$ and $\delta\phi$ give the respective power spectra for the scalar perturbations P_S and the scalar field fluctuations $P_{\delta\phi}$.

Then the power spectra for the density perturbations and the scalar field perturbations are related in the spatially flat gauge through eq.(1.47) as,

$$P_S = \frac{1}{2\epsilon}\frac{P_{\delta\phi}}{m_{pl}^2}, \tag{1.48}$$

where ϵ is the slow roll parameter expressed here in terms of H as $\epsilon = \frac{\dot{\phi}^2}{2m_{pl}^2H^2}$.

Using eq.(1.36), the power spectrum for the scalar perturbations at the horizon crossing becomes,

$$P_S(k) = \frac{1}{8\pi^2\epsilon}\left(\frac{H}{m_{pl}}\right)^2\Big|_{k=aH}. \tag{1.49}$$

Using eq.(1.24) and eq.(1.25), the power spectrum for the density perturbations can be expressed with the scalar field potential in the slow-roll approximation as,

$$P_S \simeq \frac{1}{12\pi^2 m_{pl}^6}\frac{V^3(\phi)}{V'^2(\phi)}\Big|_{k=aH}, \tag{1.50}$$

$k = aH$ indicates that the perturbations were generated outside the horizon and hence, both H and V are computed at the horizon-crossing of the wave whose wave

number is denoted by k. Due to this reason, the power spectrum is a function of the wave number k. The scalar spectrum depends on both H and ϵ. If power spectrum is independent of k, then the spectrum is scale invariant and is called the Harrison-Zeldovich spectrum. Both H and ϵ are functions of time which vary slowly with time, therefore the power spectrum is expected to exhibit slight deviation from scale invariance. Near a scale of reference, called the scalar pivot wave number k_*, the scale dependence on k of the scalar power spectrum acquires a power law form as,

$$P_S \equiv A_S \left(\frac{k}{k_*}\right)^{n_S-1}, \tag{1.51}$$

where A_S denotes the scalar perturbation amplitude and n_s denotes the scalar spectral index and the parametrization $n_S - 1$ is taken to quantify the deviation from scale invariance, $n_S = 1$ corresponds to a perfectly scale invariant state and a perfect de-Sitter limit. Hence, the running of the scalar spectral index should be very close to scale invariance, and can be defined by the slow-roll parameters,

$$n_S - 1 = 2\eta - 6\epsilon. \tag{1.52}$$

The scalar perturbations represent the density perturbations which seeded the large scale structure formation in the universe. The tensor perturbations, on the other hand, represent the primordial gravitational waves which are so weak that they travel unimpeded throughout the universe.

1.5 Tensor perturbations

The tensor perturbations are also known as the primordial gravitational waves. The tensor perturbations for flat FLRW universe can be obtained with the following form of the perturbed metric

$$ds^2 = a^2(\tau)[-d\tau^2 + (\delta_{ij} + h_{ij})dx^i dx^j], \tag{1.53}$$

where δ_{ij} is the flat space metric and h_{ij} is the tensor perturbation with $|h_{ij}| \ll \delta_{ij}$, and it satisfies the transverse and traceless conditions respectively

$$\partial_i h^{ij} = 0, \quad \delta^{ij} h_{ij} = 0.$$

Substituting the tensor perturbation in eq.(1.53) into the Einstein-Hilbert action,

$$S_{EH} = \frac{m_{pl}^2}{2} \int d\tau d^3x \sqrt{-g} R, \tag{1.54}$$

and expanding the action to second order, one gets

$$S_{EH}^{(2)} = \frac{m_{pl}^2}{8} \int d\tau d^3x a^2 [(h_{ij})^2 - (\nabla h_{ij})^2]. \tag{1.55}$$

Expressing the tensor perturbation h_{ij} in terms of the tensor mode h_k in eq.(1.55), the action becomes,

$$S_{EH}^{(2)} = \int d\tau d^3k \frac{a^2 m_{pl}^2}{4} [h_k' h_k' - k^2 h_k h_k]. \tag{1.56}$$

For normalized fields,

$$g_k = \frac{a}{2} m_{pl} h_k,$$

thus the action becomes,

$$S_{EH}^{(2)} = \frac{1}{2} \int d\tau d^3k \left[(g_k')^2 - \left(k^2 - \frac{a''}{a} \right) g_k^2 \right], \tag{1.57}$$

where g_k is equivalent to $f_k = a\delta\phi$ from eq.(1.28). Therefore, each GW polarization can be considered as a normalized field in the de Sitter space,

$$h_k = \frac{2}{m_{pl}} \delta\phi, \tag{1.58}$$

where $\delta\phi = g_k/a$. The two-point correlation function for each polarization mode is then given by,

$$\langle |h_k|^2 \rangle = \left(\frac{2}{m_{pl}} \right)^2 \langle |\delta\phi|^2 \rangle. \tag{1.59}$$

Then the power spectrum for the GW modes can be defined as the sum of the power spectra for each polarization mode. Hence, using the previous results for $P_{\delta\phi}$ and the two point correlation function for tensor perturbation, the power spectrum for the primordial GWs can be obtained,

$$P_T \equiv 2 \left(\frac{2}{m_{pl}} \right)^2 P_{\delta\phi}. \tag{1.60}$$

Using eq.(1.36), the power spectrum for primordial GWs becomes,

$$P_T = \frac{2}{\pi^2} \left(\frac{H}{m_{pl}} \right)^2 \Big|_{k=aH}. \tag{1.61}$$

Using eq.(1.24), we get the primordial GW power spectrum in the slow-roll approximation in terms of the inflaton potential as

$$P_T \simeq \frac{2}{3\pi^2 m_{pl}^4} V(\phi)\Big|_{k=aH}. \tag{1.62}$$

The GW power spectrum depends on k, and this scale dependence is defined by,

$$P_T \equiv A_T \left(\frac{k}{k_0}\right)^{n_T}, \tag{1.63}$$

where k_0 is the scale of reference called the tensor pivot wave number, and n_T is the tensor spectral index. In this case, the scale invariance corresponds to $n_T = 0$. The tensor amplitude provides direct probe to the expansion rate of the universe during inflation.

The GW power spectrum can be represented as the logarithm of the wave number k as,

$$\frac{P_T(k)}{P_T(k_0)} = \exp\left[n_T(k_0)\ln\frac{k}{k_0} + \frac{1}{2!}\alpha_T(k_0)\left(\ln\frac{k}{k_0}\right)^2 + \dots\right], \tag{1.64}$$

where $P_T(k_0)$ is power spectrum evaluated at the pivot scale. The coefficients n_T, α_T, ..., characterize the deviation of the tensor spectrum from the scale invariance and are called the running of the tensor spectral index. They can be defined by the slow-roll parameters as,

$$\begin{aligned} n_T(k) &\equiv \frac{d\ln P_T(k)}{d\ln k} \simeq -2\epsilon, \\ \alpha_T(k) &\equiv \frac{dn_T}{d\ln k} \simeq -4\epsilon[2\epsilon - \eta]. \end{aligned} \tag{1.65}$$

These parameters are determined by the equation of state during inflation and hence, can be very helpful in understanding the dynamics and phase transitions that occurred in the very early universe.

The strength of the tensor perturbation can be measured relative to the scalar perturbation through a parameter called the tensor-to-scalar ratio,

$$r \equiv \frac{P_T(k)}{P_S(k)} \simeq 16\epsilon \simeq -8n_T. \tag{1.66}$$

Thus, the tensor-to-scalar ratio is also determined by the equation of state during inflation. Physically, this parameter measures the slope of the inflaton potential.

Since inflation predicts a spectrum close to scale invariance, the potential slope is very small and is nearly flat. Therefore, r is very small and inflation models with non-zero but small r predict a small amount of primordial gravitational waves.

These primordial perturbations are believed to have left their imprints on the CMB; hence, they can be realized through their signatures on the CMB anisotropy.

Chapter 2

The Cosmic Microwave Background

The cosmic microwave background is the leftover radiation from the early universe which formed about 380,000 years after the event of the big bang. It is the oldest perceptible light in the universe. Therefore it is fundamental to the observation to understand the early universe. Actually, it originated from the recombination epoch of the early universe and is one of the major predictions of the standard cosmology [17]. Its prediction came from several studies which aimed to estimate the temperature of the universe though some of these did not explicitly mention such background radiation [21, 22, 23, 24, 25]. The first confirmation of its existence was made via its discovery made by A. Penzias and R. Wilson in 1964 [26] which supports the big bang theory and cosmological principle.

The CMB is uniform in the observable universe and its thermal variation across the sky is found to vary by only a small amount. The variation of the CMB temperature is known as the CMB anisotropy. The DMR (Differential Microwave Radiometers) experiment on the COBE (Cosmic Background Explorer) satellite in 1992 confirmed that the spectrum of the CMB has a uniform thermal blackbody function with temperature $T = 2.725$ K [27]. It also detected the temperature anisotropies on large angular scales with the fractional temperature fluctuations at the level of $\mathcal{O}(10^{-5})$. These features have been measured more precisely by several observations with the WMAP (Wilkinson Microwave Anisotropy Probe) (2003)

[28, 29], CBI (Cosmic Background Imager) (2004) [30, 31], AcBar (Arcminute Cosmology Bolometer Array Receiver) (2004) [32, 33], VSA (Very Small Array) (2004) [34, 35] instruments and BOOMERanG experiment (2005) [36, 37] and an even more detailed and refined investigation and an all-sky map of the CMB was released by Planck Cosmology probe (2015) [12, 13]. The CMB anisotropy can provide a profound information on the physical conditions of early universe [38].

Later, it is noticed that the CMB is polarized due to the Thomson scattering of photons off of electrons [39, 40]. This polarization can be of two types, known as the E-mode polarization and the B-mode polarization. The primordial density perturbations from inflation generated the E-mode polarization while the B-mode polarization was generated by two mechanisms: the first one by the primordial gravitational waves from the very early universe and the second one at late times by the gravitational lensing of E-modes. The CMB polarization has the potential to probe the surface of last scattering directly. Further, the B mode polarization can also be used to see the existence of the primordial gravitational waves.

2.1 Origin of CMB

The epoch of cosmic inflation is believed to have occurred between 10^{-36} to 10^{-32} seconds after the event of the big bang when the inflaton field decayed into relativistic particles thus releasing the potential energy of the inflaton field and filling the universe with a quark-gluon plasma [41]. After the inflationary epoch, the strong nuclear force separated from the electroweak interaction which is a combination of the electromagnetic and weak interactions. Energetic interactions between particles during this epoch were able to create exotic particles like Higgs boson, W and Z bosons. About 10^{-12} sec after the big bang, creation of W and Z bosons ended as the expansion and subsequent cooling of the universe lessened the high energy of particle interactions, and the electroweak interaction separated into electromagnetic interaction and weak interaction. During this epoch, fundamental particles like quarks, leptons and their anti-particles were constantly being created and annihilated. The temperature of the universe was very high (about 10^{15} K) which did not allow in-

stantaneous combination of quarks to form hadrons on collision. Thus the universe was an extremely hot and dense plasma of matter and energy. The fundamental interactions of weak interactions, the strong nuclear interactions, electromagnetism and gravitation interactions had taken their present forms at the end of this epoch. About 10^{-6} sec after the event of the big bang, the temperature of the universe had become sufficiently cold enough so that the quarks were able to combine to form hadrons, but still hot enough to allow the creation of not only hadron, but also its anti-particle, thus keeping the matter and anti-matter in equilibrium. However, as the universe continued to expand and cool down, production of these matter and anti-matter pairs decreased and eventually ended and were then annihilated, leaving only a small amount of hadrons. Approximately 1 sec after the event of the big bang, most of the hadrons and their antiparticles had annihilated, the universe still had a high enough temperature for the formation of leptons and their anti-particles which then existed in thermal equilibrium. However, about 10 sec later, the universe temperature became cold enough so that the leptons and their anti-particles were no longer created, but were starting to annihilate till only a small amount of leptons were left. At this time, free electrons, photons and nuclei of light elements like hydrogen were created by a process called big bang nucleosynthesis; and the universe was filled with an extremely dense plasma of these elements (photon-baryon plasma) and hence, was effectively opaque to light and other radiation. In a process called the Thomson scattering, the free electrons at that time kept on scattering the high energy photons and other radiations such that these radiations could not travel large distance. As such, the universe at that time was in a thermalized state. As the universe continued to expand, it gradually grew colder and approximately 380,000 years after the event of the big bang, the universe eventually cooled down to about 3000 K, enough for the formation of atoms by the combination of the free electrons and the nuclei; the universe became quite transparent and light could travel freely without getting scattered or knocked off course. This time period of the universe is called the era of recombination. The photons released at this time continued to travel till today, with their wavelength increasing with the expansion of the universe while continually losing their energy and hence, are perceived today as radiation with frequency and wavelength in the microwave range of the electromagnetic spec-

trum. Therefore, these are called the cosmic microwave background radiation. If one looks up at the sky, the CMB radiation seems to come from the surface of a spherical shell with the observer at the center such that radiation from all parts of the spherical surface reaches the observer at the same time. The radius of this spherical shell can be considered as the distance travelled by each photon since it was last scattered during the era of recombination, and the spherical surface is aptly named the surface of last scattering with a redshift of $z \simeq 1100$.

Between 150 million years and 1 billion years after the big bang, another phase transition stage occurred. Matter in the early universe started to condense and radiated energy strong enough to reionize the neutral hydrogen and intergalactic gas. As this happened, the universe once again became an ionized plasma, and Thomson scattering process once again took place wherein the free electrons scattered the CMB photons. At that time, the universe had expanded significantly to diffuse the matter such that the electron density was lowered and the Thomson scattering of photons was less frequent than before the recombination. This effect leaves observable anisotropies as it tries to suppress and erase the original small scale anisotropies and hence, this causes additional polarization of the CMB and leaves secondary anisotropies on the CMB anisotropy map. The expectation number of these scatterings per CMB photons is called the optical depth. Since most CMB photons did not scatter during reionization, the optical depth is expected to be ≤ 0.1.

2.2 CMB anisotropy

The intrinsic temperature of the CMB radiation can vary due to increase in radiation density via adiabatic compression, a feature known as the CMB anisotropy [42, 43]. The radiation temperature can also vary due to gravitational redshifting when the gravitational potentials between two points in space differ and evolve with time. The photon density is not uniform on the surface of last scattering, there is variation in different regions of the surface and this leads to varying intensity with the direction of observation. Regions with higher density of photons are seen as hot

spot while those with lower photon density are seen as cold spot. This leads to difference in gravitational potential across the universe. Radiation gains energy when it propagates into the gravitational potential well and it blueshifts in the process; on its quest to leave the potential well at the last scattering, it loses energy in the process of climbing out the wall of the well and hence, it redshifts. If the gravitational potential evolves with time, i.e., if, during the propagation of the radiation through the potential well, the depth of the well increases, the gravitational blueshift will be very small compared to its redshift leading to the radiation gaining an overall redshift. These effects, along with the gravitational redshifting of photons in the expanding universe comprise of the Sachs-Wolfe effect [44]. In the ΛCDM model, when the universe evolves from radiation dominated to matter dominated, this gravitational redshift during the epoch of radiation-matter equality occurs sufficiently late such that the evolution of gravitational potentials still takes place when photons decouple at the time of recombination. The Sachs-Wolfe effect takes place again when the universe undergoes phase transition from matter domination to vacuum domination. This effect is imprinted on the CMB anisotropy at the last scattering surface.

The CMB anisotropies can be described in the context of spherical harmonics as:

$$\frac{\Delta T}{T}(\hat{n}) = \sum_{lm} a_{lm} Y_{lm}(\hat{n}), \tag{2.1}$$

where $Y_{lm}(\hat{n})$ are the spherical harmonics, $a^*_{lm} = (-1)^m a_{l-m}$ are the temperature multipole coefficients, $\hat{n}$ is a unit vector with its direction being specified by angles θ and ϕ. l is the number of oscillations and can vary from 0 to ∞, m indicates the direction of oscillation on the sphere and varies from $-l$ to $+l$. $l = 0$ indicates zero oscillation and is considered as the monopole component of the CMB sky map which sets the overall scale. $l = 1$ indicates one full oscillation over the sphere and is considered as the dipole spherical harmonic component of the CMB map with three possible directions, it also exhibits the largest anisotropy. The higher order multipoles $l \leq 2$ provide more but smaller oscillations with more possible directions for the oscillations. The reciprocal of the number of oscillations l corresponds to the angular wavelength of the fluctuations in the CMB sky, hence the spherical harmonic

decomposition of the angular fluctuations give rise to multipole moments.

The CMB temperature anisotropy has zero parity (spin-0), hence it is invariant under rotation. The complex temperature multipole coefficients a_{lm} have zero mean value but have non-zero variance. This variance gives the angular power spectrum C_l:

$$\langle a_{lm} a^*_{l'm'} \rangle = C_l \delta_{ll'} \delta_{mm'}. \tag{2.2}$$

The power spectrum can be redefined in order to define the statistics of the CMB temperature map as well as the polarization map as,

$$C_l = \frac{1}{2l+1} \sum_{m=-l}^{l} a_{lm} a^*_{lm}. \tag{2.3}$$

There is a fundamental statistical uncertainty in estimating C_l which is most prominent at low multipole, called the cosmic variance, and the uncertainty scales as a sum of $(2l+1)$ terms which leads to an error of

$$\frac{\Delta C_l}{C_l} = \sqrt{\frac{2}{2l+1}}. \tag{2.4}$$

For a given l, all the $2l+1$ coefficients have the same variance, hence the power spectrum is independent of m for an isotropic sky. Inflation predicts that the scale invariant perturbations generated by inflation would be nearly constant in the spherical harmonic space and generate anisotropies, hence C_l is multiplied by $l(l+1)/2\pi$ in order to get a uniform power spectrum per logarithmic interval in l in the temperature anisotropies. Thus the power spectrum in terms of the CMB temperature anisotropy multipoles can be written with the help of eq.(2.1) as,

$$\left(\frac{\Delta T}{T}\right)^2 \equiv \frac{l(l+1)}{2\pi} C_l. \tag{2.5}$$

The CMB anisotropy spectrum may be divided into the following parts [43]: The region with $l \lesssim 100$ corresponds to primary anisotropies. Evolution of large scale isotropies have not yet occurred significantly, therefore the initial conditions of the early universe are directly reflected by these primary anisotropies. The first peak is due to the early Sachs-Wolfe effect. The primordial fluctuations in the form of scalar and tensor perturbations may also contribute to some fraction of the low multipole signal.

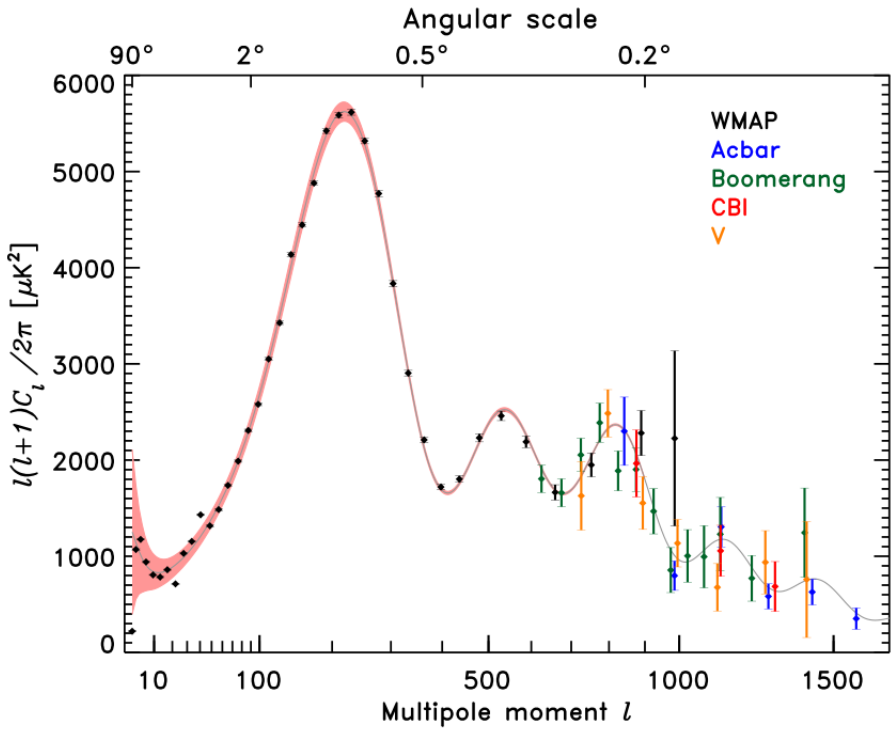

Figure 2.1: The CMB angular spectrum with the WMAP, Acbar , Boomerang, CBI and VSA experimental data. Solid line indicates theoretical prediction. Source: NASA/WMAP Science Team-lambda.gsfc.nasa.gov.

The region $100 \lesssim l \lesssim 1000$ consists of acoustic peaks and troughs. The structures arise due to acoustic oscillations of the photon-baryon plasma before the era of recombination. The high energy photons provide pressure which has the tendency to wipe out the anisotropies while the baryons tend to collapse to create overdensities due to inertia provided by the gravitational attraction of the baryons. The combined effects give rise to acoustic oscillations where the first peak gives the spatial curvature of the universe and the second peak gives the baryon densities imprinted after the recombination while the third peak determines the dark matter density.

The region $1000 \lesssim l$ is called the damping tail. The anisotropies at higher multipoles are damped due to the fact that the recombination process, i.e., the phase transition from plasma to gas is not instantaneous but happens over time; this provides thickness to the last scattering surface which also leads to the subsequent damping of the small angular scale fluctuations.

2.3 CMB Polarization

The CMB is polarized due to the Thomson scattering of incident primordial photons off of free electrons. Consider an incoming plane wave traveling along the $\hat{x}$-direction towards an electron. The corresponding electric and magnetic fields of the wave oscillate in the $y-z$ plane. If the intensity of the wave along its transverse directions $\hat{y}$ and $\hat{z}$ is equal, then this wave is unpolarized. The electron scatters this unpolarized wave in all directions. Incident radiations from the $\pm\hat{x}$-directions produce an outgoing intensity along the $\hat{y}$-direction.

The CMB is linearly polarized as a result of the quadrupole anisotropy on the surface of last scattering due to the photon flux. This CMB polarization can be decomposed into two parts which can be represented by Q and U, the Stokes parameters [45, 46]. Consider an electromagnetic wave incident along the z-direction. At a given point, the electric field vector for this wave can be written as,

$$E_x = a_x(t)\cos[w_0 t - \theta_x(t)], \tag{2.6}$$

$$E_y = a_y(t)\cos[w_0 t - \theta_y(t)], \tag{2.7}$$

where a_x and a_y represent the wave amplitudes, and θ_x and θ_y represent the phases. Both the amplitudes and the phases are functions of time and vary slowly with it.

The Stokes parameters can then be given as:

$$I = a_x^2 + a_y^2, \tag{2.8}$$

$$Q = a_x^2 - a_y^2, \tag{2.9}$$

$$U = 2a_x a_y \cos(\theta_x - \theta_y), \tag{2.10}$$

$$V = 2a_x a_y \sin(\theta_x - \theta_y), \tag{2.11}$$

where I represents the radiation intensity which is independent of the coordinate system and is always positive. Q, U and V represent the polarization states of the wave and can be either positive or negative. Q and U represent linear polarizations, both depend on the orientation of the coordinate system, here x and y axes, in the sky; Q gives polarization on the $x-y$ directions while U gives the polarization

along the axes rotated by 45°. V represents circular polarization and is therefore independent of the coordinate system on the sky and in the case of CMB, it vanishes since Thomson scattering does not induce circular polarization.

For a wave propagating along the z-axis, if the $x-y$ plane is rotated through an angle α about the direction of propagation, then the wave can be defined by the transformed Stokes parameters Q' and U':

$$Q' = Q\cos 2\alpha + U\sin 2\alpha, \tag{2.12}$$

$$U' = -Q\sin 2\alpha + U\cos 2\alpha. \tag{2.13}$$

The parameters Q and U are rotated to Q' and U' by angle 2α when the $x-y$ plane is rotated through α, i.e., they transform as a spin-2 variable and the polarization angle α is given in terms of Q and U as,

$$\alpha = \frac{1}{2}\arctan\left(\frac{U}{Q}\right). \tag{2.14}$$

Both I and V do not transform under rotation of the $x-y$ axes through an angle α, they are invariant.

Polarization in the direction $\hat{n}$ can also be represented as a complex quantity,

$$P(\hat{n}) = (Q \pm iU)(\hat{n}), \tag{2.15}$$

with the amplitude of polarization written as,

$$|P| = (Q^2 + U^2)^{\frac{1}{2}}. \tag{2.16}$$

Since the Q and U parameters transform like a spin-2 variable, they can be represented as components of a traceless symmetric 2×2 tensor,

$$\begin{bmatrix} Q & U \\ U & -Q \end{bmatrix} = \begin{bmatrix} \cos\alpha & \sin\alpha \\ -\sin\alpha & \cos\alpha \end{bmatrix} \begin{bmatrix} Q & U \\ U & -Q \end{bmatrix} \begin{bmatrix} \cos\alpha & -\sin\alpha \\ \sin\alpha & \cos\alpha \end{bmatrix}. \tag{2.17}$$

The polarization tensor $P_{\mu\nu}$ is then traceless, $g^{\mu\nu}P_{\mu\nu} = 0$ and symmetric, $P_{\mu\nu} = P_{\nu\mu}$, and for an orthogonal but not orthonormal coordinate basis (θ, ϕ),

$$P_{\mu\nu}(\hat{n}) = \frac{1}{2}\begin{bmatrix} Q(\hat{n}) & -U(\hat{n})\sin\theta \\ -U(\hat{n})\sin\theta & -Q(\hat{n})\sin^2\theta \end{bmatrix}. \tag{2.18}$$

The parameters Q and U rotate by an angle 2α when the coordinate axes are rotated in clockwise manner by an angle α around $\hat{n}$ as,

$$(Q' \pm iU')(\hat{n}) = e^{\mp 2i\alpha}(Q \pm iU)(\hat{n}). \tag{2.19}$$

Hence, polarization is also a spin-2 variable, and the parameters Q and U have spin weights $+2$ and -2 respectively. One can decompose the polarization and its complex conjugate in the spin-weighted basis in terms of the spherical harmonics of spin-2 ${}_{\pm 2}Y_{lm}$ as,

$$\begin{aligned} T(\hat{n}) &= \sum_{lm} a_{T,lm} Y_{lm}(\hat{n}), \\ (Q \pm iU)(\hat{n}) &= \sum_{lm} a_{\pm 2,lm}\ {}_{\pm 2}Y_{lm}(\hat{n}), \end{aligned} \tag{2.20}$$

and the expansion coefficients are defined by,

$$\begin{aligned} a_{T,lm} &= \int d\hat{n} Y^*_{lm}(\hat{n}) T(\hat{n}), \\ a_{\pm 2,lm} &= \int d\hat{n}\ {}_{\pm 2}Y^*_{lm}(\hat{n})(Q \pm iU)(\hat{n}), \\ &= \left[\frac{(l+2)!}{(l-2)!}\right]^{-\frac{1}{2}} \int d\hat{n} Y^*_{lm}(\hat{n})[(\partial^{\mp})^2 (Q \pm iU)(\hat{n})], \end{aligned} \tag{2.21}$$

where the coefficient $a_{\pm 2,lm}$ can be regarded as the expansion of the quantities $(\partial^-)^2(Q + iU)$ and $(\partial^+)^2(Q - iU)$ in Y_{lm} respectively and (∂^-) and (∂^+) are the spin-lowering and spin-raising operators which lower or raise the spin-weight of a function respectively as,

$$\begin{aligned} {}_sY^*_{lm} &= (-1)^{m+s}\ {}_{-s}Y_{lm}, \\ \partial^+\ {}_sY_{lm} &= [(l-s)(l+s+1)]^{\frac{1}{2}}\ {}_{s+1}Y_{lm}, \\ \partial^-\ {}_sY_{lm} &= -[(l+s)(l-s+1)]^{\frac{1}{2}}\ {}_{s-1}Y_{lm}, \\ \partial^-\partial^+\ {}_sY_{lm} &= -(l-s)(l+s+1)\ {}_sY_{lm}. \end{aligned} \tag{2.22}$$

The polarization on the sky can be characterized with the help of the expansion coefficients $a_{\pm 2,lm}$ whose linear combinations lead to the following components of polarization:

$$\begin{aligned} a_{E,lm} &= -\frac{1}{2}(a_{2,lm} + a_{-2,lm}), \\ a_{B,lm} &= \frac{i}{2}(a_{2,lm} - a_{-2,lm}). \end{aligned} \tag{2.23}$$

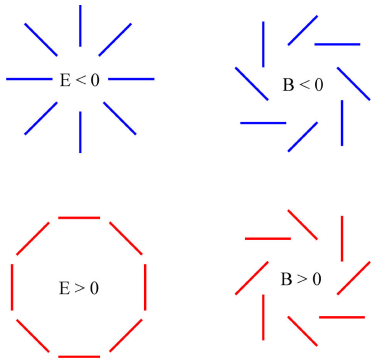

Figure 2.2: The E-mode and B-mode polarization patterns of CMB. Source: spie.org.

The E and B variables characterize the real space polarization fields Q and U respectively and can be expanded in terms of $Y_{lm}(\hat{n})$ as

$$\begin{aligned} E(\hat{n}) &= \sum_{lm} a_{E,lm} Y_{lm}(\hat{n}), \\ B(\hat{n}) &= \sum_{lm} a_{B,lm} Y_{lm}(\hat{n}). \end{aligned} \tag{2.24}$$

These polarization fields are invariant under rotation but under parity transformation, E and B behave differently; E-modes possess $(-1)^l$ parity while B-modes carry $(-1)^{l+1}$ parity ($l = 2$, $m = 0$) on the sphere, hence the pattern of $E(\hat{n})$ remains invariant while the $B(\hat{n})$ pattern changes sign. Thus, E and B can be considered as analogous to the electric and magnetic modes of polarization where E is the curl-free gradient component with no handedness while B is the divergence-free curl component with handedness of the CMB polarization.

One can characterize the CMB perturbations with the auto-correlation power spectra of T, E and B, and the T and E cross-correlation power spectrum as:

$$\begin{aligned} C_l^{TT} &= \frac{1}{2l+1} \sum_m \langle a_{T,lm} a_{T,lm}^* \rangle, \\ C_l^{EE} &= \frac{1}{2l+1} \sum_m \langle a_{E,lm} a_{E,lm}^* \rangle, \\ C_l^{BB} &= \frac{1}{2l+1} \sum_m \langle a_{B,lm} a_{B,lm}^* \rangle, \\ C_l^{TE} &= \frac{1}{2l+1} \sum_m \langle a_{T,lm} a_{E,lm}^* \rangle. \end{aligned} \tag{2.25}$$

The temperature and polarization anisotropies of the CMB are very small and are also expected to obey the statistics of Gaussianity, and hence the universe is con-

sidered to be statistically isotropic which implies that,

$$\begin{aligned}
\langle a_{T,lm} a^*_{T,l'm'} \rangle &= C_l^{TT} \delta_{ll'} \delta_{mm'}, \\
\langle a_{E,lm} a^*_{E,l'm'} \rangle &= C_l^{EE} \delta_{ll'} \delta_{mm'}, \\
\langle a_{B,lm} a^*_{B,l'm'} \rangle &= C_l^{BB} \delta_{ll'} \delta_{mm'}, \\
\langle a_{T,lm} a^*_{E,l'm'} \rangle &= C_l^{TE} \delta_{ll'} \delta_{mm'}, \\
\langle a_{T,lm} a^*_{B,l'm'} \rangle &= \langle a_{E,lm} a^*_{B,lm} \rangle = 0. \qquad (2.26)
\end{aligned}$$

The E-mode polarization spectrum and the temperature anisotropy spectrum are directly out of phase, hence these spectra are cross-correlated to give TE-modes. On the other hand, since B possesses parity opposite to both T and E, the cross correlation between T and B or E and B vanishes unless there exist interactions with no parity violation. The power spectra C_l^{TT}, C_l^{EE}, C_l^{BB} and C_l^{TE} are specified by the primordial perturbations. The auto-correlation angular power spectrum of E-modes of CMB can be given by [47, 48]

$$\begin{aligned}
C_l^{EE} &= (4\pi)^2 \int k^2 dk P_T(k) \\
&\quad \times \Big| \int_0^{\tau_0} d\tau g(\tau) h_k(\tau) \left[-j_l(x) + j_l''(x) + \frac{2 j_l(x)}{x^2} + \frac{4 j_l'(x)}{x} \right] \Big|^2, \qquad (2.27)
\end{aligned}$$

and the auto-correlation angular power spectrum B-modes of CMB is [47, 48]

$$C_l^{BB} = (4\pi)^2 \int k^2 dk P_T(k) \times \Big| \int_0^{\tau_0} d\tau g(\tau) h_k(\tau) \left[2 j_l'(x) + \frac{4 j_l(x)}{x} \right] \Big|^2, \qquad (2.28)$$

where, $x = k(\tau_0 - \tau)$, the visibility function is represented by $g(\tau) = \kappa'(\tau) e^{-\kappa}$,its peak defines the recombination era and denotes the probability of a CMB photon being last scattered at the redshift z, and $\kappa' = a n_e x_e \sigma_T$ gives the differential optical depth for the Thomson scattering where n_e denotes the electron density, x_e gives the ionization fraction, σ_T denotes the Thomson cross-section. Integration of the differential optical depth with respect to the conformal time τ gives the total optical depth as, $\kappa(\tau) = \int_\tau^{\tau_0} \kappa'(\tau) d\tau$. $j_l(x)$ represents the spherical Bessel function of order l.

The E-modes are believed to be generated from the Thomson scattering in the matter plasma, and hence they are signatures of primordial density perturbations

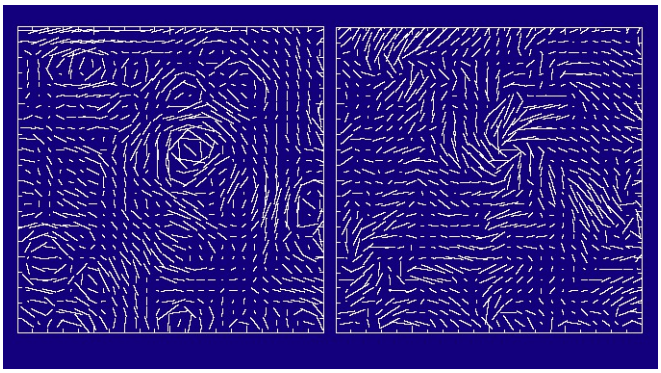

Figure 2.3: The CMB polarization field decomposed into E-modes (left panel) and B-modes (right panel). Source: astrobites.org.

while the B-modes are believed to be generated by the primordial GWs. The E and B modes have different patterns in the polarization sky and their anisotropy spectra are believed to have different shapes and amplitudes. The E-mode polarization is either orthogonal or parallel to the direction of the plane wave propagation whereas the B-mode polarization crosses the plane wave at 45°. The full polarization pattern of the CMB sky is simply a random superposition of these polarization patterns. Hence the CMB polarization field can be decomposed into E modes and B modes which would help in separating the contributions of the primordial gravitational waves from those of the density perturbations. However, since the generation of the CMB polarization occurred during the recombination epoch for only a very short period of time, the polarization anisotropy is expected to be much smaller than the temperature anisotropy, a case which is not much altered by secondary anisotropies during reionization epoch. Thus, the primordial density and metric perturbations can be realized through their imprints on the CMB in the form of specific polarization.

2.4 BB-mode correlation angular power spectrum of CMB

The primordial GWs generated during the very early universe are believed to have left their signatures on the polarization pattern of the CMB sky in the form of swirling pattern with an odd parity, called the B-mode polarization [48, 49]. The

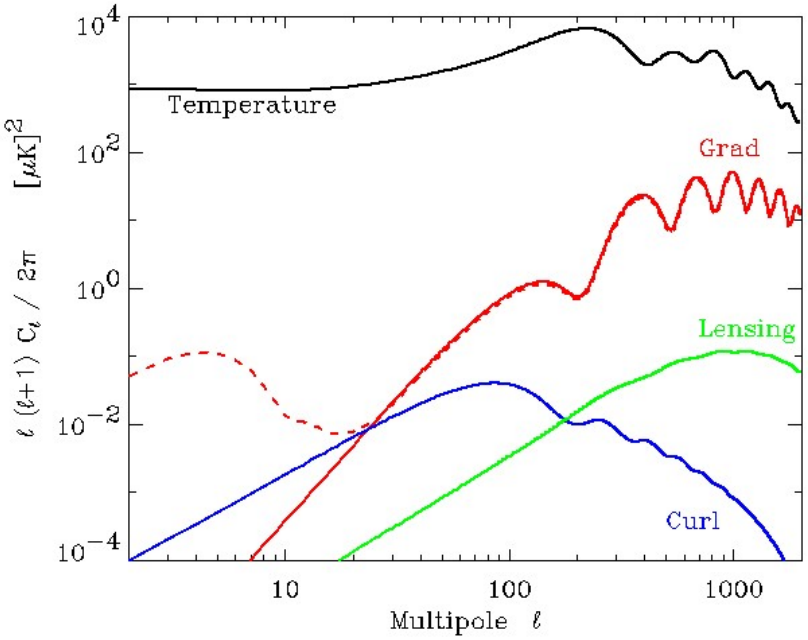

Figure 2.4: The CMB angular power spectrum for temperature anisotropy (black), E-mode polarization (gradient component) (red), B-mode polarization (curl component) (blue) and lensing of E-modes (green). Source: bicep.caltech.edu.

B-modes, unlike the E-modes, cannot be created directly by the scattering of photons off of free electrons during phase transitions as in the recombination epoch. On the other hand, during such phenomenon which occurred at the last scattering, the primordial GWs present at that instant would imprint a local quadrupole anisotropy to the CMB photons, thus providing a linear polarization. The transverse nature of the GW polarization breaks the symmetry of the plane wave thereby producing the B-mode polarization. Since density perturbations do not directly give rise to B-modes, the B-modes directly reflect the existence of primordial gravitational perturbations and hence, detection of B-modes would provide excellent insights into the primordial gravitational waves, their amplitude and spectrum and their contributions. The amplitude of the gravitational waves varies directly as the expansion rate of the universe during inflation, this in turn varies directly as the square of the energy scale of inflation. Thus, if the inflationary energy scale is close to 10^{16} GeV, then the primordial GWs would provide a potentially detectable signal.

Most of the inflationary models predict a small amount of primordial gravitational waves whose power spectrum is close to scale invariance. The relative

amplitude of the auto-correlation spectrum of B-modes of the CMB can provide a constraint on the tensor-to-scalar ratio, which is the strength of the tensor perturbation relative to the scalar perturbation. The BB-mode angular power spectrum has a large bump around $l \leq 10$ due to the re-scattering of the temperature quadrupole by the reionized plasma during the reionization epoch. The primordial GW signal peaks around the scale of $l \simeq 100$ and then drops rapidly after that in the BB-mode angular spectrum. This is due to the fact that on small angular scales, the primordial GWs have reentered the horizon and had enough time for their amplitudes to redshift away by the time recombination takes place.

Gravitational lensing of CMB which is the deflection of CMB photons by the large scale structure gravitational potential converts some pattern of E-mode polarization into that of B-mode polarization on small angular scales, i.e., at higher multipole of the CMB spectrum [50]. This type of B-mode has been observed by the South Pole Telescope in 2013. This lensed B-mode signal imprints a new observable on the CMB which provides an important cosmological probe into the large scale structures which would be very useful in constraining some cosmological parameters like the neutrino mass.

There are various experiments measuring the CMB anisotropy which include ground based, balloon and space based missions. The ground based interferometers include DASI [9, 10], BICEP2 and Keck Array [14], South Pole Telescope [16], CBI [30, 31], Acbar [32, 33] and VSA [34, 35]. The first detection of the CMB polarization was made by DASI. The BOOMERanG experiment is a balloon observation which discovered in 2000 that the universe is close to flat [36, 37]. Space based missions include COBE [27], WMAP [28, 29] and Planck spacecraft [12, 13] which make measurements of the large scale CMB anisotropies to high precision. Ambitious goals of these space based missions in observing CMB include measurements of gravitational lensing and B-mode polarization.

Observation of primordial GW background or even B-modes would give not only evidence of inflation, but also the strength of the inflaton potential. This would provide an excellent probe into the physics of the inflationary epoch.

Chapter 3

Inflation and BB mode Correlation Angular Power Spectrum of CMB

Inflation is a widely known scenario introduced to resolve several shortcomings of the standard model of cosmology [17, 18, 19]. According to inflationary scenario the early universe expanded exponentially within a brief period of time. There are many inflationary models introduced to address one or other unresolved questions plaguing the standard model of cosmology [51]. All the models agree that the inflation seeded the formation of galaxies in the universe, however recent CMB anisotropy data constrains several inflation models [52]. The inflation also gave rise to the induction and evolution of primordial gravitational waves which can be realized through the CMB polarization. The primordial gravitational waves are believed to have been generated quantum mechanically through a mechanism known as parametric amplification, hence they are expected to be in a certain quantum state called the squeezed vacuum state [53, 54, 55, 56]. Therefore, this feature is also expected to be reflected on the polarization and anisotropy of the CMB. Therefore the study of the CMB polarization due to primordial GWs is very crucial for the confirmation of the inflationary scenario itself and validating models of inflation [57, 58]. Moreover the study of primordial gravitational waves effect on CMB not only helps to test the existence of primordial gravitational waves but also the potential existence of these GWs in the squeezed quantum vacuum state.

As discussed, there exist many models of inflation and some models propose that

the inflationary process was driven by a single scalar field while others suggest more than one scalar field. Slow-roll inflation models with single scalar field predict an almost Gaussian distribution of the density perturbations and scale invariant spectrum while the models with multiple scalar fields predict non-adiabatic and isocurvature perturbations and hence non-Gaussian distribution. However, the Planck 2013 result suggested negligible level of non-Gaussianity which seems to be consistent with the prediction of single scalar field inflation models [59]. At the same time recent observations of the CMB indicate large-scale anomalies in the fluctuations of CMB, wherein a hemispherical asymmetry exists across the CMB sky. This was first hinted by WMAP and confirmed by Planck. This garnered several explanations, one of the attempted explanations suggests that single field models are incapable of producing such asymmetry without violating the homogeneity and isotropy but multi field inflation models can account for it [60]. These studies indicate that for favoring single or multi field inflationary models, one needs alternative tests rather than the Gaussianity test alone.

This chapter is aimed to study whether the primordial GWs exist in the squeezed quantum vacuum state and thermal state for several slow roll inflation models through the BB-mode auto-correlation angular power spectrum of the CMB with the joint analysis data of BICEP2/Keck and Planck missions. Also an attempt is made to validate the slow-roll single field vs multiple field issue by studying the BB-mode angular power spectrum of CMB with the joint BICEP2/Keck and Planck (BKP) analysis data.

3.1 Inflation models

In the simplest inflationary scenario, a scalar field rolls down its potential towards its true vacuum and encounters friction along its potential. Once it reaches its true vacuum, it oscillates and decays into relativistic particles and this process is immediately followed by reheating of the universe. Some important constraints on the inflation models are: sufficient amount of expansion must take place for the resolution of the isotropy, homogeneity and flatness problems, the fractional

energy density of the early universe at that instant should be sufficiently low, the amplitudes of primordial scalar and tensor perturbations must be (approximately) consistent with the CMB anisotropies, the spectral index of the scalar perturbations and the tensor-to-scalar ratio must be very close to scale invariance. The most recent tensor-to-scalar ratio constraint, $r < 0.07$ as the upper bound and the lower bound $r \simeq \mathcal{O}(10^{-3})$ comes from the analysis of the joint data of BICEP2/Keck Array and Planck [61]. Next, we briefly discuss several slow-roll inflation models which are interested in the present study. We also compute the relevant parameters for each inflation model that are required for the further study and analysis of the present work.

3.1.1 Quadratic chaotic inflation model

The quadratic chaotic inflation model is a simple power law type model with a single massive inflaton field [19]. In this model, the scalar field after rolling down its potential, rests at its vacuum but then gets displaced to higher state due to quantum or perhaps, thermal fluctuations, and then it rolls back to its true vacuum. This mechanism repeats itself and whenever this event happens, cosmic inflation occurs, blowing up the region in which the scalar field gets displaced out of its vacuum state. When the scalar field finally rests at its true vacuum, it decays and causes the universe to reheat. The scalar field of the quadratic chaotic inflation model has an effective potential,

$$V(\phi) = \frac{1}{2}m^2\phi^2, \tag{3.1}$$

where $m = 1.53 \times 10^{13}$ GeV represents the inflaton mass.

Using eqs.(1.25) and (3.1), the slow-roll parameters for the quadratic chaotic inflation model are calculated as,

$$\begin{aligned} \epsilon &= 8.26 \times 10^{-3}, \\ \eta &= 8.26 \times 10^{-3}. \end{aligned} \tag{3.2}$$

Using eq.(1.62) and the potential eq.(3.1), the initial value of the power spectrum for the tensor perturbations is calculated for the quadratic chaotic inflation model

and is calculated as $P_T = 3.21 \times 10^{-10}$. By taking the power spectrum value for the scalar perturbations to be $P_S = 2.43 \times 10^{-9}$ and using eq.(1.66), the estimated tensor-to-scalar ratio for the quadratic chaotic inflation model is $r = 0.132$ and tensor spectral index is found by using eq.(1.65) as $n_T = -1.65 \times 10^{-2}$.

3.1.2 Quartic chaotic inflation model

The quartic chaotic inflation model is also a simple power law inflation with a scalar field which has a self-interacting term [62]. This model suggests the existence of not only the inflaton but also a curvaton scalar field at late times and the primordial perturbations come from both their contributions. The curvaton itself does not drive the inflation but generates curvature fluctuations after the decay of the inflaton field. The potential of the scalar field for the quartic chaotic inflation model is,

$$V(\phi) = \frac{1}{4}\lambda\phi^4, \tag{3.3}$$

where $\lambda = 5.94 \times 10^{-14}$ GeV indicates the scalar self-coupling.

Using the potential eq.(3.3) and eq.(1.25), the slow-roll parameters for the quartic chaotic inflation model are found as,

$$\begin{aligned} \epsilon &= 1.626 \times 10^{-2}, \\ \eta &= 2.439 \times 10^{-2}. \end{aligned} \tag{3.4}$$

Using eq.(1.62) and the potential, eq.(3.3), for the scalar field of the quartic chaotic inflation model, the calculated initial value of tensor power spectrum is $P_T = 2.426 \times 10^{-10}$. Using the above potential with the power spectrum of the scalar perturbations $P_S = 2.43 \times 10^{-9}$ and eq.(1.66), the tensor-to-scalar ratio is calculated to be $r = 0.26$ and the spectral index for tensor perturbations is found using eq.(1.65) as $n_T = -3.25 \times 10^{-2}$.

3.1.3 Coleman-Weinberg inflation model

The potential for Coleman-Weinberg inflation model is studied in the context of spontaneous symmetry breaking which is induced by radiative corrections giving

rise to logarithmic function [63, 64, 65]. The Coleman-Weinberg inflation model is based on single scalar field which has the following normalized effective potential as,

$$V(\phi) = M^4 \left[1 + \alpha \left(\frac{\phi}{\sigma}\right)^4 \ln\left(\frac{\phi}{\sigma}\right)\right], \tag{3.5}$$

where $\alpha = 4e$, $M = 10^{16}$ GeV, $\sigma = 10m_{pl}$ sets the typical vacuum expectation value at which inflation takes place.

By substituting the potential eq.(3.5) in eq.(1.25), the obtained slow-roll parameters for the Coleman-Weinberg inflation model are

$$\epsilon = 4.86 \times 10^{-4}, \tag{3.6}$$

$$\eta = -4.42 \times 10^{-2}. \tag{3.7}$$

For the Coleman-Weinberg inflation model, the initial value of the tensor power spectrum is calculated with the help of eq.(3.5) and eq.(1.62), and the obtained value is $P_T = 1.89 \times 10^{-11}$. Tensor-to-scalar ratio for this model, by using eq.(1.66) with the scalar power spectrum value $P_S = 2.43 \times 10^{-9}$, is obtained as $r = 7.77 \times 10^{-3}$ and the tensor spectral index is found using eq.(1.65) as $n_T = -9.72 \times 10^{-4}$.

3.1.4 New inflation model

In the new inflation model, it is assumed that the scalar field has a flat plateau but no barrier so that it slowly rolls down towards its vacuum. When it reaches its true vacuum, it oscillates and decays. Inflation at the last stage is not driven by the scalar energy density but by the energy density of the vacuum state. The potential of the scalar field for this model is based on that of the Coleman-Weinberg model with a quartic interacting scalar field [63, 66],

$$V(\phi) = \frac{1}{4}\lambda\phi^4 \left(\ln\frac{\phi}{\sigma} - \frac{1}{4}\right) + \frac{\lambda\sigma^4}{16}, \tag{3.8}$$

where $\lambda = 2.36 \times 10^{-14}$ GeV indicates the quartic self-coupling of the field and $\sigma = 10m_{pl}$ is the vacuum expectation value of the scalar field at minimum.

Using eq.(1.25) and the potential (3.8), the obtained slow-roll parameters for the

new inflation model are

$$\epsilon = 1.16 \times 10^{-2}, \qquad \eta = 1.86 \times 10^{-3}. \tag{3.9}$$

Using the potential (3.8) and eq.(1.62), initial value of the power spectrum of primordial GWs for the new inflation model is calculated as $P_T = 4.52 \times 10^{-10}$. By using eq.(1.65), the tensor spectral index for the new inflation model is found as $n_T = -2.32 \times 10^{-2}$. Using the power spectrum of density perturbations, $P_S = 2.43 \times 10^{-9}$ and eq.(1.66), the calculated tensor-to-scalar ratio value for the new inflation model is $r = 0.186$.

3.1.5 Inverse monomial inflation model

The inverse monomial inflation model is a single scalar field slow-roll inflationary model and is studied here in the context of quintessential inflation [67, 68, 69]. The potential of the scalar field is initially flat to ensure enough time for resolution of the horizon problem, then it becomes steep so that part of the scalar field energy density gets converted to entropy, then this is followed by gradual decrease in the potential slope. The kinetic energy dominates the scalar field after the end of inflation and radiation dominates the universe at later time. The scalar field need not necessarily decay and reheating tends to occur naturally even when the potential has no global minimum, gravitational particle production leads to radiation during the exponential expansion. The effective potential of the inverse monomial inflation model can be expressed as,

$$V(\phi) = M^4 \left(\frac{\phi}{m_{pl}} \right)^{-p}, \tag{3.10}$$

where $p = 3$ is a positive parameter and the ratio $M/m_{pl} = 10^{-1}$.

Using eq.(1.25) and eq.(3.10), the slow-roll parameters are calculated for the inverse monomial inflation model and are obtained as,

$$\epsilon = 1.25 \times 10^{-4}, \tag{3.11}$$

$$\eta = 3.33 \times 10^{-4}. \tag{3.12}$$

Therefore the calculated initial value of tensor power spectrum by using eq.(1.62) and the potential eq.(3.10) for inverse monomial inflation model is $P_T = 4.86 \times 10^{-12}$. Using eq.(1.66) with the scalar power spectrum value $P_S = 2.43 \times 10^{-9}$, the calculated tensor-to-scalar ratio for this inflation model can be obtained, $r = 2.0 \times 10^{-3}$ and the tensor spectral index is found by using eq.(1.65) as $n_T = -2.50 \times 10^{-4}$.

3.1.6 Higgs inflation model

The Higgs inflation model is based on the single Higgs field, which is considered to non-minimally couple with gravity and is considered to play the role of the scalar field [70]. When the field $\phi \gg m_{pl}$, the associated potential is flat enough for the slow roll inflation process to take place. The field can be described using the following effective potential,

$$V(\phi) = M^4(1 + e^{-\sqrt{2/3}\phi/m_{pl}})^{-2}. \tag{3.13}$$

For the Higgs inflation model, the corresponding slow-roll parameters are calculated with eq.(1.25) and eq.(3.13), and the results are

$$\begin{aligned} \epsilon &= 1.77 \times 10^{-4}, \\ \eta &= -1.48 \times 10^{-2}. \end{aligned} \tag{3.14}$$

Using eqs.(1.62) and (3.13), the initial value of the tensor power spectrum for the Higgs inflation model is obtained as, $P_T = 6.87 \times 10^{-12}$. By using the power spectrum for the scalar perturbation $P_S = 2.43 \times 10^{-9}$ and eq.(1.66), the tensor-to-scalar ratio for the Higgs inflation model is calculated as $r = 2.83 \times 10^{-3}$ with tensor spectral index found using eq.(1.65) as $n_T = -3.53 \times 10^{-4}$.

3.1.7 R2 inflation model

The $R2$ inflation model is also known as the Starobinsky inflation model and here $R2$ means the square of Ricci scalar. This model is based on the higher order gravitational terms as quantum corrections to general relativity with the assumption that the early universe underwent an inflationary de Sitter period [18]. The scalar

field degree of freedom comes from the higher order gravitation term itself. The $R2$ inflation model can be expressed in the form of Einstein gravity with a normalized inflaton field which has the effective potential,

$$V(\phi) = M^4(1 - e^{-\sqrt{2/3}\phi/m_{pl}})^2. \tag{3.15}$$

The slow-roll parameters for the $R2$ inflation model are calculated with effective potential eq.(3.15) and eq.(1.25), the obtained values for the parameters are

$$\begin{aligned} \epsilon &= 2.03 \times 10^{-4}, \\ \eta &= -1.63 \times 10^{-2}. \end{aligned} \tag{3.16}$$

Using eqs.(1.62) and eq.(3.15), the initial value of the primordial GW power spectrum for the Starobinsky inflation model is, $P_T = 7.9 \times 10^{-12}$. Using eq.(1.66) with the scalar power spectrum value $P_S = 2.43 \times 10^{-9}$, the tensor-to-scalar ratio for the R2 model is calculated to be $r = 3.25 \times 10^{-3}$, and the tensor spectral index is found using eq.(1.65) as $n_T = -4.06 \times 10^{-4}$.

3.1.8 Arctan inflation model

The arctan inflation model is a single scalar field model and often studied as a toy model [71, 72]. It is a large field model which starts at a large value and then evolves to a minimum at the origin. The inflation process ends when the slow-roll condition is violated. The potential for the scalar field can be expressed by,

$$V(\phi) = M^4 \left[1 - \arctan\left(\frac{\phi}{\mu}\right)\right], \tag{3.17}$$

where $\mu/m_{pl} = 10^{-2}$ is a free parameter which characterizes the typical vacuum expectation value at which inflation takes place and the ratio $M/m_{pl} = 10^{-3}$.

Using eq.(1.25) with the potential eq.(3.17), the parameters of the slow-roll condition for the arctan inflation model are found as,

$$\epsilon = 8.62 \times 10^{-4}, \tag{3.18}$$

$$\eta = 3.0 \times 10^{-2}. \tag{3.19}$$

Using eqs.(1.62) and (3.17), the estimated initial value of the tensor power spectrum for the arctan inflation model is $P_T = 3.35 \times 10^{-11}$. Using the power spectrum of the scalar perturbation $P_S = 2.43 \times 10^{-9}$ and eq.(1.66), the tensor-to-scalar ratio for this inflation model is calculated as, $r = 1.38 \times 10^{-2}$ and the tensor spectral index is found using eq.(1.65) as $n_T = -1.72 \times 10^{-3}$.

3.1.9 Natural inflation model

In the natural inflation model, the role of the scalar field is considered to be played by the Nambu-Goldstone boson which arises whenever global symmetry is spontaneously broken and can give rise to an epoch of inflation naturally [73, 74]. The scenario for the natural inflation model is very close to the chaotic inflationary scenario. The scalar field in the natural inflation model has an associated effective potential,

$$V(\phi) = M^4 \left[1 + \cos\left(\frac{\phi}{f}\right)\right], \tag{3.20}$$

where $f/m_{pl} = 10^2$, this corresponds to the symmetry breaking energy scale and $M/m_{pl} = 10^{-2}$.

The slow-roll parameters for the natural inflation model are calculated by using the potential eq.(3.20) and eq.(1.25), and the obtained values are

$$\epsilon = 1.29 \times 10^{-3}, \tag{3.21}$$

$$\eta = 1.24 \times 10^{-3}. \tag{3.22}$$

Using eq.(1.62) and eq.(3.1), the initial power spectrum of the tensor perturbation for the natural inflation model is calculated as $P_T = 5.027 \times 10^{-11}$. Using eq.(1.66) with the scalar power spectrum value $P_S = 2.43 \times 10^{-9}$, the tensor-to-scalar ratio for this inflation model is, $r = 2.06 \times 10^{-2}$ and the tensor spectral index is found using eq.(1.65) as $n_T = -2.58 \times 10^{-3}$.

3.1.10 Radiatively corrected quadratic chaotic inflation model

The radiatively corrected quadratic chaotic inflation is a simple quadratic chaotic inflation model studied under the assumption that the scalar field interacts with the fermion field thus leading to the quantum radiative correction which takes the form of a logarithmic function [19, 75]. The scalar field potential for radiatively corrected quadratic chaotic inflation model can be written as,

$$V(\phi) = \frac{1}{2}m^2\phi^2 - \frac{g^4}{16\pi^2}\phi^4 \ln\left(\frac{\phi}{m_{pl}}\right), \tag{3.23}$$

where g is the Yukawa coupling and mass of the scalar field $m = 3.44 \times 10^{12}$ GeV.

For the radiatively corrected quadratic chaotic inflation model, the associated slow-roll parameters are calculated by using eqs.(1.25) and (3.23) and are found as

$$\begin{aligned} \epsilon &= 1.86 \times 10^{-3}, \\ \eta &= 1.86 \times 10^{-3}. \end{aligned} \tag{3.24}$$

Using eq.(1.62) and eq.(3.23), the calculated initial value of the GW power spectrum for the radiatively corrected quadratic chaotic inflation model is $P_T = 7.25 \times 10^{-11}$. With the power spectrum of the density perturbation $P_S = 2.43 \times 10^{-9}$ and by using eq.(1.66), the tensor-to-scalar ratio is calculated as $r = 2.98 \times 10^{-2}$ and the tensor spectral index is found using eq.(1.65) as $n_T = -3.72 \times 10^{-3}$.

3.1.11 Loop inflation model

In the loop inflation scenario, the flatness of the scalar field potential is altered by symmetry breaking which produces quantum radiative corrections in which one loop order correction takes the form of a logarithmic function [76, 77, 78]. The phase transition with symmetry breaking occurs only after the scalar field drops to its critical value below which all the vacuum expectation values adjust rapidly to their supersymmetric values. The scalar field associated with the loop inflation model has an effective potential given by,

$$V(\phi) = M^4\left[1 + \alpha \ln\left(\frac{\phi}{m_{pl}}\right)\right], \tag{3.25}$$

where $\alpha = g^2/16\pi^2$ tunes the strength of radiative effects and $M = 10^{16}$ GeV.

Using the potential eq.(3.25) and eq.(1.25), the obtained slow-roll parameters for the loop inflation model are

$$\epsilon = 3.09 \times 10^{-3}, \tag{3.26}$$

$$\eta = -2.06 \times 10^{-2}. \tag{3.27}$$

Using eq.(1.62) and eq.(3.25), the estimated initial value of the GW power spectrum for the loop inflation model is $P_T = 1.2 \times 10^{-10}$. Using eq.(1.66) with the scalar power spectrum value $P_S = 2.43 \times 10^{-9}$, the tensor-to-scalar ratio for this inflation model is found to be, $r = 4.34 \times 10^{-2}$ and the tensor spectral index is found using eq.(1.65) as $n_T = -6.18 \times 10^{-3}$.

3.1.12 Hybrid inflation model

The hybrid inflation model is a multi-scalar field slow-roll inflation model and it has the effective potential [79, 80],

$$V = \frac{1}{4\lambda}(M^2 - \lambda\sigma^2)^2 + \frac{1}{2}m^2\phi^2 + \frac{1}{2}g^2\phi^2\sigma^2, \tag{3.28}$$

where $M = 1.21 \times 10^{16}$ GeV and $m = 3.65 \times 10^{11}$ GeV are the masses of the ϕ field and σ field respectively, and $\lambda = 1$ and $g = 8 \times 10^{-4}$ are the respective self-coupling terms. The ϕ field provides the initial inflationary mechanism and thus it determines the inflationary period while the σ field both determines the rate and triggers the end of inflation. When the ϕ field rolls down to the minimum of its potential after the slow-roll, it displaces the σ field from its minimum potential. This action leads to fast roll and then symmetry breaking of the σ field, thus abruptly ending the inflation.

The parameters of slow-roll for the hybrid inflation model are found by using eq.(1.25) and the potential eq.(3.28) and are

$$\epsilon = 2.65 \times 10^{-4},$$

$$\eta = 1.47 \times 10^{-4}. \tag{3.29}$$

Using the eq.(3.28) and eq.(1.62), the initial value of tensor power spectrum with the hybrid inflation model is obtained as $P_T = 1.03 \times 10^{-11}$. Using eq.(1.66) with the scalar power spectrum value $P_S = 2.43 \times 10^{-9}$, the calculated tensor-to-scalar ratio is $r = 4.24 \times 10^{-3}$ and the tensor spectral index is found using eq.(1.65) as $n_T = -5.3 \times 10^{-4}$.

3.2 Gravitational waves in expanding universe

The primordial gravitational waves are basically seeded from the cosmic inflation of the early universe. The tensor perturbation for the perturbed flat FLRW metric is given in eq.(1.53) and its properties are discussed in Chapter 1. In quantum theory, the tensor perturbation or the primordial gravitational wave field can be expressed as a collection of the wave modes in the Fourier space as,

$$h_{ij}(\mathbf{x},\tau) = \frac{D}{(2\pi)^{\frac{3}{2}}} \int_{-\infty}^{+\infty} \frac{d^3\mathbf{k}}{\sqrt{2k}} \sum_{p=+,\times}^{2} [h_k^{(p)}(\tau) c_k^{(p)} \varepsilon_{ij}^{(p)}(\mathbf{k}) e^{i\mathbf{k}.\mathbf{x}} + h_k^{(p)*}(\tau) c_k^{(p)\dagger} \varepsilon_{ij}^{(p)*}(\mathbf{k}) e^{-i\mathbf{k}.\mathbf{x}}], \tag{3.30}$$

where $D = \sqrt{16\pi} l_{pl}$ is the constant of normalization, $l_{pl} = \sqrt{G}$ represents the Planck length and k denotes the wave number; $\varepsilon_{ij}^{(p)}$, $p = +, \times$ are the linear, symmetric and transverse-traceless polarizations which satisfy the conditions,

$$\varepsilon_{ij}^{(p)} \delta^{ij} = 0, \quad \varepsilon_{ij}^{(p)} k^i = 0, \quad \varepsilon_{ij}^{(p)} \varepsilon^{(p')ij} = 2\delta_{pp'}, \quad \varepsilon_{ij}^{(p)}(\mathbf{-k}) = \varepsilon_{ij}^{(p)}(\mathbf{k}).$$

The creation and annihilation operators $c_k^{(p)\dagger}$ and $c_k^{(p)}$ satisfy the following commutation relations,

$$[c_k^{(p)}, c_{k'}^{(p')\dagger}] = \delta_{pp'} \delta^3(k - k'),$$

$$[c_k^{(p)}, c_{k'}^{(p')}] = [c_k^{(p)\dagger}, c_{k'}^{(p')\dagger}] = 0.$$

The Heisenberg equations of motion govern the evolution of the creation and annihilation operators,[1]

$$\frac{d}{d\tau} c_{\mathbf{k}}^{\dagger}(\tau) = -i[c_k^{\dagger}(\tau), \mathcal{H}_{gw}], \tag{3.31}$$

$$\frac{d}{d\tau} c_{\mathbf{k}}(\tau) = -i[c_k(\tau), \mathcal{H}_{gw}], \tag{3.32}$$

[1]From here onwards, the index (p) is dropped for notational convenience.

where $\mathcal{H}_{gw}$ is the Hamiltonian for the primordial gravitational waves.

The initial vacuum state can be defined as,

$$c_k|0\rangle = 0.$$

The Bogoliubov transformations for the annihilation and creation operators are

$$c_{\mathbf{k}}(\tau) = u_k(\tau)c_{\mathbf{k}}(0) + v_k(\tau)c^{\dagger}_{\mathbf{k}}(0), \tag{3.33}$$

$$c^{\dagger}_{\mathbf{k}}(\tau) = u^*_k(\tau)c^{\dagger}_{\mathbf{k}}(0) + v^*_k(\tau)c_{\mathbf{k}}(0), \tag{3.34}$$

where $c_{\mathbf{k}}(0)$ and $c^{\dagger}_{\mathbf{k}}(0)$ indicate the initial values of the annihilation and creation operators respectively, $u_k(\tau)$ and $v_k(\tau)$ are complex functions which satisfy the condition

$$|u_k|^2 - |v_k|^2 = 1.$$

The evolution equation of the primordial GWs in the flat FLRW universe can be expressed in the Fourier space as,

$$h''_k(\tau) + 2Hh'_k(\tau) + k^2h_k(\tau) = 0, \tag{3.35}$$

here H denotes the Hubble parameter in the conformal time. The gravitational wave mode can be rescaled with the help of the mode function as,

$$h_k(\tau)a(\tau) = \mu_k(\tau). \tag{3.36}$$

where the mode functions can have the following form

$$\mu_k(\tau) = u_k(\tau) + v^*_k(\tau). \tag{3.37}$$

Using eq.(3.36) in eq.(3.35), the equation of motion in terms of the mode function becomes,

$$\mu''_k(\tau) + \left(k^2 - \frac{a''}{a}\right)\mu_k(\tau) = 0. \tag{3.38}$$

When $k^2 \gg a''/a$, the mode is inside the Hubble radius, which corresponds to the short wavelength limit and the solution to the eq.(3.38) gives simple plane wave solution as,

$$\mu_k(\tau) \simeq C_{\pm}(k)e^{\pm ik\tau}, \tag{3.39}$$

which indicates that,

$$h_k(\tau) \simeq \frac{C_{\pm}(k)e^{\pm ik\tau}}{a(\tau)}. \tag{3.40}$$

In this case, the tensor mode is over the potential barrier and the wave does not interact with the potential barrier and hence propagates with an amplitude which decreases with time.

For the long wavelength limit, $k^2 \ll a''/a$, the mode is under the potential barrier and eq.(3.38) has the solution

$$\mu_k(\tau) \simeq A_k a(\tau) + B_k a(\tau) \int^{\tau} \frac{d\tau}{a^2(\tau)}, \tag{3.41}$$

which implies that,

$$h_k(\tau) \simeq A_k + B_k \int^{\tau} \frac{d\tau}{a^2(\tau)}, \tag{3.42}$$

which exhibits presence of both constant mode and decaying mode; the wave interacts with the barrier and gets amplified above $h_k(\eta) \propto 1/a(\eta)$ in the adiabatic regime. Since this is the case, the constant mode implies an adiabatic growth, and the mode is frozen outside the Hubble radius.

3.3 Tensor power spectrum in squeezed vacuum state

The primordial gravitational waves are believed to have been generated quantum mechanically in the very early universe. It is believed that the strong and variable gravitational field during inflation induced the generation of the primordial GWs through the parametric amplification mechanism of the zero-point quantum fluctuations. Due to the parametric amplification, the initial quantum vacuum state with no graviton evolves into a quantum state with multiple particles called the squeezed vacuum state. The squeezed quantum vacuum state can be defined as [81],

$$|\xi\rangle = S(\xi)|0\rangle, \tag{3.43}$$

where $S(\xi)$ is the single mode squeezing operator, $\xi = r_s e^{i\gamma}$ is a complex variable with r_s being the squeezing parameter and γ represents squeezing angle and are

respectively ranged as $0 \leq r_s < \infty$ and $0 \leq \gamma \leq 2\pi$. The single mode squeezing operator is defined as,

$$S(\xi) = \exp\left[\frac{1}{2}\xi^* c^2 - \frac{1}{2}\xi c^{\dagger 2}\right]. \tag{3.44}$$

The unitary transformations on the creation and annihilation operators induced by the squeezing operator S lead to,

$$\begin{aligned} c_k^\dagger &= S^\dagger(\xi) c^\dagger S(\xi) = c^\dagger \cosh r_s - c e^{-i\gamma} \sinh r_s, \\ c_k &= S^\dagger(\xi) c S(\xi) = c \cosh r_s - c^\dagger e^{i\gamma} \sinh r_s, \end{aligned} \tag{3.45}$$

and the creation and annihilation operators have the following mean values in vacuum state:

$$\begin{aligned} \langle 0|c_{\mathbf{k}}^\dagger(\tau)|0\rangle &= \langle 0|c_{\mathbf{k}}(\tau)|0\rangle = 0, \\ \langle 0|c_{\mathbf{k}}^\dagger(\tau) c_{\mathbf{k}'}^\dagger(\tau)|0\rangle &= u_k^*(\tau) v_{k'}^* \delta^3(\mathbf{k}+\mathbf{k}'), \\ \langle 0|c_{\mathbf{k}}(\tau) c_{\mathbf{k}'}(\tau)|0\rangle &= u_k(\tau) v_{k'} \delta^3(\mathbf{k}+\mathbf{k}'), \\ \langle 0|c_{\mathbf{k}}^\dagger(\tau) c_{\mathbf{k}'}(\tau)|0\rangle &= v_k^*(\tau) v_{k'} \delta^3(\mathbf{k}-\mathbf{k}'), \\ \langle 0|c_{\mathbf{k}}(\tau) c_{\mathbf{k}'}^\dagger(\tau)|0\rangle &= u_k(\tau) u_{k'}^* \delta^3(\mathbf{k}-\mathbf{k}'). \end{aligned} \tag{3.46}$$

The complex functions $u_k(\tau)$ and $v_k(\tau)$ can be represented in terms of the squeezing parameter r_s, squeezing angle γ and the rotation angle θ_s as,

$$\begin{aligned} u_k &= e^{i\theta_s} \cosh r_s, \\ v_k &= e^{-i(\theta_s - 2\gamma)} \sinh r_s. \end{aligned} \tag{3.47}$$

and their equations of motion in the FLRW universe become

$$\begin{aligned} i\frac{du_k}{d\tau} &= k u_k + i\frac{a'}{a} v_k^*, \\ i\frac{dv_k}{d\tau} &= k v_k + i\frac{a'}{a} u_k^*. \end{aligned} \tag{3.48}$$

The squeezing parameter, squeezing angle and rotation angle are then governed by the following equations of motion [82],

$$\begin{aligned} r_s' &= \frac{a'}{a}\cos 2\gamma, \\ \gamma' &= -k - \frac{a'}{a}\sin 2\gamma \coth 2r_s, \\ \theta_s' &= -k - \frac{a'}{a}\sin 2\gamma \tanh r_s. \end{aligned} \tag{3.49}$$

To study the effect of primordial GWs in the squeezed vacuum state on the CMB spectrum in the form of the B-mode polarization for various inflation models requires the computation of tensor power spectrum in the squeezed vacuum state. The power spectrum for the primordial GWs can be obtained with the two-point correlation function of the GW mode, h_k as,

$$\langle h_{\mathbf{k}} h^*_{\mathbf{k}'} \rangle = \frac{2\pi^2}{k^3} P_T(k) \delta^3(\mathbf{k} - \mathbf{k}'), \tag{3.50}$$

where the angle bracket indicates the variance of the GW field and P_T is the power spectrum of the primordial GW.

Using eq.(3.30) and eq.(3.37), the gravitational wave field can be written as a combination of the mode function and the annihilation and creation operators as,

$$h_{\mathbf{k}}(\mathbf{x}, \tau) = \frac{D}{a(\tau)(2\pi)^{\frac{3}{2}}} \int_{-\infty}^{+\infty} d^3\mathbf{k} [\mu_k(\tau) c_k + \mu^*_k(\tau) c^\dagger_k] e^{i\mathbf{k}.\mathbf{x}}. \tag{3.51}$$

Using eq.(3.45) and eq.(3.46), the mean square value of the gravitational wave, eq.(3.51), can be computed in the squeezed vacuum state and the obtained result is,

$$\langle h_{\mathbf{k}} h^*_{\mathbf{k}'} \rangle = \frac{D^2}{a^2} [(|u_k|^2 + |v_k|^2)|\mu_k|^2 + u_k v_k \mu_k^2 + u^*_k v^*_k \mu^{*2}_k] \delta^3(\mathbf{k} - \mathbf{k}'), \tag{3.52}$$

which can be written explicitly in terms of the squeezing parameter and squeezing angle as,

$$\langle h_{\mathbf{k}} h^*_{\mathbf{k}'} \rangle = \frac{D^2}{a^2} \left[(1 + 2\sinh^2 r_s)|\mu_k|^2 + \frac{1}{2} \sinh 2r_s (\mu_k^2 e^{i\gamma} + \mu^{*2}_k e^{-i\gamma}) \right] \delta^3(\mathbf{k} - \mathbf{k}'). \tag{3.53}$$

Therefore comparing the standard two point correlation eq.(3.50) with the two point correlation of the GW modes in the squeezed quantum vacuum state, eq.(3.53), gives the power spectrum of the primordial GWs in the squeezed vacuum state as,

$$P_T(k) = \frac{k^3}{2\pi^2} \frac{D^2}{a^2} \left[(1 + 2\sinh^2 r_s)|\mu_k|^2 + \frac{1}{2} \sinh 2r_s (\mu_k^2 e^{i\gamma} + \mu^{*2}_k e^{-i\gamma}) \right]. \tag{3.54}$$

During inflation, considering the quasi de Sitter universe, the scale factor and the conformal time are related as $a(\tau) = \frac{-1}{H\tau(1-\epsilon)}$.

For constant slow roll parameter ϵ value, the equation of motion can be expressed as [83],

$$\mu''_k + \left[k^2 - \frac{1}{\tau^2} \left(\vartheta^2 - \frac{1}{4} \right) \right] \mu_k = 0, \tag{3.55}$$

where $\vartheta = \frac{3}{2} + \epsilon$ for small value of ϵ which leads to the tensor spectral index $n_T = -2\epsilon = 3 - 2\vartheta$. which has the general solution:

$$\mu_k(\tau) = \sqrt{-\tau}[C_1(k)\mathbb{H}_\vartheta^{(1)}(-k\tau) + C_2(k)\mathbb{H}_\vartheta^{(2)}(-k\tau)], \tag{3.56}$$

where $\mathbb{H}_\vartheta^{(1)}$ and $\mathbb{H}_\vartheta^{(2)}$ represent the Hankel functions of the first and second kinds, and C_1 and C_2 denote the integration constants.

For short wavelength limit ($k >> aH$), the modes can be approximated using the flat spacetime solutions as,

$$\mu_k^0(\tau) = \frac{1}{\sqrt{2k}} e^{-ik\tau}. \tag{3.57}$$

Using eq.(3.57), the integration constants become,

$$\begin{aligned} C_1(k) &= \frac{\sqrt{\pi}}{2} \exp\left[i\left(\vartheta + \frac{1}{2}\right)\left(\frac{\pi}{2}\right)\right], \\ C_2(k) &= 0. \end{aligned} \tag{3.58}$$

For long wavelength limit ($k << aH$), eq.(3.56) gives

$$\mu_k(\tau) = e^{i\left(\vartheta - \frac{1}{2}\right)\left(\frac{\pi}{2}\right)} 2^{\vartheta - \frac{3}{2}} \frac{\Gamma(\vartheta)}{\Gamma\left(\frac{3}{2}\right)} \frac{1}{\sqrt{2k}} (-k\tau)^{\frac{1}{2} - \vartheta}. \tag{3.59}$$

Using eq.(3.59) in eq.(3.54), the power spectrum for the long wavelength limit ($k << aH$) becomes,

$$P_T(k) = D^2 \left(\frac{H}{2\pi}\right)^2 \left(\frac{k}{aH}\right)^{3-2\vartheta} \left[1 + 2\sinh^2 r_s + \sinh 2r_s \cos\left(\gamma + \left(\vartheta - \frac{1}{2}\right)\pi\right)\right]. \tag{3.60}$$

The power spectrum for the primordial gravitational waves can then be written in terms of the tensor spectral index n_T as

$$P_T(k) = A_T(k_0) \left(\frac{k}{k_0}\right)^{n_T} \left[1 + 2\sinh^2 r_s + \sinh 2r_s \cos\left(\gamma + (2 - n_T)\frac{\pi}{2}\right)\right], \tag{3.61}$$

where $A_T(k_0) = D^2 \left(\frac{H_{k0}}{2\pi}\right)^2$ is the constant of normalization, H_{k0} indicates that the Hubble parameter is computed at $aH = k_0$, and k_0 is the pivot wave number. It is clear from the above equation that in the absence of the squeezing effect, the tensor power spectrum recovers to that of ordinary vacuum case.

Eq.(3.61) gives the power spectrum for primordial GWs in the squeezed quantum vacuum state. If the primordial GWs indeed exist in such state, then the squeezing

effect is also expected to have some signature in the B-mode polarization of the CMB anisotropy spectrum. The variance of the GW field is an explicit oscillatory function of time, hence leading to non-stationary background. Hence, the squeezing effect implies that the resulting state can be treated as a background of stochastic standing waves thus leaving oscillatory characteristics in the CMB angular power spectrum. Thus, the primordial GWs in the squeezed vacuum state form a non-stationary background which can provide a unique signature essential in distinguishing it from a background created from a stochastic stationary background by other sources or processes which could not produce oscillatory features in the CMB angular power spectrum.

3.4 BB-mode angular power spectrum of CMB in squeezed vacuum state

In this section, we study the BB-mode angular power spectrum by placing the primordial GWs in the squeezed vacuum state for various slow-roll inflation models. For each inflation model, the BB-mode angular power spectrum of CMB is implemented with the expression (2.28) given by,

$$C_l^{BB} = (4\pi)^2 \int k^2 dk\, P_T(k) \Big| \int_0^{\tau_0} d\tau g(\tau) h_k(\tau) \left[2j_l'(x) + \frac{4j_l(x)}{x} \right] \Big|^2, \quad (3.62)$$

where, $x = k(\tau_0 - \tau)$, $g(\tau) = \kappa'(\tau)e^{-\kappa}$ is the visibility function whose peak defines the recombination era and denotes the probability of the CMB photon being last scattered at the redshift z, and κ' denotes the differential optical depth for the surface of last scattering and $j_l(x)$ denotes the spherical Bessel function of order l.

By using eq.(3.62), the BB-mode spectrum of CMB for the primordial GWs in the squeezed vacuum state for the various slow-roll inflation models are computed by taking the calculated initial value of the power spectrum of the GWs corresponding to each inflation model as well as the tensor spectral index. The BB-mode spectrum for each slow-roll inflation model is generated with the help of CAMB code. For this, the optical depth value is taken to be $\kappa = 0.08$, and the tensor and scalar pivot wave numbers are respectively taken to be 0.002 Mpc^{-1} and 0.05 Mpc^{-1}. The BB-mode

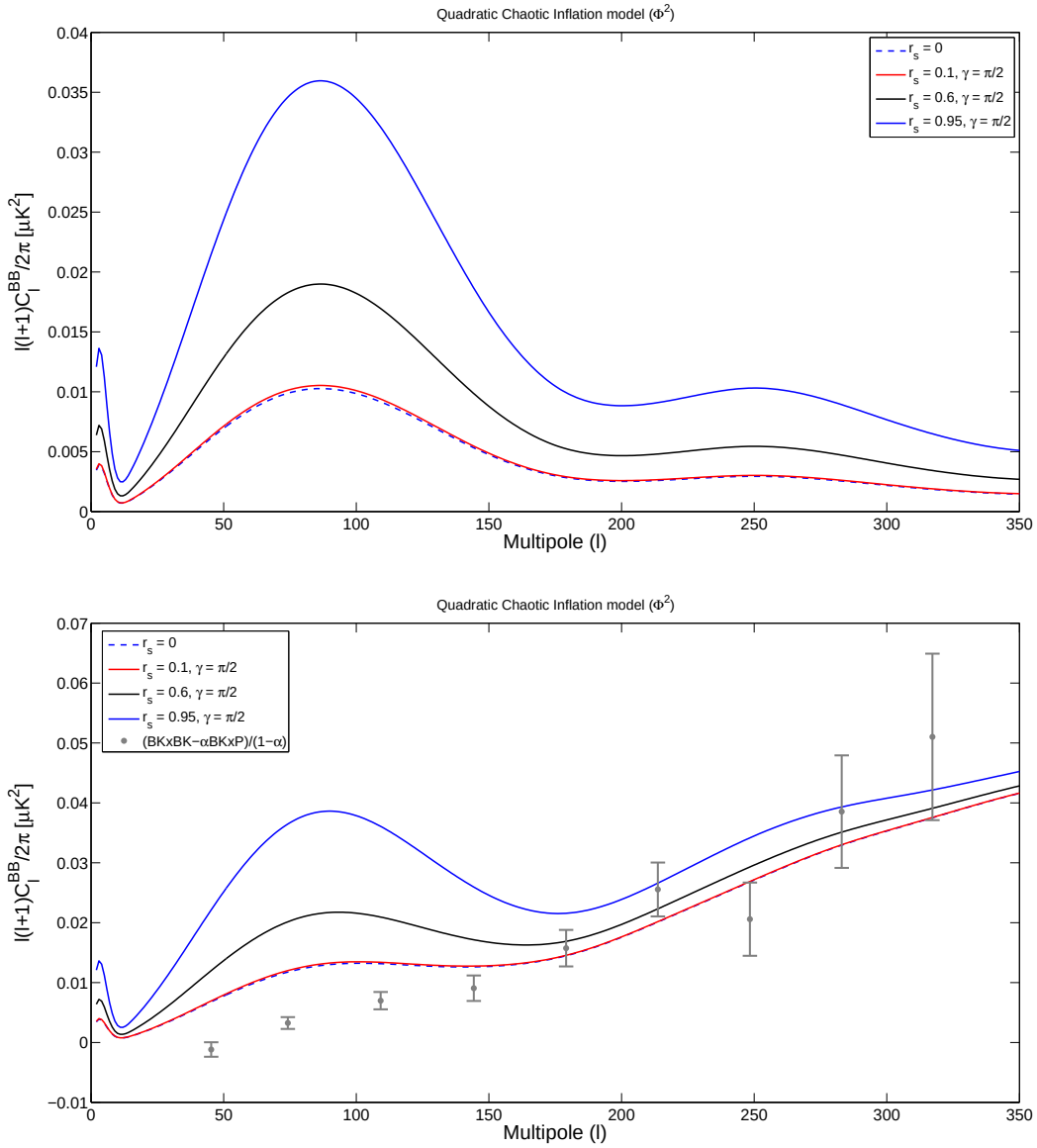

Figure 3.1: The BB-mode angular spectrum of CMB for the quadratic chaotic inflation model with unlensed (upper panel) and lensed (lower panel) effects for various values of squeezing parameters with the joint BKP data.

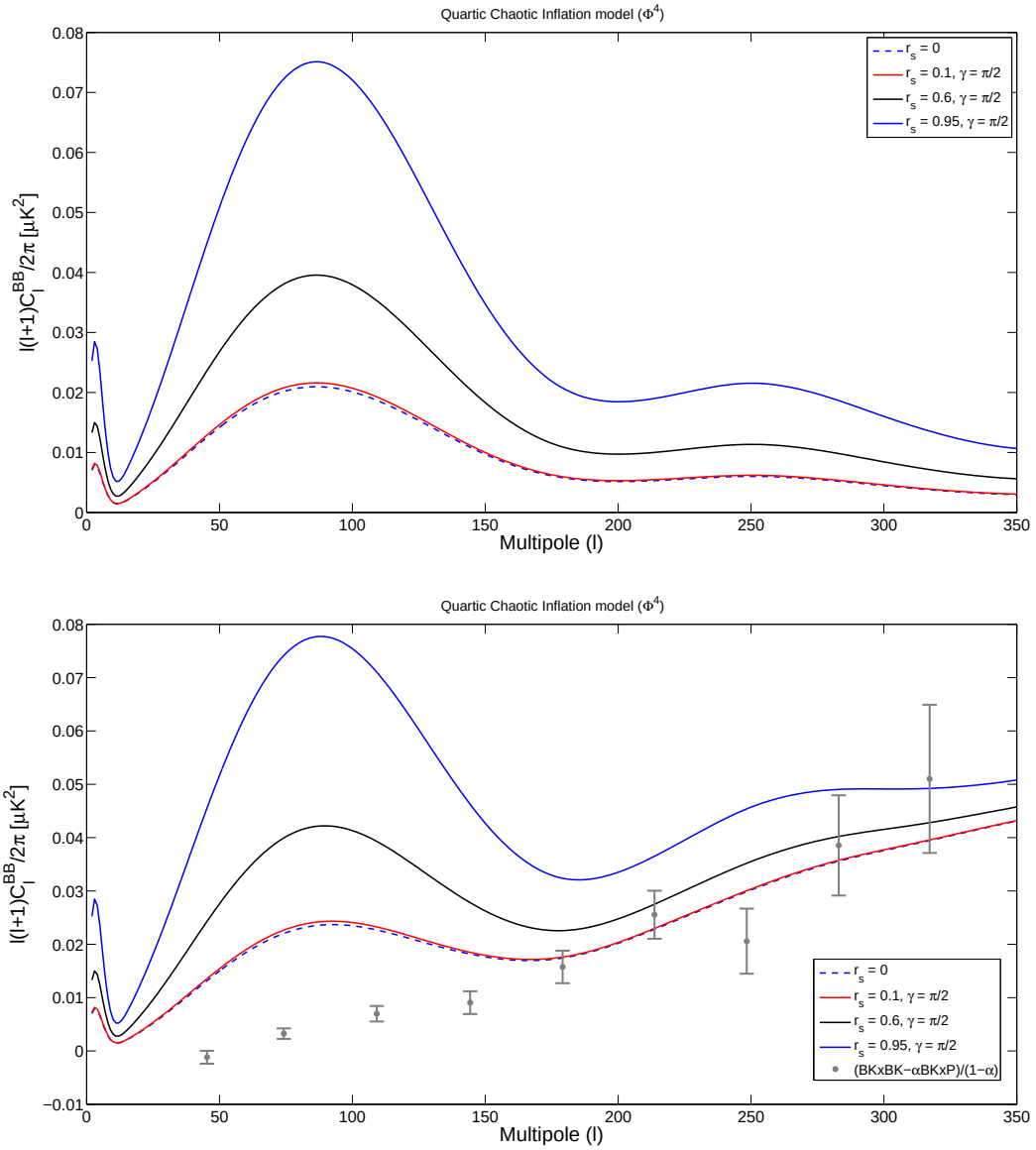

Figure 3.2: The BB-mode angular spectrum of CMB for the quartic chaotic inflation model with unlensed (upper panel) and lensed (lower panel) effects for various values of squeezing parameters with the joint BKP data.

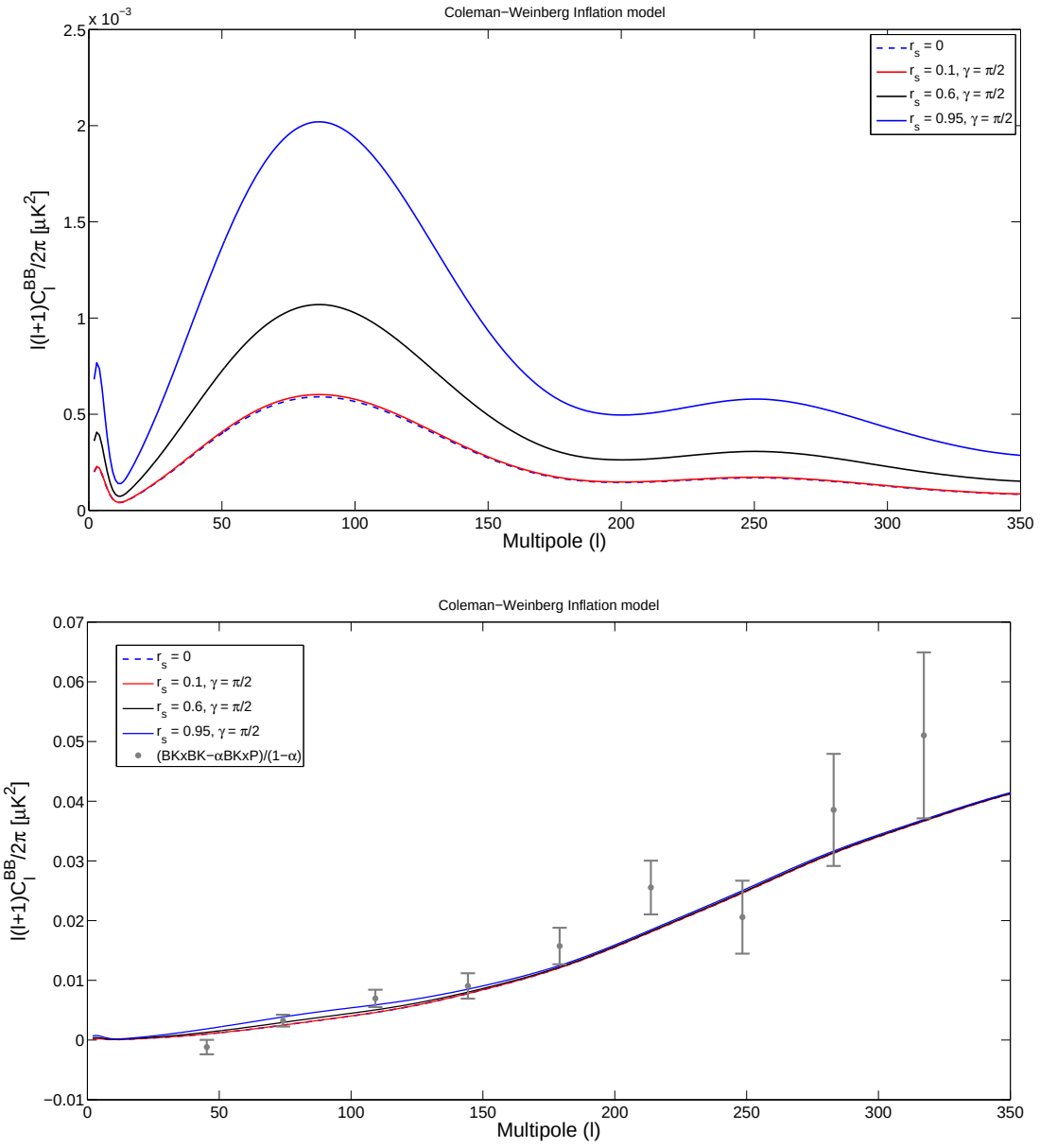

Figure 3.3: The BB-mode angular spectrum of CMB for the Coleman-Weinberg inflation model with unlensed (upper panel) and lensed (lower panel) effects for various values of squeezing parameters with the joint BKP data.

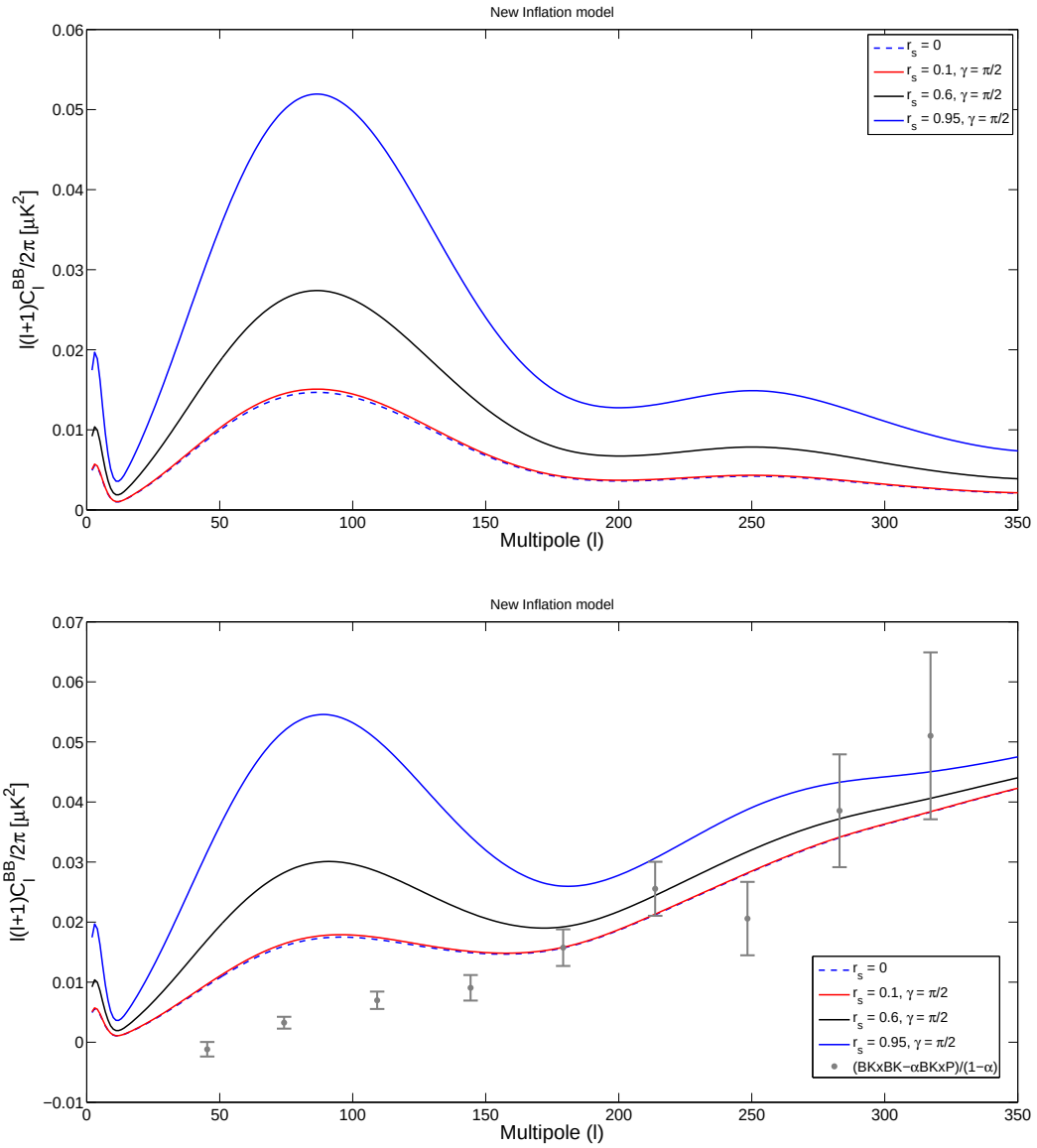

Figure 3.4: The BB-mode angular spectrum of CMB for the new inflation model with unlensed (upper panel) and lensed (lower panel) effects for various values of squeezing parameters with the joint BKP data.

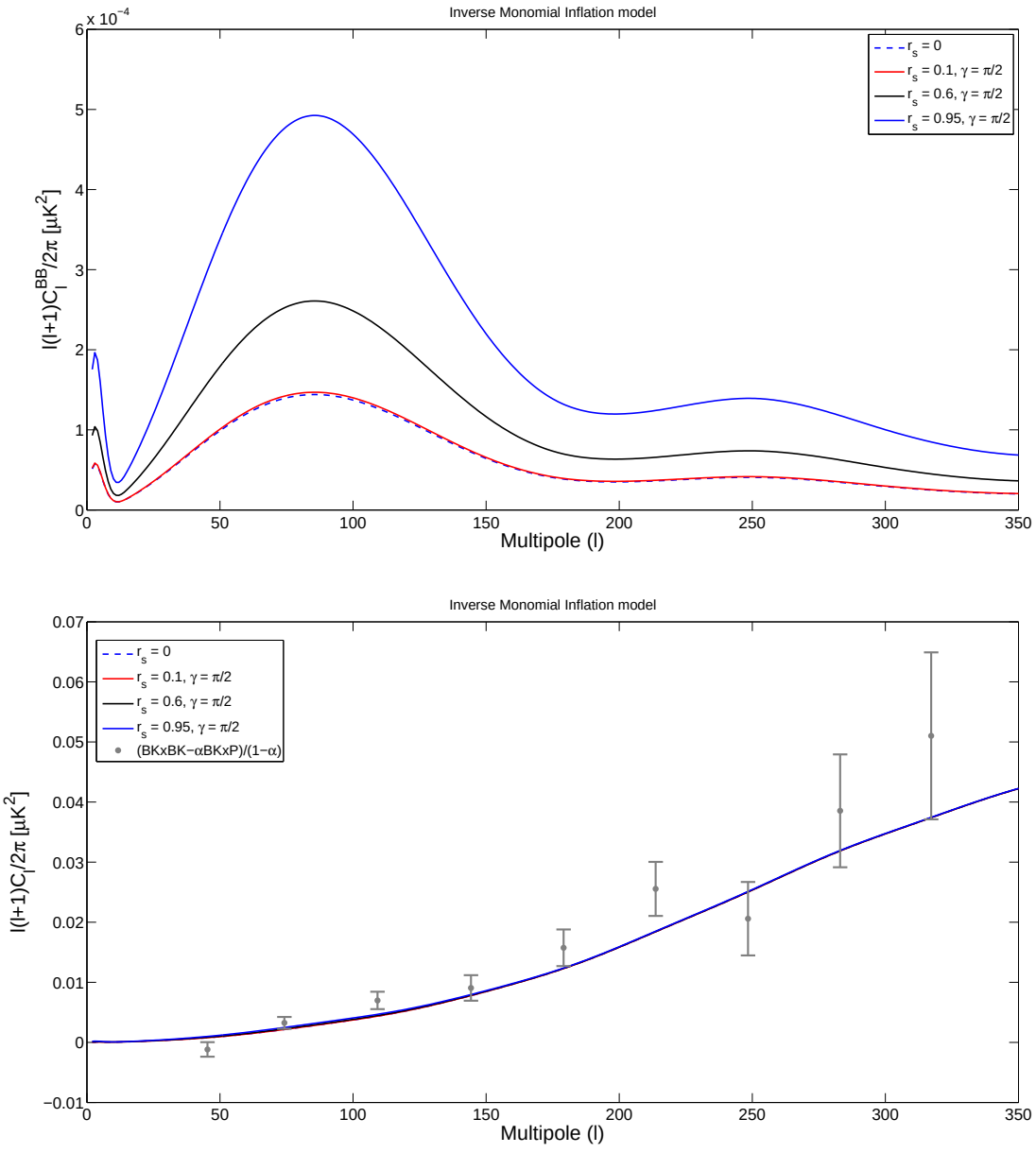

Figure 3.5: The BB-mode angular spectrum of CMB for the inverse monomial inflation model with unlensed (upper panel) and lensed (lower panel) effects for various values of squeezing parameters with the joint BKP data.

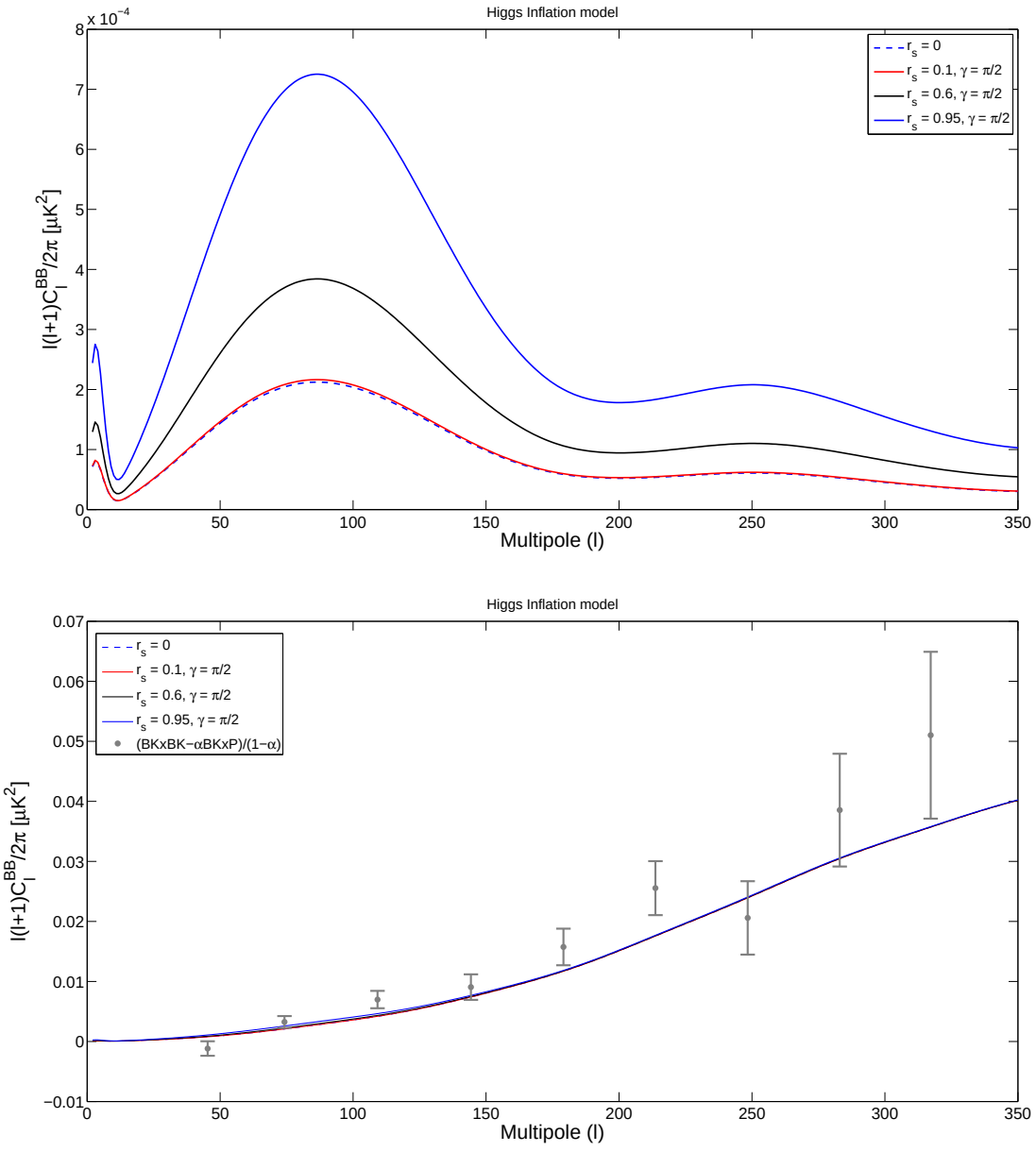

Figure 3.6: The BB-mode angular spectrum of CMB for the Higgs inflation model with unlensed (upper panel) and lensed (lower panel) effects for various values of squeezing parameters with the joint BKP data.

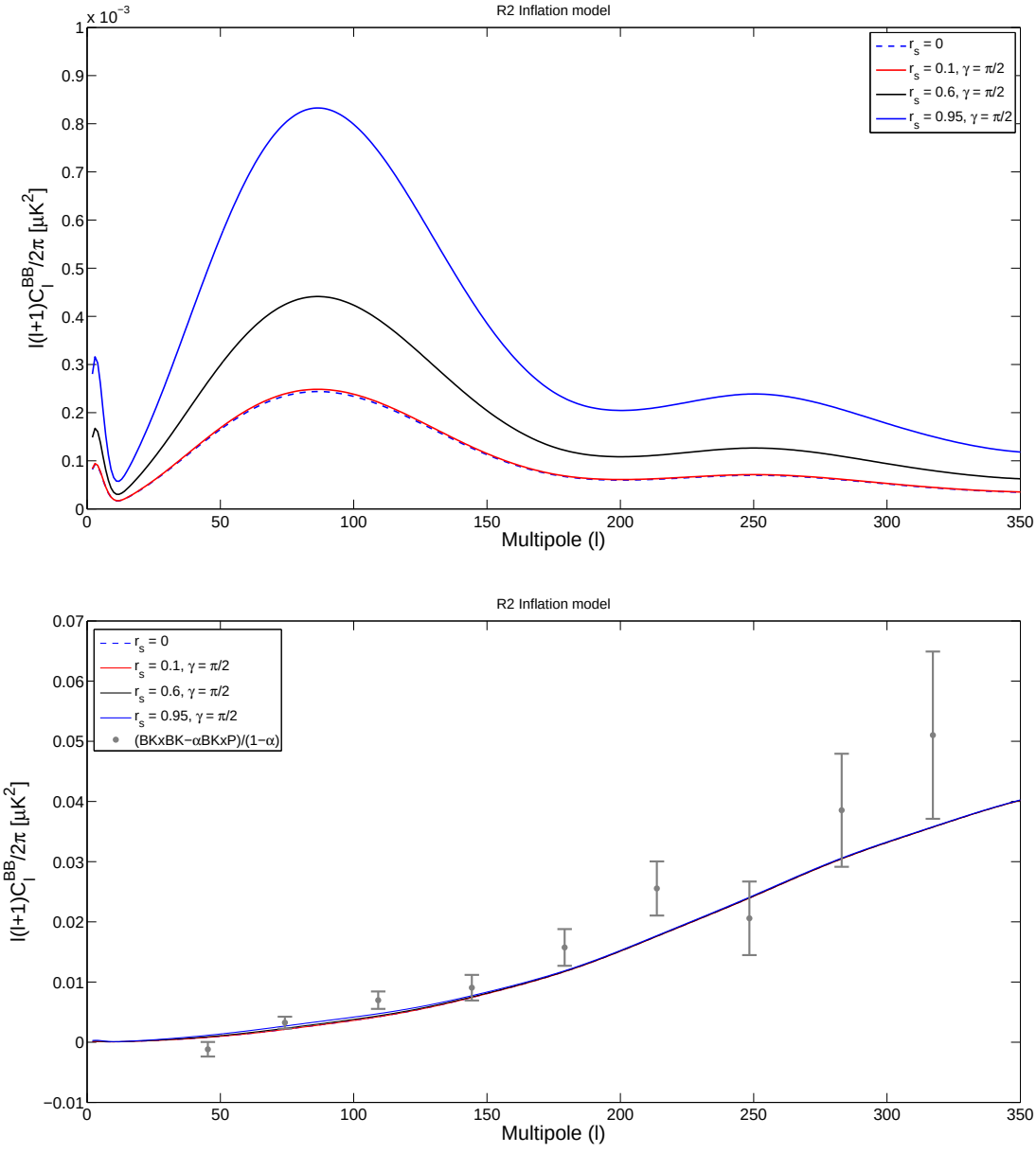

Figure 3.7: The BB-mode angular spectrum of CMB for the Starobinsky (R2) inflation model with unlensed (upper panel) and lensed (lower panel) effects for various values of squeezing parameters with the joint BKP data.

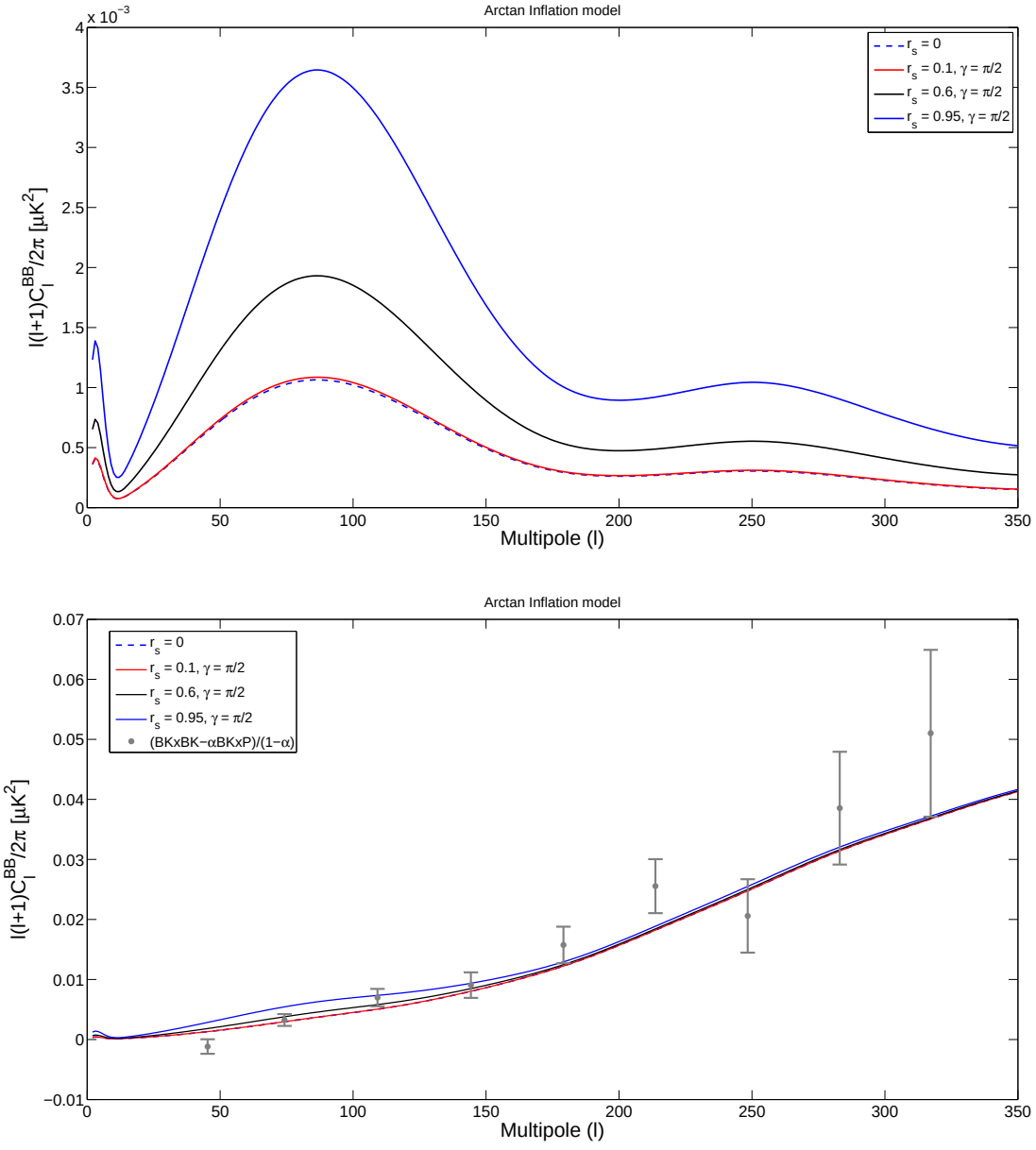

Figure 3.8: The BB-mode angular spectrum of CMB for the arctan inflation model with unlensed (upper panel) and lensed (lower panel) effects for various values of squeezing parameters with the joint BKP data.

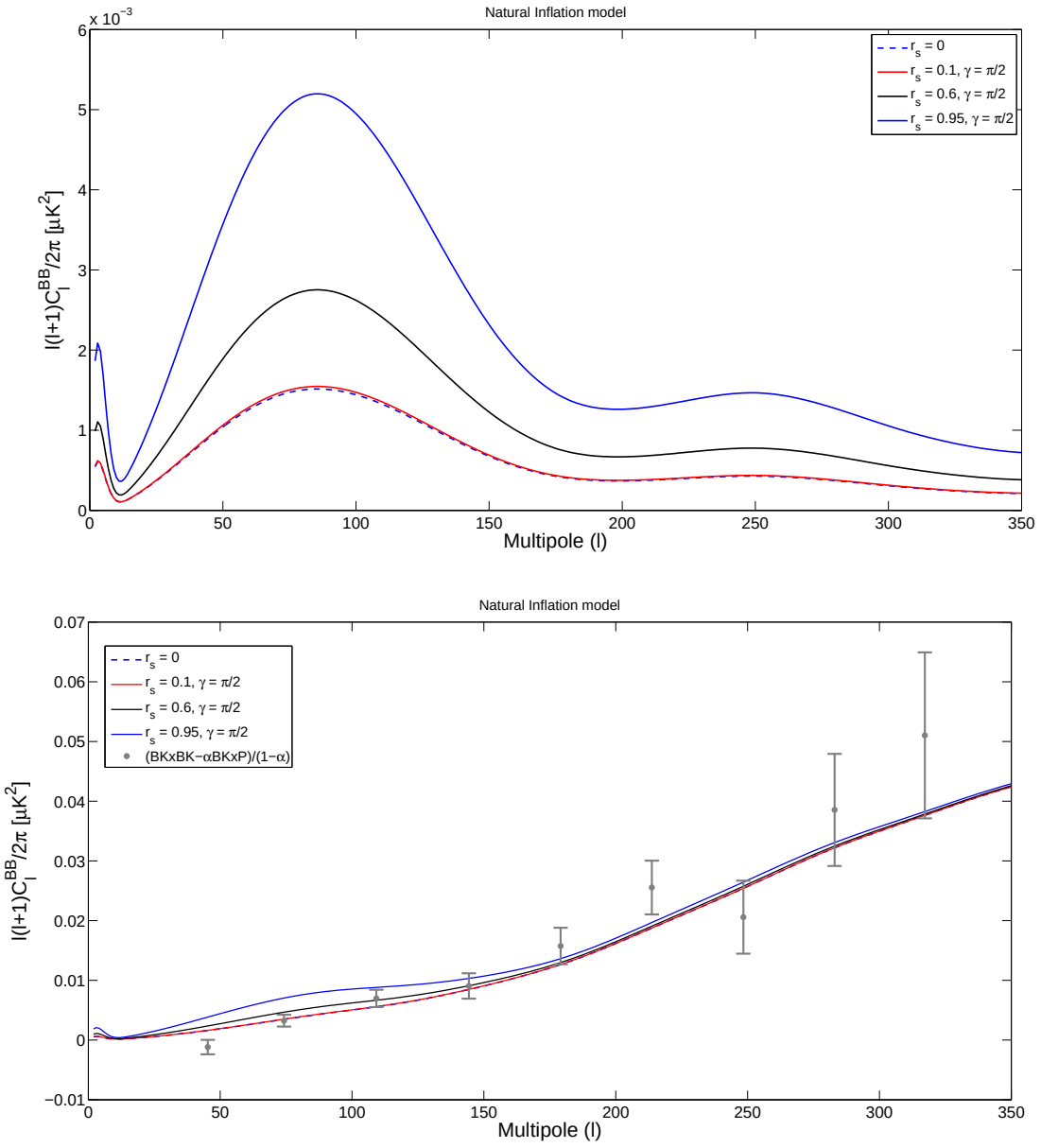

Figure 3.9: The BB-mode angular spectrum of CMB for the natural inflation model with unlensed (upper panel) and lensed (lower panel) effects for various values of squeezing parameters with the joint BKP data.

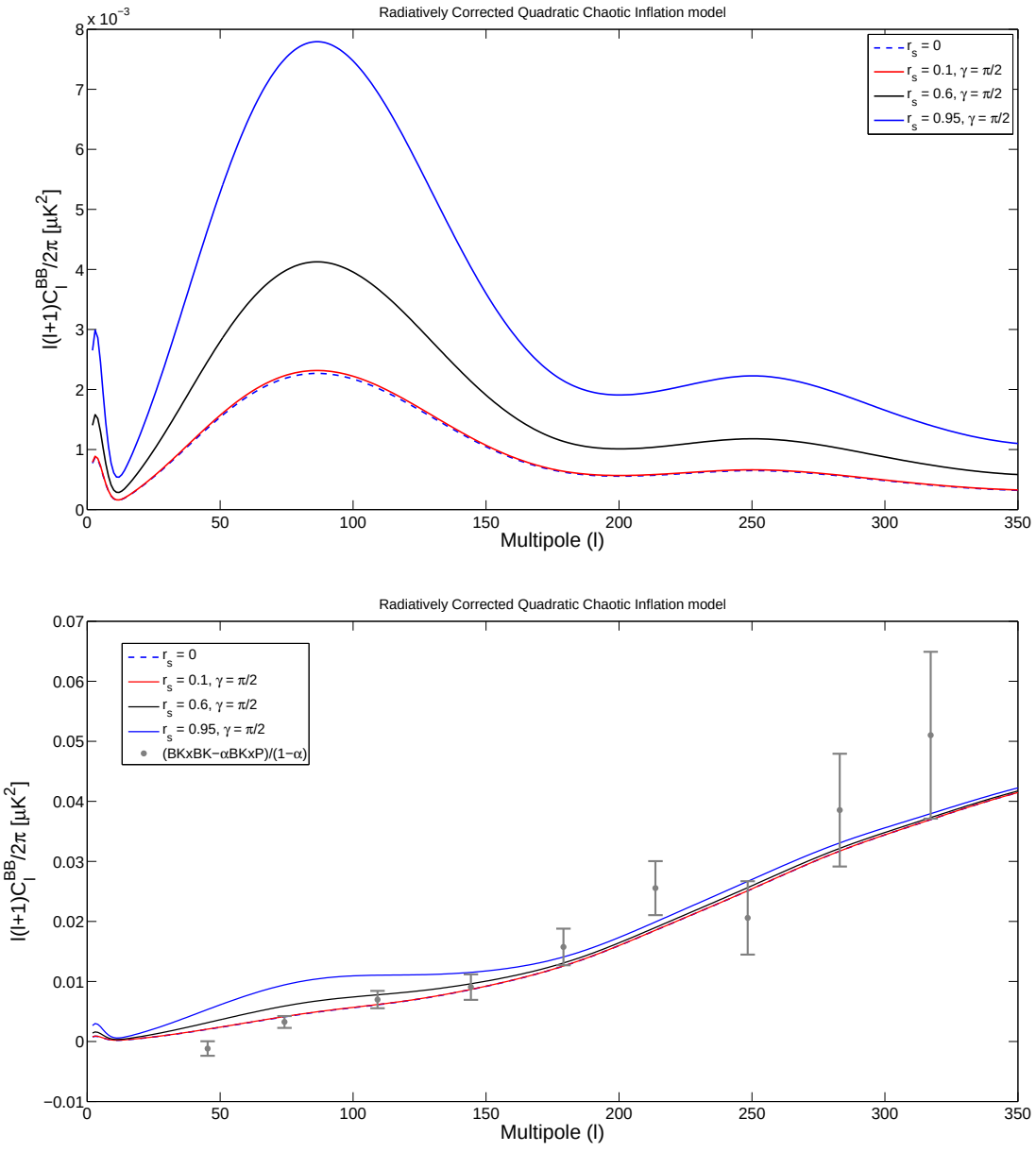

Figure 3.10: The BB-mode angular spectrum of CMB for the radiatively corrected quadratic chaotic inflation model with unlensed (upper panel) and lensed (lower panel) effects for various values of squeezing parameters with the joint BKP data.

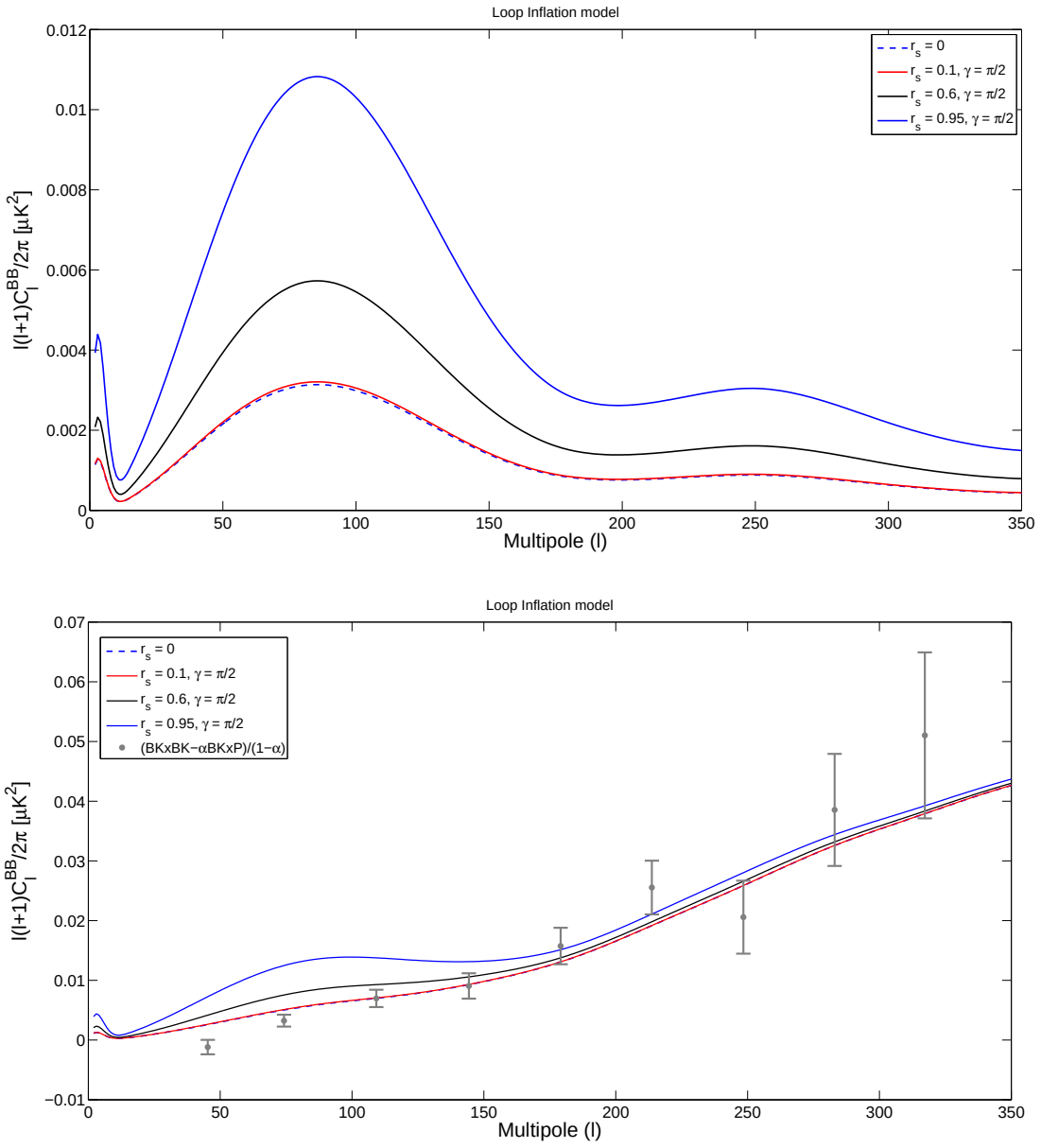

Figure 3.11: The BB-mode angular spectrum of CMB for the loop inflation model with unlensed (upper panel) and lensed (lower panel) effects for various values of squeezing parameters with the joint BKP data.

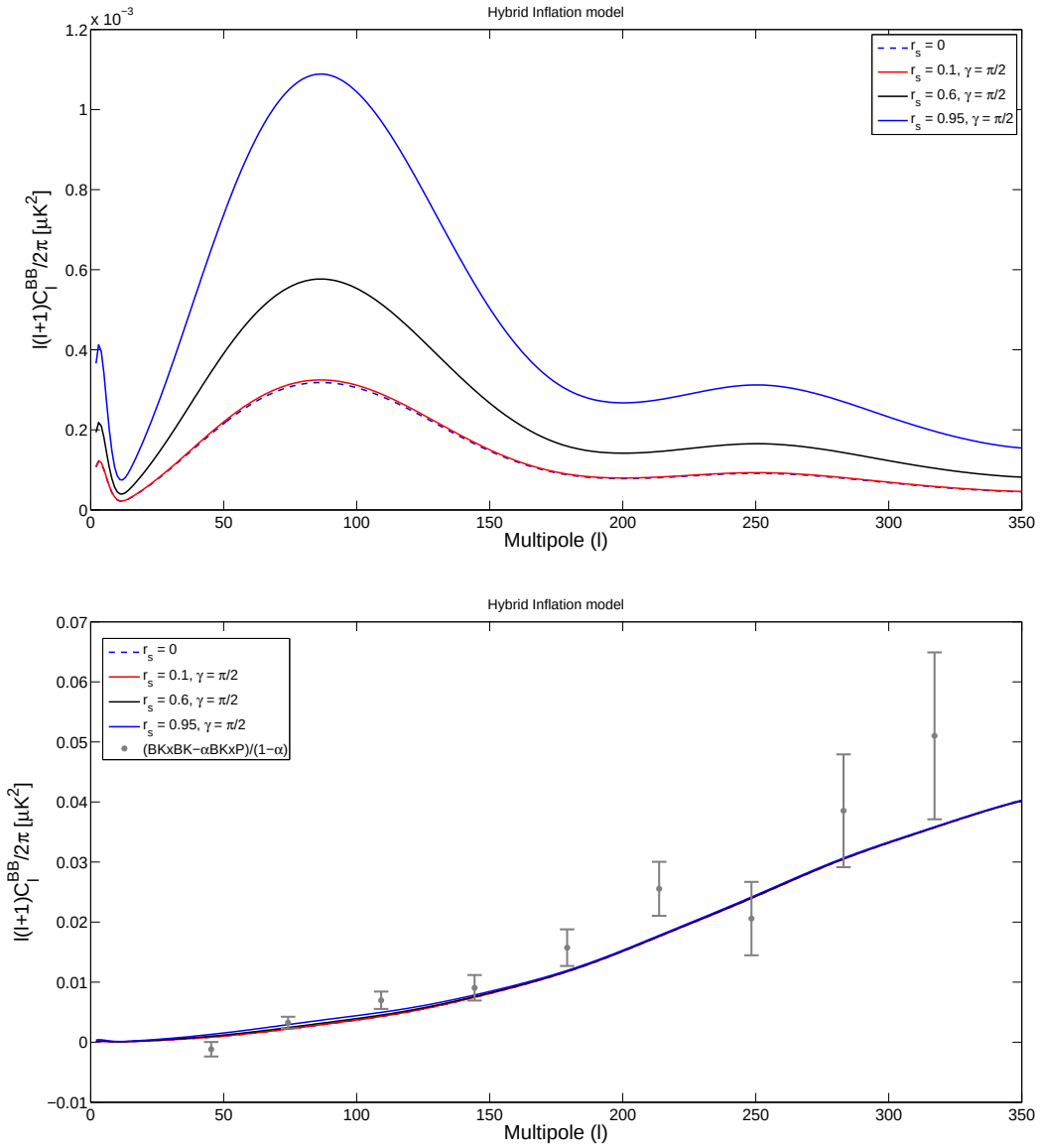

Figure 3.12: The BB-mode angular spectrum of CMB for the hybrid inflation model with unlensed (upper panel) and lensed (lower panel) effects for various values of squeezing parameters with the joint BKP data.

correlation spectra are obtained for several values of the squeezing parameter and squeezing angle. The estimated BB-mode spectrum of CMB for all the inflationa models are compared with the analysis data of the BICEP2/Keck Array at 150 GHz and Planck at 353 GHz collaboration where the limit is (BK x BK - α BK x P)/(1 - α) at the fiducial value $\alpha = \alpha_{fid} = 0.04$, taken after the elimination of the dust contribution in the BICEP2 band which is 0.04 times more than that in the Planck band.

The obtained CMB spectrum for B-mode auto-correlation by placing the primordial GWs in the squeezed vacuum state with various squeezing parameter values for unlensed and lensed cases are presented with the BKP collaboration data, for the quadratic chaotic inflation model in Fig.(3.1), for the quartic chaotic inflation model in Fig.(3.2), for the general Coleman-Weinberg inflation model in Fig.(3.3), for the new inflation model in Fig.(3.4), for the inverse monomial inflation model in Fig.(3.5), for the Higgs inflation model in Fig.(3.6), for the R2 inflation model in Fig.(3.7), for the arctan inflation model in Fig.(3.8), for the natural inflation model in Fig.(3.9), for the quadratic chaotic inflation model with radiative corrections in Fig.(3.10), for the loop inflation model in Fig.(3.11), and for the hybrid inflation model in Fig.(3.12).

The analysis of the results shows that the B-mode auto-correlation power spectrum of CMB with the primordial GWs in the squeezed vacuum state for the slow-roll inflation models like the Coleman-Weinberg, the R2, the Higgs, the inverse monomial and the hybrid inflation models are found to highly agree with the joint BKP data. On the other hand, the B-mode auto-correlation angular power spectrum of CMB corresponding to the natural inflation model, the loop, the arctan and the radiatively corrected quadratic chaotic inflation models are marginally favored by the BKP data with the squeezing effect on the primordial gravitational waves, hence these inflationary models are not ruled out. Further, it can be seen that in absence of the squeezing effect on the primordial gravitational waves, the BB-mode angular spectrum for these inflation models recover the power spectrum of the ordinary vacuum case.

Thus the study of the BB-mode angular power spectrum of CMB for various inflation models with the joint BKP data shows that the existence of the primordial GWs in the squeezed vacuum state cannot be ruled out with the current data.

3.5 BB-mode angular power spectrum of CMB in thermal vacuum state

Before the era of recombination, the universe was in a very hot and dense state filled with nuclei and a large number of free electrons in which no atom could form due to the extreme high temperature. In such a state, Thomson scattering occurred where the free electrons scattered the high energy photons, making the universe at that epoch effectively opaque to radiations and hence, thermalized. As the universe expanded, it eventually cooled down to a point where the nuclei and free electrons could combine to form a neutral hydrogen atom; the universe became transparent and the photons and other particles and radiation could travel long distances freely without getting obstructed. The light released at this time is what we perceive today and are called the cosmic microwave background. Among the thermalized particles which decoupled after the recombination were the gravitons. It is believed that due to these thermalized gravitons, there would occur stimulated emission process into the thermal background of gravitational waves which would amplify the tensor perturbations generated during inflation thus bringing about some change in the B-mode angular spectrum of the CMB by a temperature dependent factor [83]. Therefore, the thermal effect of the primordial gravitational waves can also be expected to reflect on the BB-mode correlation power spectrum of the CMB. Moreover, if the primordial GWs exist in the squeezed vacuum state, then the thermal and squeezing effects are expected to be reflected on the B-mode correlation angular spectrum of the CMB. Therefore it is interesting to study the combined effects of the thermal and squeezing of primordial gravitational waves on the B-mode correlation power spectrum for various slow-roll inflation models with the joint BKP data.

To study the thermal effect on the BB-mode correlation spectrum of the CMB, it is necessary to compute the angular spectrum in the thermal state. Time-dependent

thermal state can be described as [84, 85],

$$|0(\beta),\tau\rangle = \tilde{T}(\theta_k)|0,\tau\rangle, \tag{3.63}$$

where $\tilde{T}(\theta_k) = \exp[-\theta_k(\beta)\{\tilde{c}_k(\tau)c_k(\tau) - c_k^\dagger(\tau)\tilde{c}_k^\dagger(\tau)\}]$ is the thermal operator. The parameter $\theta(\beta)$ is temperature-dependent and can be defined through the following relations,

$$\begin{aligned} \cosh\theta_k(\beta) &= (1-e^{-\beta k})^{-\frac{1}{2}}, \\ \sinh\theta_k(\beta) &= e^{-\frac{\beta k}{2}}(1-e^{-\beta k})^{-\frac{1}{2}}, \end{aligned} \tag{3.64}$$

where $\beta = \frac{1}{T}$ and T is the associated temperature parameter.

Then according to the Bogoliubov transformation the annihilation operator in the Hilbert space and tilde space respectively becomes,

$$\begin{aligned} c_k(\beta,\tau) &= T(\theta)c_k T^\dagger(\theta) \\ &= c_k(\tau)\cosh\theta_k(\beta) + \tilde{c}_k^\dagger(\tau)\sinh\theta_k(\beta), \qquad (3.65) \\ \tilde{c}_k(\beta,\tau) &= T(\theta)\tilde{c}_k T^\dagger(\theta) \\ &= \tilde{c}_k(\tau)\cosh\theta_k(\beta) + c_k^\dagger(\tau)\sinh\theta_k(\beta). \qquad (3.66) \end{aligned}$$

The Hermitian conjugate of the above equations lead to the following equations for the creation operator in the Hilbert space and tilde space $c_k^\dagger(\beta,\tau)$ and $\tilde{c}_k^\dagger(\beta,\tau)$ respectively,

$$\begin{aligned} c_k^\dagger(\beta,\tau) &= T(\theta)c_k^\dagger T^\dagger(\theta) \\ &= c_k^\dagger(\tau)\cosh\theta_k(\beta) + \tilde{c}_k(\tau)\sinh\theta_k(\beta), \qquad (3.67) \\ \tilde{c}_k^\dagger(\beta,\tau) &= T(\theta)\tilde{c}_k^\dagger T^\dagger(\theta) \\ &= \tilde{c}_k^\dagger(\tau)\cosh\theta_k(\beta) + c_k(\tau)\sinh\theta_k(\beta). \qquad (3.68) \end{aligned}$$

Consider the vacuum state, then the annihilation and creation operators in eq.(3.30) satisfy the following relations,

$$\begin{aligned} \langle c_k^\dagger c_{k'}\rangle &= \delta^3(\mathbf{k}-\mathbf{k}'), \qquad (3.69) \\ \langle c_k c_{k'}\rangle &= \langle c_k^\dagger c_{k'}^\dagger\rangle = 0. \qquad (3.70) \end{aligned}$$

Thereby using the above equations, eq.(3.69) modifies to [86],

$$\langle c_k^\dagger c_{k'} \rangle = \left(1 + \frac{2}{e^{\frac{k}{T}} - 1}\right) \delta^3(\mathbf{k} - \mathbf{k}'). \tag{3.71}$$

Hence using eqs.(3.30) and (3.71), the two point correlation for the primordial gravitational waves in thermal state is computed and hence comparing with the standard two point correlation (3.50), the power spectrum for primordial GWs in the thermal state can be written as,

$$P_T(k) = A_T(k_0) \left(\frac{k}{k_0}\right)^{n_T} \coth\left[\frac{k}{2T}\right], \tag{3.72}$$

where A_T is the normalization constant and k_0 is the tensor pivot wave number. Hence the power spectrum of primordial GWs in the combined squeezed and thermal states can be written as,

$$P_T(k) = A_T(k_0) \left(\frac{k}{k_0}\right)^{n_T} \left[1 + 2\sinh^2 r_s + \sinh 2r_s \cos\left(\gamma + (2 - n_T)\frac{\pi}{2}\right)\right] \coth\left[\frac{k}{2T}\right]. \tag{3.73}$$

Note that when thermal effect is absent ($T = 0$), the power spectrum takes its form in the squeezed vacuum state. Further, the tensor power spectrum in the ordinary vacuum state can be recovered in absence of the thermal and squeezing effects.

By substituting the expression for the tensor power spectrum in the combined thermal and squeezing states, eq.(3.73) in eq.(3.62), the B-mode correlation spectrum for various values of the squeezing parameters and temperature parameter with various slow-roll inflation models can be computed. The BB-mode angular spectrum for various inflationary models are obtained with the CAMB code with corresponding initial value of the tensor power spectrum and tensor spectral index. The optical depth value is taken to be $\kappa = 0.08$, and the tensor and scalar pivot wave numbers are respectively taken to be 0.002 Mpc^{-1} and 0.05 Mpc^{-1}.

The obtained lensed BB-mode correlation power spectrum of CMB by considering the primordial GWs in the combined thermal and squeezed states for all the slow-roll inflationary models are analyzed and compared with the collaboration data of BICEP2/Keck Array at 150 GHz and Planck at 353 GHz where the limit is (BK x BK - α BK x P)/(1 - α) at the fiducial value $\alpha = \alpha_{fid} = 0.04$, evaluated by elim-

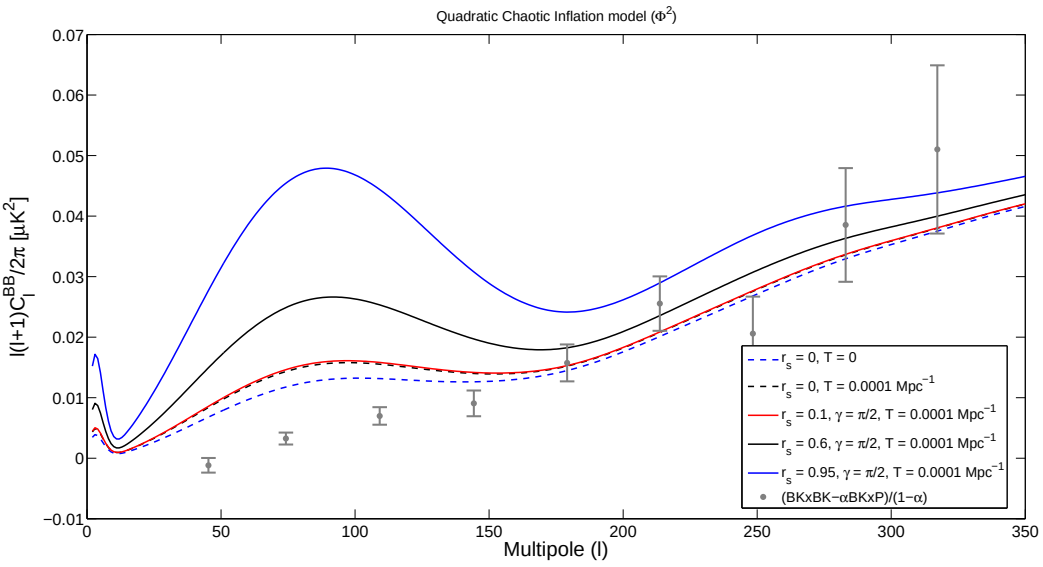

Figure 3.13: The BB-mode angular spectrum of CMB for the quadratic chaotic inflation model with lensing effect for the various values of squeezing parameters and thermal effect with the joint BKP data.

inating the dust contribution in the BICEP2 band which is 0.04 times more than that in the Planck band.

The resulting BB-mode spectrum of CMB with various values of the squeezing parameters with lensing effects are presented with the BKP joint data, for the quadratic chaotic inflation model in Fig.(3.13), for the quartic chaotic inflation model in Fig.(3.14), for the general Coleman-Weinberg inflation model in Fig.(3.15), for the new inflation model in Fig.(3.16), for the inverse monomial inflation model in Fig.(3.17), for the Higgs inflation model in Fig.(3.18), for the R2 inflation model in Fig.(3.19), for the arctan inflation model in Fig.(3.20), for the natural inflation model in Fig.(3.21), for the quadratic chaotic inflation model with radiative corrections in Fig.(3.22), for the loop inflation model in Fig.(3.23) and for the hybrid inflation model in Fig.(3.24).

The study of the BB-mode correlation spectrum of CMB by considering the primordial GWs in the thermal and squeezed vacuum states for various slow-roll inflation models with the joint BKP data shows that the power level of the BB-mode angular power spectrum increases due to the quantum and thermal effects. Note that from the initial vacuum state upto the end of the inflationary period, the squeezing

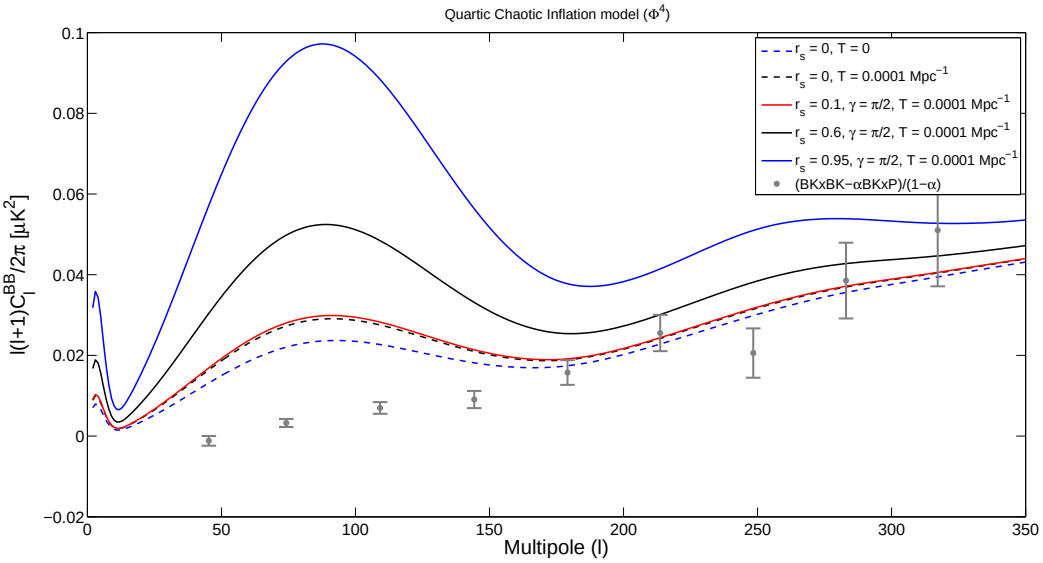

Figure 3.14: The BB-mode angular spectrum of CMB for the quartic chaotic inflation model with lensing effect for various values of squeezing parameter and thermal effect with the joint BKP data.

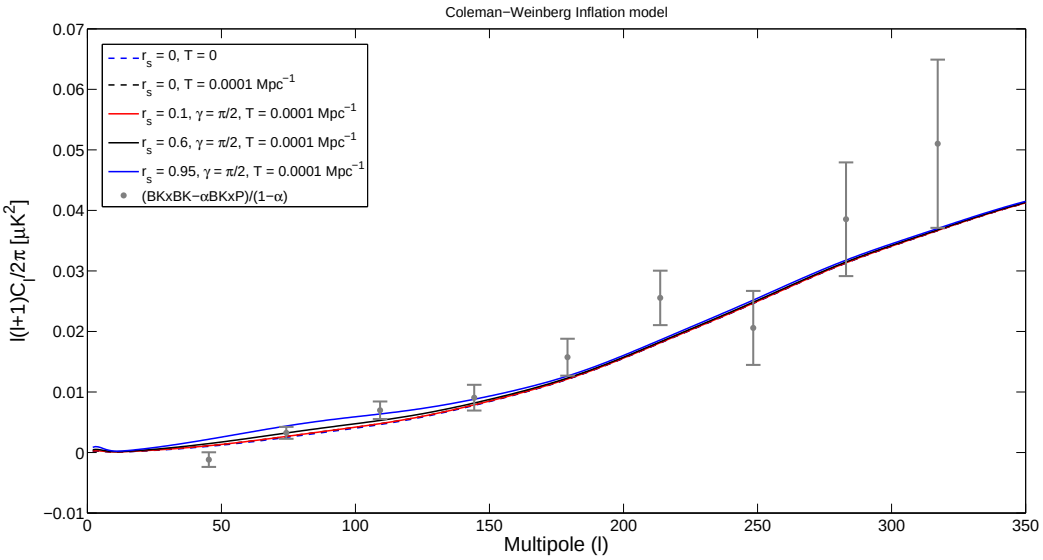

Figure 3.15: The BB-mode angular spectrum of CMB for the Coleman-Weinberg inflation model with lensing effect for various values of squeezing parameter and thermal effect with the joint BKP data.

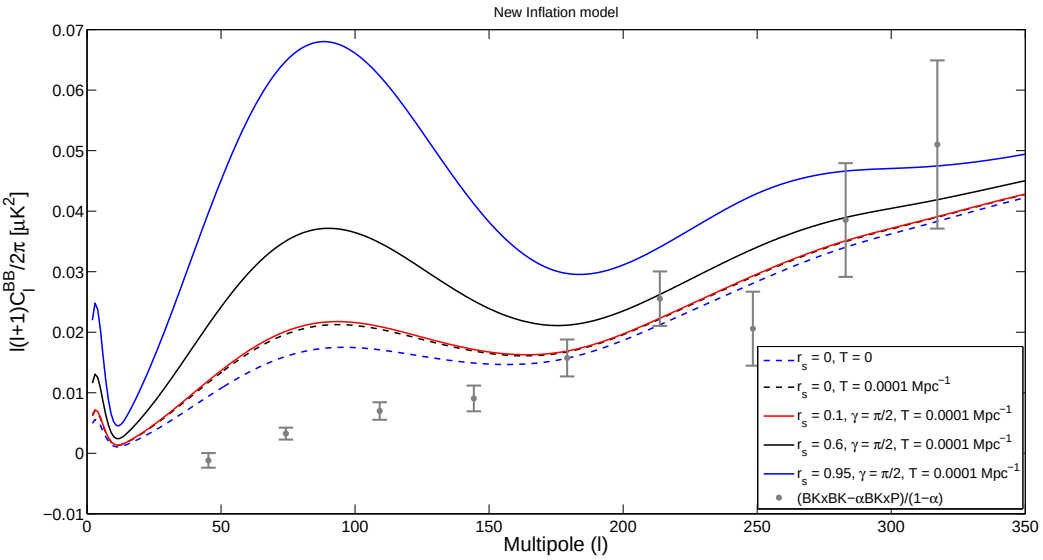

Figure 3.16: The BB-mode angular spectrum of CMB for the new inflation model with lensing effect for various values of squeezing parameter and thermal effect with the joint BKP data.

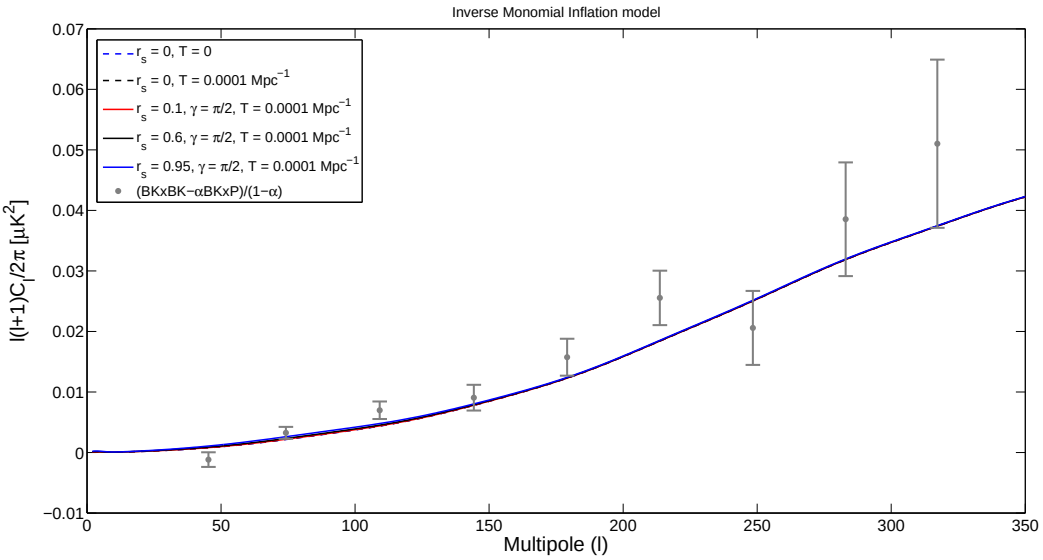

Figure 3.17: The BB-mode angular spectrum of CMB for the inverse monomial inflation model with lensing effect for various values of squeezing parameter and thermal effect with the joint BKP data.

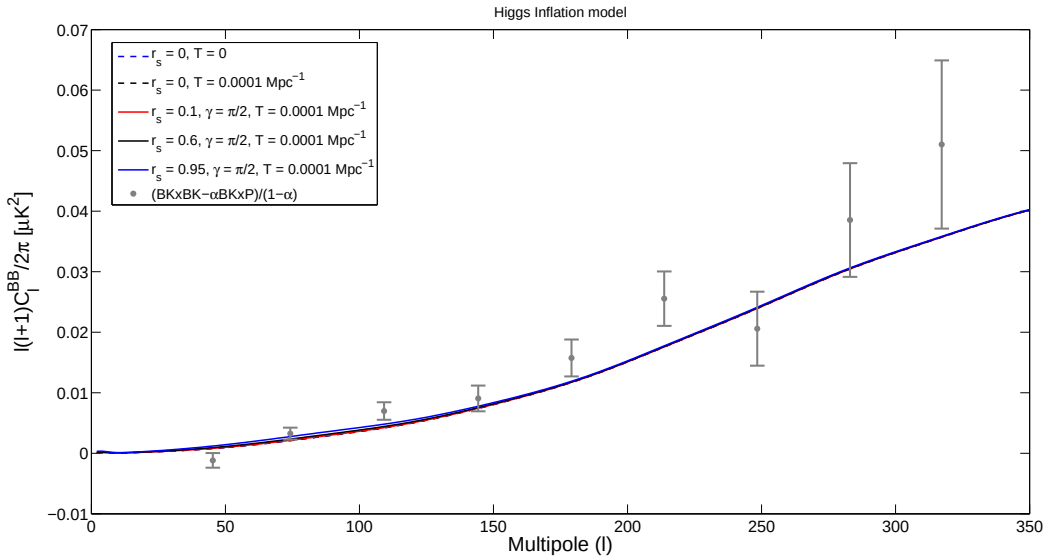

Figure 3.18: The BB-mode angular spectrum of CMB for the Higgs inflation model with lensing effect for various values of squeezing parameter and thermal effect with the joint BKP data.

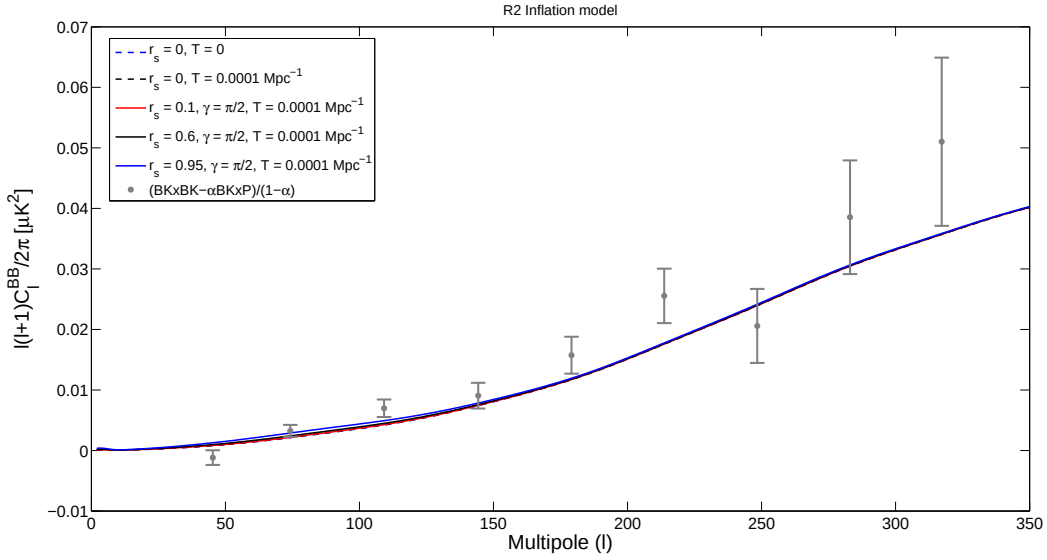

Figure 3.19: The BB-mode angular spectrum of CMB for the R2 inflation model with lensing effect for various values of squeezing parameter and thermal effect with the joint BKP data.

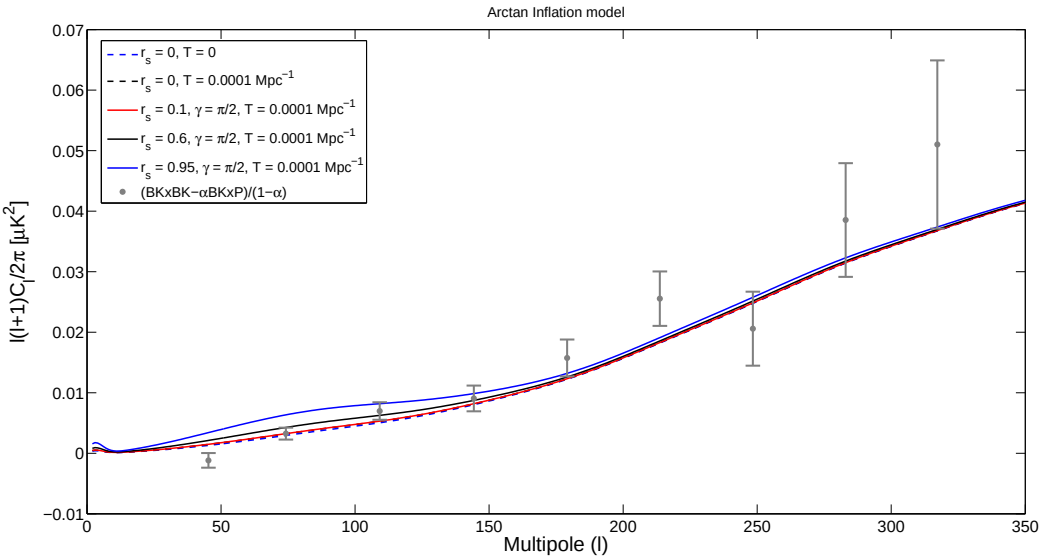

Figure 3.20: The BB-mode angular spectrum of CMB for the arctan inflation model with lensing effect for various values of squeezing parameter and thermal effect with the joint BKP data.

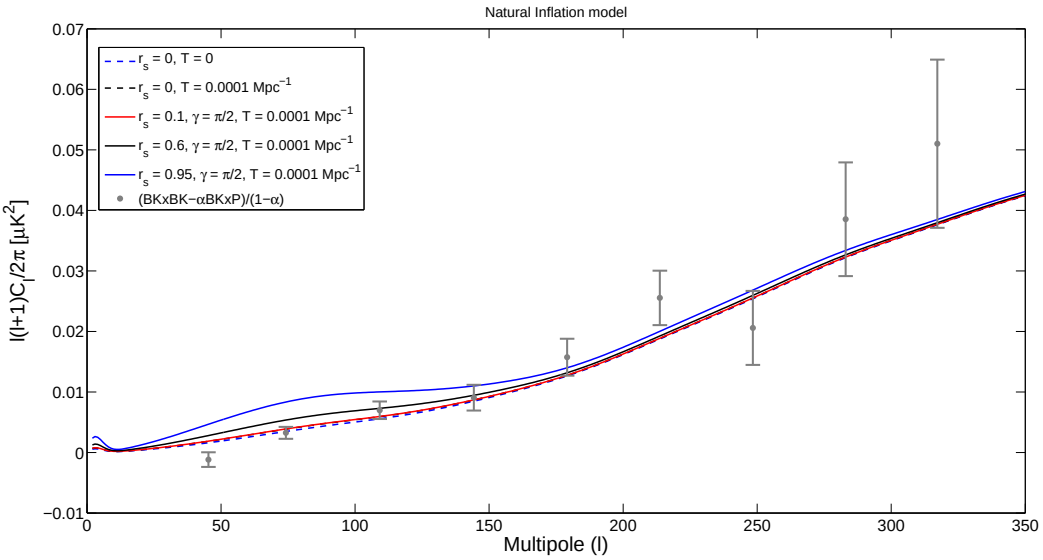

Figure 3.21: The BB-mode angular spectrum of CMB for the natural inflation model with lensing effect for various values of squeezing parameter and thermal effect with the joint BKP data.

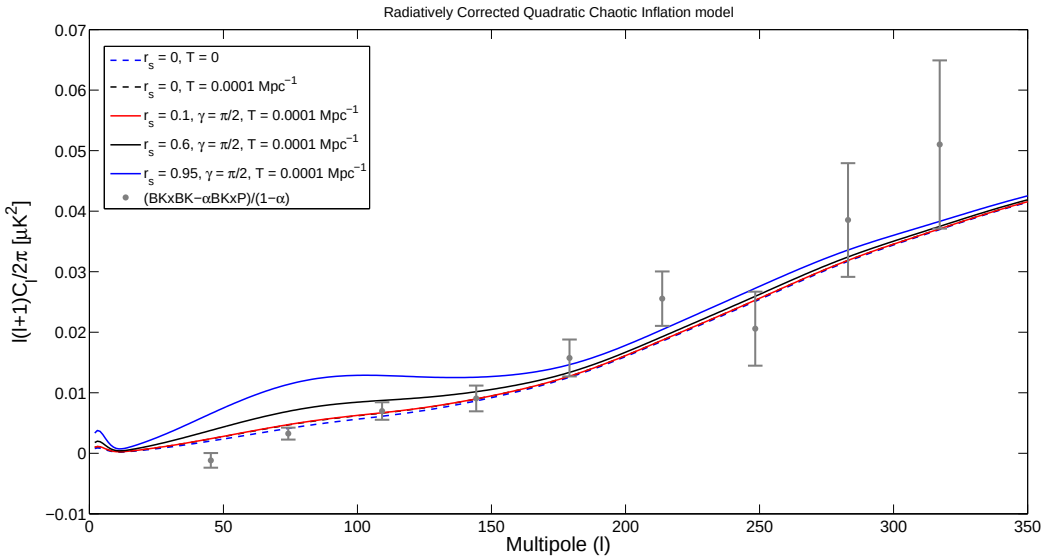

Figure 3.22: The BB-mode angular spectrum of CMB for the radiatively corrected quadratic chaotic inflation model with lensing effect for various values of squeezing parameter and thermal effect with the joint BKP data.

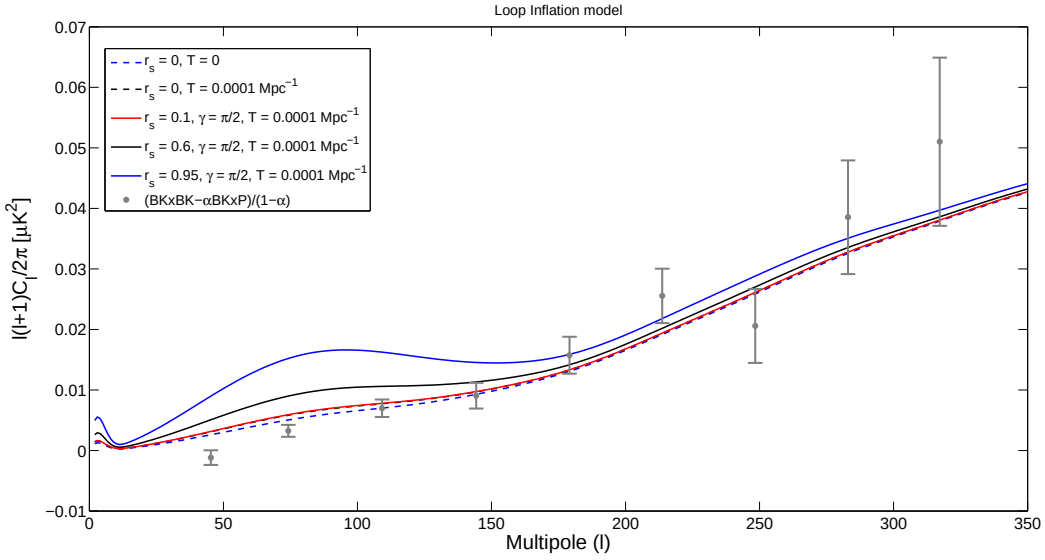

Figure 3.23: The BB-mode angular spectrum of CMB for the loop inflation model with lensing effect for various values of squeezing parameter and thermal effect with the joint BKP data.

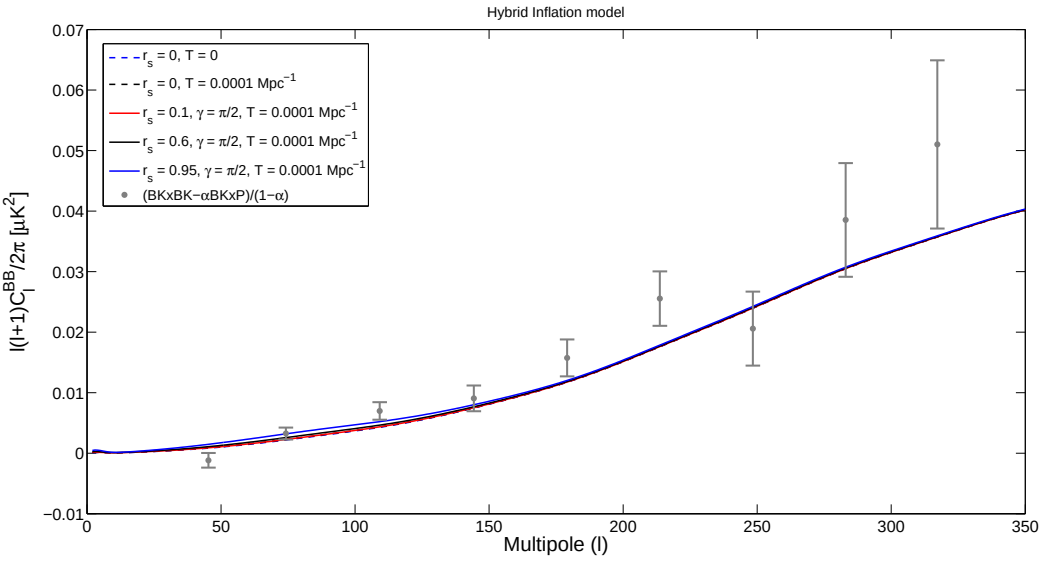

Figure 3.24: The BB-mode angular spectrum of CMB for the hybrid inflation model with lensing effect for various values of squeezing parameter and thermal effect with the joint BKP data.

parameter has gone from $r_s = 0$ to $r_s = 1$ [56], hence the squeezing parameters have been chosen to reflect this increase during this period. It can be seen that for the chosen squeezing parameters, the BB-mode correlation angular spectrum for the quadratic chaotic inflation model, the quartic chaotic inflation model and the new inflation model with the thermal and squeezing effects are out of the limit of the joint BKP data, hence these models are not favorable while the angular spectrum of CMB for various values of squeezing parameters and with thermal effect for the hybrid inflation model, which is a multi-field inflation model is found within the limit. The rest of the models with the combined thermal and squeezing effects are also found to be within the limit and are either highly or moderately favored by the current data.

3.6 Discussions

We have studied the BB-mode correlation angular power spectrum of CMB for several slow-roll inflation models by placing the primordial GWs in the thermal and squeezed vacuum states and the resulting angular power spectra are compared with the recent joint analysis result from BICEP2/Keck Array at 150 GHz and Planck

at 353 GHz data. Note that in this study, the anisotropy due to lensing (which smooths out the acoustic peaks at intermediate to smaller angular scales of the power spectrum) is included in correspondence with the data given by the used analysis data. The estimate limit on the B-mode auto-correlation spectrum of CMB data has been calculated from the power spectra of the TT and TE cross-correlations of the CMB. From the analysis of the present study, the potential existence of the primordial gravitational waves in the thermal and/or squeezed vacuum states is not ruled out. Further, it has been observed that there is increase in power level due to both thermal and squeezing effects. It can also be seen that squeezing effect would provide a helpful platform in constraining the inflation models. Note that at smaller angular scale, i.e., at higher multipoles, angular power spectrum is contaminated due to the lensing effect where the E-mode is converted into B-mode, hence the angular power spectrum at higher multipoles is ignored for the analysis. It can be observed that for each inflation model, with increase in squeezing parameter, power level of the angular power spectrum also increases. It can also be observed that larger the deviation from scale invariance, stronger is the squeezing effect, i.e., squeezing effect is more prominent in inflation models with larger values of tensor-to-scalar ratio and smaller values of tensor spectral index. The squeezing parameters used in the present study and analysis are the expected values during the inflationary period. Hence, the effect of squeezing offers a useful constraint on inflation models using the limit from the recent data.

In the present BB-mode angular power spectrum of CMB study, we considered single as well as multiple field slow-roll inflationary models. From the analysis of the results of the work for various inflation models with B-mode auto correlation angular spectrum of CMB with joint data of the BICEP2/Keck Array and Planck mission, neither single nor multi-field inflation models are ruled out completely. Thus the issue of single field inflation model vs multiple field inflation model is found unsolved with the present study of the BB-mode auto-correlation power spectrum of CMB.

Chapter 4

Primordial Massive Gravitational Waves and BB mode of CMB

According to the general theory of relativity, gravitational waves propagate with the speed of light in the free space, hence a quanta of gravitational field called the graviton, a spin-2 particle which mediates the force of gravitation is expected to be massless. However, starting from the idea of an arbitrary spin-2 field with non-zero mass in a flat spacetime proposed by Fierz and Pauli in the 1930s [87], the theory of massive gravity has gained a lot of interest and has been studied enormously, and a consistent theory involving graviton with non-zero mass could be a viable alternative theory to the general relativity theory as introduction of mass term produces modification to the latter. It has been suggested that if graviton does have mass and if the mass is comparable to the Hubble parameter, then at cosmological distances, it would provide repulsive effect which could lead to late time cosmic acceleration, thereby suggesting that instead of the dark energy being responsible for the accelerating expansion of the universe, massive gravity might be responsible for the current accelerating stage of the universe [88, 89]. The theory of general relativity is an established one with countless successes and finding a consistent theory which could stand as an alternative or modification to it poses a big challenge, and the theory of massive gravity is no exception.

The graviton, when massless, has two tensor modes (spin-2). However, when endowed with mass, it acquires five polarization modes with two additional vector

modes (spin-1) and a scalar mode (spin-0) apart from the already present two tensor modes. For the general graviton mass parameters, the theory possesses a negative kinetic energy called ghost mode which leads to instabilities [90]. The mass parameters were then carefully tuned such that the ghost mode no longer appears in the theory and were then called the Fierz-Pauli mass terms. However, on switching from the massive to massless limit, the vector modes are separated from the tensor modes but the scalar mode retains a strong coupling to the trace of energy-momentum tensor which causes a discontinuity called the van Dam-Veltman-Zakharov (vDVZ) discontinuity which prevents reproduction of general relativity theory [91, 92]. A non-linear treatment of these degrees of freedom to free the massive gravity theory of the vDVZ discontinuity was developed by Vainshtein [93], but it was later shown by Boulware and Deser (BD) that this non-linear treatment of the Fierz-Pauli theory reintroduces the ghost mode, called the BD ghost [90]. Since then, several theories have been proposed to acquire a consistent theory of massive gravity free from all these pathologies. One of these theories is the de Rham-Gabadadze-Tolley (dRGT) theory which is fully non-linear and has the capability of completely eliminating the ghost mode in the decoupling limit using higher order corrections [94, 95]. This theory has been proved and improved by Hassan and Rosen [96]. However, in this theory, neither flat nor closed FLRW cosmological solutions do not exist unless one violates the cosmological principle, i.e., the notion of a homogeneous and isotropic universe on large scales. To avoid this, more theories which could accommodate the notion of open universes with self-acceleration and one which allows closed/flat/open FLRW universes, both proposed by Gumrukcuoglu, Lin and Mukohyama [97, 98, 99] and the minimal theory of massive gravity proposed by De Felice and Mukohyama [100, 101] have been put forward to provide a non-linear completion of dRGT theory which, at the same time accommodates the cosmological principle. Another potentially consistent theory involves the spontaneous breaking of Lorentz invariance which results in the graviton acquiring mass. The Lorentz violating massive gravity admits the FLRW cosmological solution and has been studied extensively and shown to be free of pathologies like ghosts, instabilities and the vDVZ discontinuity [102, 103, 104].

While attempts have been made to construct a consistent theory of massive gravity which can evade all pathologies, several attempts have also been made to constrain the mass of graviton. Most of these bounds on the mass of graviton come from astrophysical observations while a couple are from theoretical and phenomenological studies. The estimate bounds on the mass of graviton vary widely. From the analysis of coupling between bound galaxy clusters, the upper bound for the graviton mass has been estimated to be 2×10^{-62} g ($m_{gw} < 10^{-29}$ eV) at the graviton's Compton wavelength $\lambda_g > 10^{19}$ km [105] and from the analysis of the dynamics of the solar system, the estimated upper limit for graviton mass is 7.68×10^{-55} g ($m_{gw} < 7.2 \times 10^{-23}$ eV) at $\lambda_g > 2.8 \times 10^{12}$ km [106]. The observations of stellar-mass compact inspiral using ground based interferometers and that of supermassive black hole binary inspiral using space based interferometer bounded the upper limit for graviton mass to be 3.678×10^{-62} g and 3.678×10^{-65} g respectively [107]. From the parameters of expansion of the universe, the upper limit on the mass of the graviton has been calculated to be 4.5×10^{-66} g [108]. The observations of the orbital decay of the binary systems of pulsars PSR B1913+16 and PSR B1534+12, bounded the upper limit for graviton mass to be 1.4×10^{-52} g ($m_{gw} < 7.6 \times 10^{-20}$ eV) at $\lambda_g > 6.6 \times 10^8$ km [109]. From the comparison of the times of arrival of gravitational waves and optical light from white dwarf binaries, graviton mass has been estimated to be less than 10^{-56} g ($m_{gw} < 6 \times 10^{-24}$ eV) [110]. Phenomenological approach estimates the mass of graviton to be approximately 2.0432×10^{-72} g by using fundamental constants [111]. From the first direct observation of gravitational waves GW150914 originating from black hole mergers, assuming a modified dispersion relation for these waves, calculation for the bound on the mass of graviton yields $m_{gw} < 1.2 \times 10^{-22}$ eV at the graviton Compton wavelength $\lambda_g > 4.2 \times 10^{11}$ km [112]. In the de Sitter background, provided that the kinetic term for the scalar cosmological perturbations is positive definite, the Higuchi bound sets an absolute lower bound on the graviton mass as $m_{gw}^2 \geq 2H^2$ [113]. Massive graviton is also expected to affect the primordial gravitational waves and the bound for the mass of primordial graviton has been estimated from the exponential decay of the Yukawa potential which puts the mass to be $m_{gw} < 10^{-30}$ eV at $\lambda_g > 10^{20}$ km [104, 114]. The lower bound for primordial graviton mass has also been calculated to be about

10^{-32} eV [115, 116]. If the graviton indeed has mass, then this mass, however small it may be, is expected to have an observable effect on the B-mode polarization of the CMB anisotropy spectrum [114, 117].

The present work is based on the Lorentz violating massive gravity theory to study the effect of massive primordial gravitational waves on the BB-mode correlation angular power spectrum of CMB with the recent analysis data of Planck and BICEP2/Keck Array collaboration for several slow-roll inflation models. The work also aims to constrain the mass of the primordial GWs from the BB-mode spectrum of CMB with the joint data of Planck and BICEP2/Keck Array.

4.1 Lorentz violating massive gravity

The Lorentz violating massive gravity theory considers the modification of general relativity by graviton mass terms which break the Lorentz invariance about the flat spacetime. These mass terms are different from both the general graviton mass terms for which the theory possesses ghosts and the Fierz-Pauli mass terms for which the theory is free of ghost mode but suffer from vDVZ discontinuity. For the Lorentz-violating massive gravity, the ghost instability and the vDVZ discontinuity can be evaded such that the theory can switch from massive to massless limit without discontinuity.

The action for the Lorentz violating massive gravity model is given by [103, 104],

$$S = \int d^4x\sqrt{-g}[-m_{pl}^2 R + \Lambda^4 F(Z^{ij})], \tag{4.1}$$

which is a linear combination of the Einstein-Hilbert action and the Goldstone action respectively, F is a function of the Goldstone field, metric components and its derivatives, the parameter Λ characterizes the cutoff energy scale for low energy effective theory. The Goldstone field leads to spontaneous breaking of the Lorentz symmetry. Ordinary matter field is assumed to have minimal coupling with gravity.

The action depends on the Goldstone field derivatives through an argument Z^{ij},

which can be obtained with the help of the following expressions,

$$\begin{aligned} Z^{ij} &= X^q W^{ij}, \\ X &= \Lambda^{-4} g^{\alpha\beta} \partial_\alpha \zeta^0 \partial_\beta \Phi^0, \\ W^{ij} &= \Lambda^{-4} g^{\alpha\beta} \partial_\alpha \Phi^i \partial_\beta \Phi^j - \frac{V^i V^j}{X}, \\ V^i &= \Lambda^{-4} g^{\alpha\beta} \partial_\alpha \Phi^0 \partial_\beta \Phi^i, \end{aligned} \tag{4.2}$$

which ensures the non-pathological behavior (absence of rapid instabilities and ghosts) of the perturbations about the vacuum solutions; $\Phi^0(x)$, $\Phi^i(x)$, $(i = 1, 2, 3)$ are the four scalar fields and q is considered as a constant free parameter.

After setting the Goldstone fields to their vacuum values, the vacuum solutions corresponding to the flat FLRW metric can be written as

$$\begin{aligned} g_{\alpha\beta} &= a^2 \eta_{\alpha\beta}, \\ \Phi^0 &= \Lambda^2 t, \\ \Phi^i &= \Lambda^2 x^i. \end{aligned} \tag{4.3}$$

where $\eta_{\alpha\beta}$ is the flat space metric.

The metric $g_{\alpha\beta}$ with perturbations can be written as

$$g_{\alpha\beta} = a^2 \eta_{\alpha\beta} + \delta g_{\alpha\beta}, \tag{4.4}$$

where the metric perturbations $\delta g_{\alpha\beta}$ are considered as perturbations about the Minkowski background metric and are taken after the spontaneous Lorentz symmetry breaking, and they can be separated into the components of the scalar, vector and tensor fields as given in eq.(1.38).

On substituting the vacuum solutions in eq.(4.3) and the decomposition of perturbation metric in eq.(1.38) into the action eq.(4.1), the Lagrangian becomes [118],

$$L_m = \frac{m_{pl}^2}{2}(m_0^2 h_{00} h_{00} + 2m_1^2 h_{0i} h_{0i} - m_2^2 h_{ij} h_{ij} + m_3^2 h_{ii} h_{jj} - 2m_4^2 h_{00} h_{ii}), \tag{4.5}$$

where $h_{\alpha\beta}$ correspond to perturbations about the Minkowski spacetime; the mass

parameters can be expressed in terms of the function F and its derivatives as,

$$\begin{aligned} m_0^2 &= \frac{\Lambda^4}{m_{pl}^2}[XF_X + 2X^2F_{XX}], \\ m_1^2 &= \frac{2\Lambda^4}{m_{pl}^2}[-XF_X - WF_W + \frac{1}{2}XWF_{VV}], \\ m_2^2 &= \frac{2\Lambda^4}{m_{pl}^2}[WF_W - 2W^2F_{WW2}], \\ m_3^2 &= \frac{\Lambda^4}{m_{pl}^2}[WF_W + 2W^2F_{WW1}], \\ m_4^2 &= -\frac{\Lambda^4}{m_{pl}^2}[XF_X + 2XWF_{XW}], \end{aligned} \tag{4.6}$$

where

$$\begin{aligned} W &= -1/3\delta_{ij}W^{ij}, \\ \frac{\partial F}{\partial X} &= F_X, \\ \frac{\partial^2 F}{\partial X^2} &= F_{XX}, \\ \frac{\partial F}{\partial W^{ij}} &= F_W\delta_{ij}, \\ \frac{\partial^2 F}{\partial V^i \partial V^j} &= F_{VV}\delta_{ij}, \\ \frac{\partial^2 F}{\partial W^{ij}\partial W^{kl}} &= F_{WW1}\delta_{ij}\delta_{kl} + F_{WW2}(\delta_{ik}\delta_{jl} + \delta_{ij}\delta_{jk}), \\ \frac{\partial^2 F}{\partial X \partial W^{ij}} &= F_{XW}\delta_{ij}. \end{aligned} \tag{4.7}$$

Using the decomposition of the perturbed metric given in eq.(1.38) into the mass Lagrangian in eq.(4.5), where $a^2 h_{\alpha\beta} = \delta g_{\alpha\beta}$, and in the Einstein-Hilbert Lagrangian and adding them, one gets for tensor field,

$$(\partial^\alpha \partial_\alpha + m_2^2)h_{ij} = 0, \tag{4.8}$$

which is the Klein-Gordon equation for a massive plane wave propagating in the $\hat{z} = \hat{\mathbf{k}}$ direction. In the massless limit, $m_2 = 0$, the above equation recovers the massless general relativity case. The mass parameter m_2 represents the graviton mass, a mass of helicity-2 mode. From now on, the graviton mass will be denoted by m_{gw} instead of m_2.

4.2 Primordial massive gravitational waves

The evolution of the primordial massive GW field $h_{ij}^{(m)}$ in the Fourier space is given by,

$$h_{ij}^{(m)\prime\prime}(\tau) + 2Hh_{ij}^{(m)\prime}(\tau) + k^2 h_{ij}^{(m)}(\tau) + a^2 m_{gw}^2 h_{ij}^{(m)}(\tau) = 0, \tag{4.9}$$

where the field in quantum language can be written in the Fourier space as,

$$\begin{aligned} h_{ij}^{(m)}(\mathbf{x},\tau) &= \frac{D}{(2\pi)^{\frac{3}{2}}}\int_{-\infty}^{\infty}\frac{d^3\mathbf{k}}{\sqrt{2E_k}}[h_{ij}^{(m)(p)}(\tau)c_{ij}^{(m)(p)}\varepsilon_{ij}^{(m)(p)}(\mathbf{k})e^{i\mathbf{k}.\mathbf{x}} \\ &\quad + h_{ij}^{(m)(p)*}(\tau)c_{ij}^{(m)(p)\dagger}\varepsilon_{ij}^{(m)(p)*}(\mathbf{k})e^{-i\mathbf{k}.\mathbf{x}}], \end{aligned} \tag{4.10}$$

where the normalization constant $D = \sqrt{16\pi}l_{pl}$, E_k is the energy of the mode, (p) is the polarization index and the superscript (m) stands for the massive gravitational waves.

The dynamical equation of motion for primordial massive GWs can then be written as,

$$h_k^{(m)\prime\prime}(\tau) + 2Hh_k^{(m)\prime}(\tau) + (k^2 + a^2 m_{gw}^2)h_k^{(m)}(\tau) = 0. \tag{4.11}$$

From here onwards, the polarization index (p) and the mass index (m) are dropped for notational convenience. Using the expression of the mode function in eq.(3.36), the equation of motion of the GWs in the FLRW universe can be described as,

$$\mu_k''(\tau) + \left(k^2 + a^2 m_{gw}^2 - \frac{a''}{a}\right)\mu_k(\tau) = 0, \tag{4.12}$$

where the dispersion relation can be written as

$$\frac{k^2}{a^2} + m_{gw}^2 = w^2, \tag{4.13}$$

and w is known as the effective frequency.

For the adiabatic vacuum, eq.(4.11) has the solution [119],

$$h_k(\eta) \propto e^{-iwa\tau}. \tag{4.14}$$

For super-horizon mode, $w^2 \ll H^2$, the mode stays outside the horizon and the tensor amplitudes are frozen; the mode remains constant and therefore its magnitude is,

$$|h_k| = \mathcal{A}(k), \quad \tau < \tau_k, \tag{4.15}$$

where $\mathcal{A}(k) = \frac{H_{ex}}{m_{pl}k^{3/2}}$ is the tensor mode amplitude which is evaluated at the time of its generation, H_{ex} is the rate of expansion during horizon exit and τ_k is the time of horizon re-entry.

Assume that the horizon re-entry takes place sufficiently rapidly at horizon crossing time $\tau \simeq \tau_k$, that is, when the effective frequency of the mode is comparable to the rate of cosmic expansion, $w^2 \simeq H^2$, the mode with comoving momentum k re-enters the horizon, then eq.(4.14) can be rewritten as

$$h_k(\tau) = \frac{\mathcal{C}(k)}{\sqrt{w_k a_k^3}} e^{-iwa\tau}, \qquad \tau \simeq \tau_k, \tag{4.16}$$

where $w_k \equiv w(\tau_k) = H_k$ indicates horizon re-entry.

With the expansion of the universe, the modes re-enter the horizon and are then called sub-horizon modes with $w^2 \gg H^2$. Once they enter the horizon, they oscillate and their amplitudes are no longer constant. Its solution can then be expressed with eq.(4.14):

$$h_k(\tau) = \frac{\mathcal{C}(k)}{\sqrt{w(\tau)a^3(\tau)}} e^{-iwa\tau}, \qquad \tau > \tau_k, \tag{4.17}$$

where $\mathcal{C}(k)$ is a constant of integration.

Using eq.(4.15), eq.(4.16) and eq.(4.17), we get

$$\frac{|h_k(\tau)|}{\mathcal{A}(k)} = \sqrt{\frac{w_k}{w(\tau)} \frac{a_k^3}{a^3(\tau)}}, \qquad \tau > \tau_k. \tag{4.18}$$

Replacing w by k/a and τ_k by τ_k^{GR}, the superscript GR indicating the massless GR case, we get the corresponding solution in the massless case as

$$\frac{|h_k^{GR}(\tau)|}{\mathcal{A}(k)} = \frac{a_k^{GR}}{a(\tau)}, \qquad \tau > \tau_k^{GR}. \tag{4.19}$$

The power spectrum for massive GWs is defined by the two-point correlation function which can be expressed in terms of effective frequency as

$$P(w_0) \equiv \frac{d}{d\ln w_0} \langle 0|h_{ij}(\mathbf{x},\tau)h^{ij}(\mathbf{x},\tau)|0\rangle, \tag{4.20}$$

where

$$\langle 0|h_{ij}(\mathbf{x},\tau)h^{ij}(\mathbf{x},\tau)|0\rangle = \frac{D^2}{2\pi^2}\int_0^\infty k^2 |h_k(\tau)|^2 \frac{dk}{k}. \tag{4.21}$$

Therefore one gets

$$P(w_0) = \frac{w_0^2}{w_0^2 - m_{gw,0}^2} \frac{2k^3}{\pi^2} |h_k(\tau_0)|^2, \tag{4.22}$$

where

$$k = a_0 \sqrt{w_0^2 - m_{gw,0}^2},$$
$$\frac{d}{d \ln w_0} \left(\frac{dk}{k} \right) = \frac{w_0^2}{w_0^2 - m_{gw,0}^2}.$$

Using eq.(4.18), the power spectrum for the massive GWs is obtained as

$$\begin{aligned} P(w_0) &= \frac{2k^3}{\pi^2} \mathcal{A}^2(k) \left(\frac{k' a_k}{k a_0} \right)^2 \frac{w_k a_k}{w_0 a_0} \\ &= \left(\frac{k' a_k}{k a_0} \right)^2 \frac{w_k a_k}{w_0 a_0} P(k), \end{aligned} \tag{4.23}$$

where $k' = a_0 w_0$ and $P(k) = \frac{2k^3}{\pi^2} \mathcal{A}^2(k)$ represents the initial power spectrum of the primordial GWs.

Using eq.(4.19), the power spectrum for the massless GW case can also be written as

$$P_{GR}(w_0) = \left(\frac{a_{k'}^{GR}}{a_0} \right)^2 P(k'). \tag{4.24}$$

By taking the ratio of eq.(4.23) to eq.(4.24), we obtain

$$\begin{aligned} \frac{P(w_0)}{P_{GR}(w_0)} &= \frac{P(k)}{P(k')} \left(\frac{k' a_k}{k a_{k'}^{GR}} \right)^2 \frac{w_k a_k}{w_0 a_0} \\ &= \frac{P(k)}{P(k')} S^2(w_0), \end{aligned} \tag{4.25}$$

where the enhancement factor $S(w_0)$ can be written as

$$S(w_0) = \frac{k' a_k}{k a_{k'}^{GR}} \sqrt{\frac{w_k a_k}{w_0 a_0}}. \tag{4.26}$$

During horizon re-entry, the mass term has become dominant, hence the corresponding dispersion relation can be written as,

$$w_k \simeq m_{gw}(\tau_k). \tag{4.27}$$

Horizon re-entry takes place simultaneously for all long wavelength modes provided the rate of cosmic expansion is comparable to the effective mass of the GWs,,

$$H(\tau_k) \simeq m_{gw}(\tau_k).$$

Therefore, we have $\tau_k \simeq \tau_{hc}$, $a_k \simeq a_{hc}$, $\mathcal{H}_k \simeq H$ and $w_{hc} \simeq m_{gw}(\tau_{hc}) = \frac{k_{hc}}{a_{hc}}$. Hence, it can be assumed that the mass is a growing function of time, and further considering that the mass term dominates the effective frequency till present time,

$$w_0 \simeq m_{gw,0} \equiv m_{gw} = \frac{k_0}{a_0},$$
$$k' \simeq k_0.$$

For long wavelength modes, the enhancement factor becomes

$$S(w_0) \simeq \frac{a_{hc}}{a_{k_0}^{GR}} \sqrt{\frac{k_{hc}}{k_0}} \left(\frac{w_0^2}{m_{gw}^2} - 1 \right)^{-\frac{1}{2}}. \tag{4.28}$$

The short wavelength modes with non-zero mass have enhancement factor close to unity and hence their behavior is almost indistinguishable from their massless counterparts and therefore, they are not considered in the present study.

4.3 BB-mode spectrum of CMB and mass constraint of primordial GWs

This section is to study the B-mode auto-correlation power spectrum of the CMB for the massive primordial GWs for several slow-roll inflation models namely the R2 inflation model, the arctan inflation model, the Higgs inflation model, the inverse monomial inflation model, the loop inflation model and the hybrid inflation model with the joint analysis data BICEP2/Keck Array and Planck mission and hence to get bound on the primordial graviton mass. The power spectrum for the massive primordial GWs can be written as

$$P_T(k) = A_T(k_0) \left(\frac{k}{k_0} \right)^{n_T} S^2(w_o). \tag{4.29}$$

where $A_T(k_0)$ is the normalization constant, $S(w_o)$ is the enhancement factor given by eq.(4.28), k_0 denotes the tensor pivot wave number and n_T denotes the tensor spectral index, which depends on the effective potential of each inflation model. It can be noted that the tensor power spectrum for the massive primordial GWs differ from the massless case only by the enhancement factor.

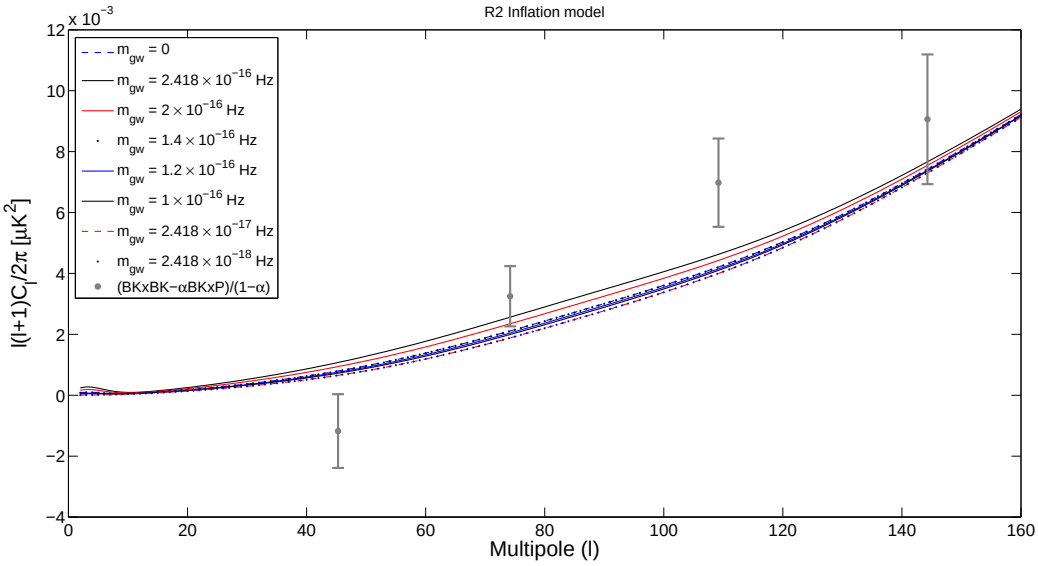

Figure 4.1: The BB-mode correlation angular spectrum of CMB for the Starobinsky (R2) inflation model ($n_T = -4.06 \times 10^{-4}$) for various values of graviton mass with the joint BKP data.

Using eq.(4.29) and eq.(3.62), the BB-mode correlation power spectrum can be computed and generated for the inflation models under the present study. The B-mode auto-correlation spectrum of CMB is generated for each inflation model with the help of CAMB code by taking the initial value of the tensor power spectrum, tensor spectral index and the tensor-to-scalar ratio corresponding to each model computed in Chapter 3 and also by using the value of the tensor pivot scale as $k_0 = 0.002$ Mpc^{-1} and the scalar pivot wave number as $k_* = 0.05$ Mpc^{-1}.

The obtained lensed BB-mode power spectrum of CMB for the primordial massive GWs with the aforementioned slow-roll inflationary models are compared with the joint data of BICEP2/Keck Array at 150 GHz and Planck at 353 GHz, where the limit is (BK x BK - α BK x P)/(1 - α) at the fiducial value $\alpha = \alpha_{fid} = 0.04$, evaluated after the elimination of the dust contribution in the BICEP2 band which is 0.04 times more than that in the Planck band.

The resulting lensed BB-mode angular spectrum of CMB for the primordial massive GWs are presented for the R2 inflation model shown in Fig.(4.1), the arctan inflation model in Fig.(4.2), the Higgs inflation model in Fig.(4.3), the inverse monomial inflation model in Fig.(4.4), the loop inflation model shown in Fig.(4.5) and the

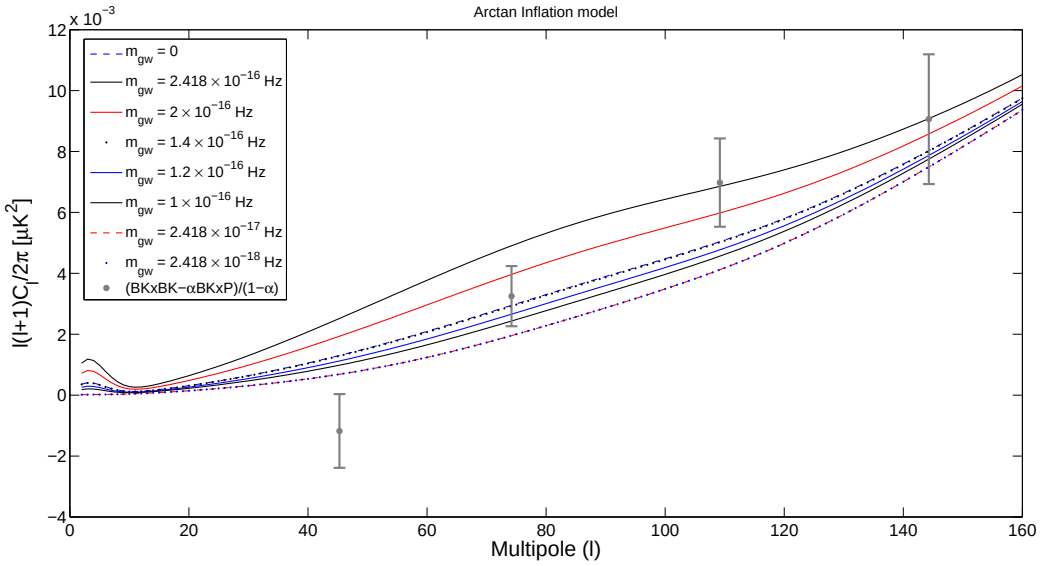

Figure 4.2: The lensed BB-mode correlation angular spectrum of CMB for the arctan inflation model ($n_T = -1.72 \times 10^{-3}$) for various values of graviton mass with the joint BKP data.

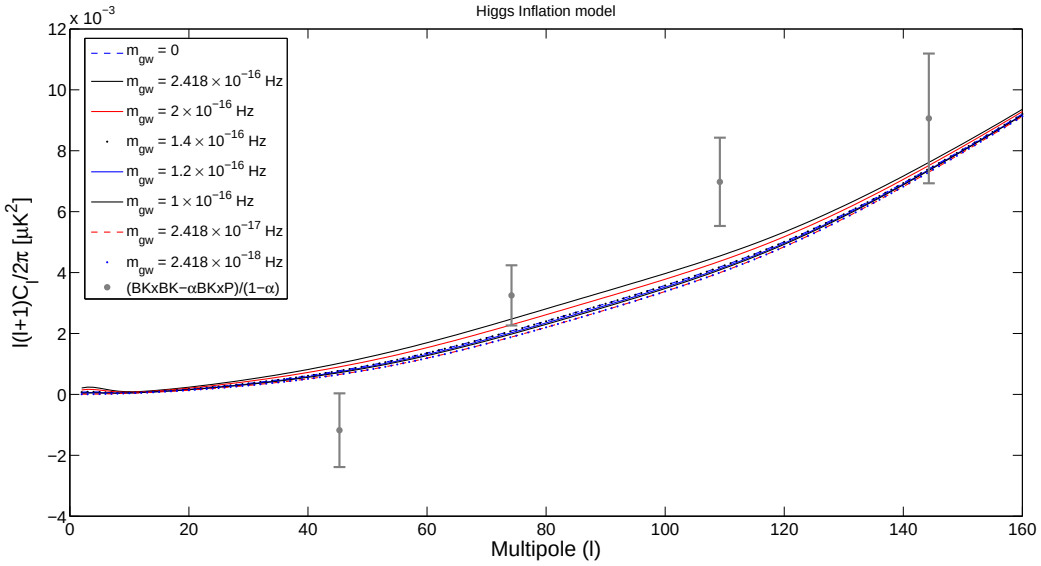

Figure 4.3: The lensed BB-mode correlation angular spectrum of CMB for the Higgs inflation model ($n_T = -3.53 \times 10^{-4}$) for various values of graviton mass with the joint BKP data.

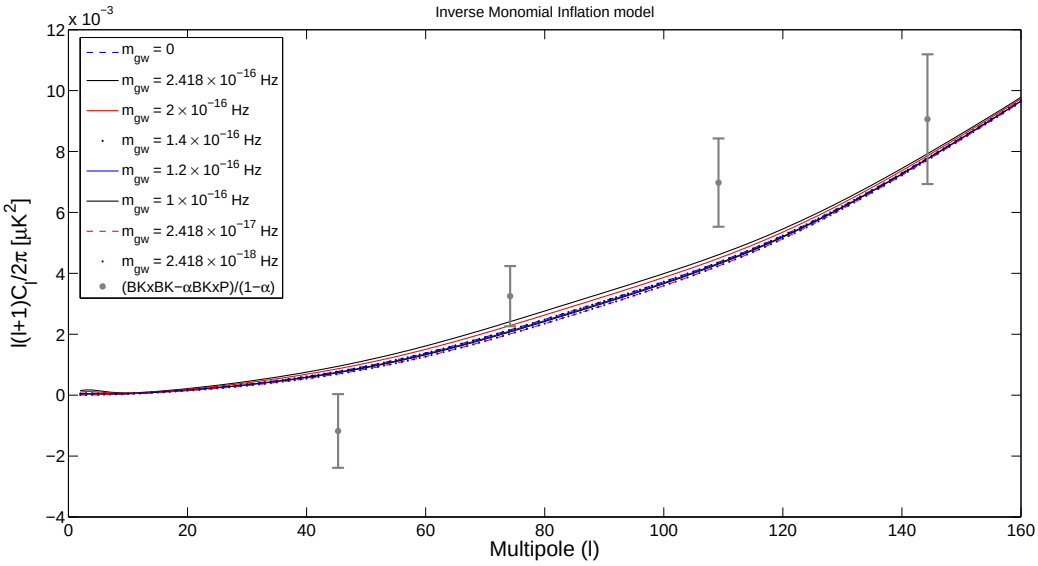

Figure 4.4: The lensed BB-mode correlation angular spectrum of CMB for the inverse monomial inflation model ($n_T = -2.50 \times 10^{-4}$) for various values of graviton mass with the joint BKP data.

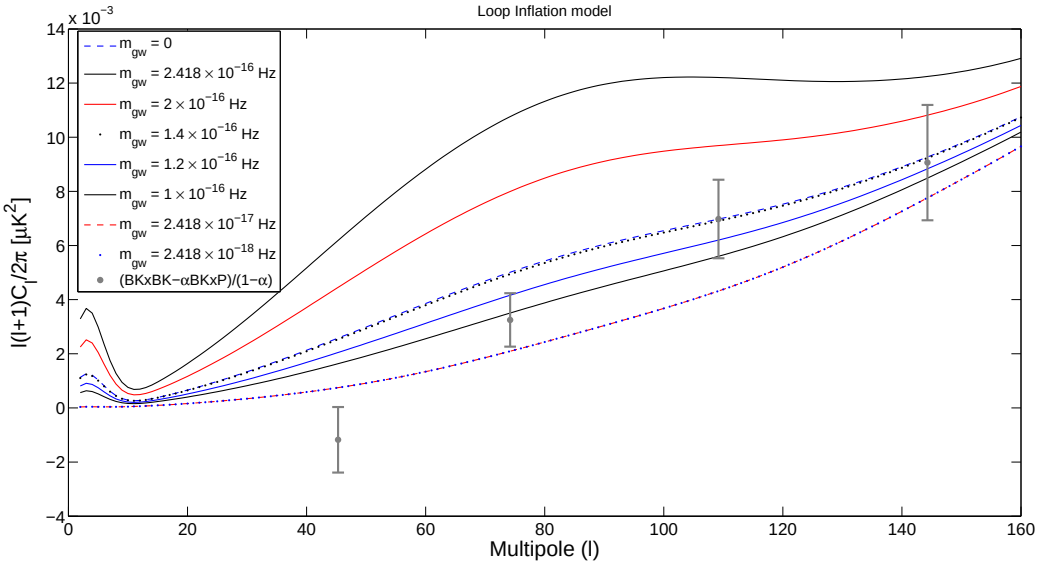

Figure 4.5: The lensed BB-mode correlation angular spectrum of CMB for the loop inflation model ($n_T = -6.18 \times 10^{-3}$) for various values of graviton mass with the joint BKP data.

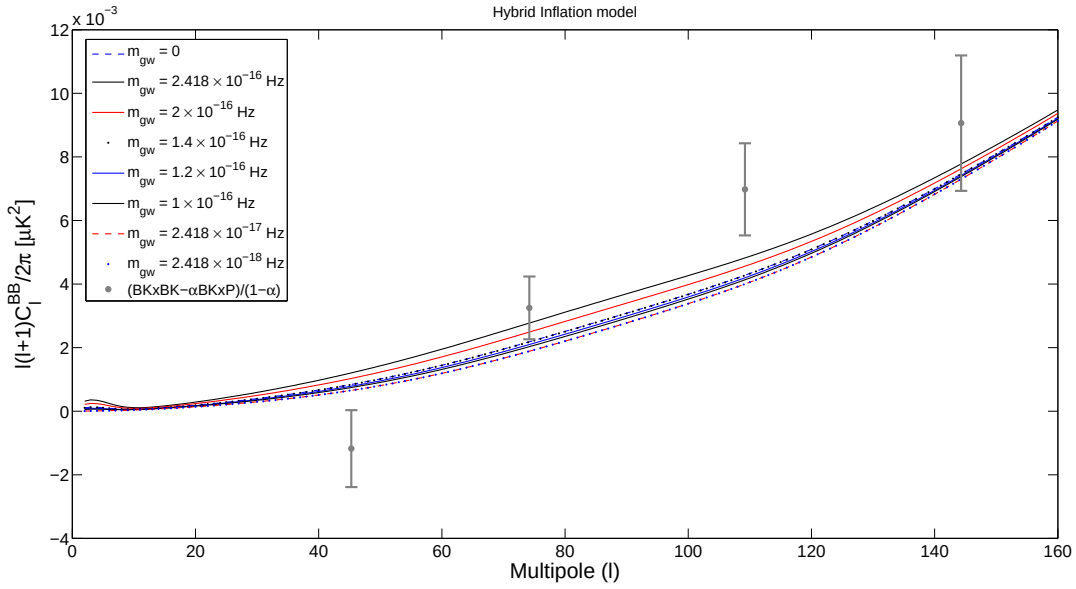

Figure 4.6: The lensed BB-mode correlation angular spectrum of CMB for the hybrid inflation model ($n_T = -6.18 \times 10^{-3}$) for various values of graviton mass with the joint BKP data.

hybrid inflation model in Fig.(4.6). It can be seen that for each inflation model, for the primordial gravitational waves with mass $m_{gw} \gtrsim 1.4 \times 10^{-16}$ Hz ($\equiv 5.79 \times 10^{-31}$ eV), there is enhancement in the power level of the power spectrum compared with its massless counterpart while there is decrease in the power level in the case of $m_{gw} < 1.4 \times 10^{-16}$ Hz. Therefore, the BB-mode correlation spectrum of CMB for gravitational waves with mass $m_{gw} \simeq 1.4 \times 10^{-16}$ Hz is found almost comparable to its massless counterpart. The increase/decrease in the power level of BB-mode power spectrum of CMB for the massive GWs is greater for inflation models with larger deviation (n_T) from scale invariance. For each slow-roll inflation model, the angular power spectrum for the gravitational waves with masses $m_{gw} = 2.418 \times 10^{-17}$ Hz ($\equiv 10^{-31}$ eV) and $m_{gw} = 2.418 \times 10^{-18}$ Hz ($\equiv 10^{-32}$ eV) are found marginally within the limit of the joint BICEP2/Keck Array and Planck data at higher multipoles, which indicates that the lower limit for the graviton mass may be higher than these masses. At the same time, it can be seen from the figures that the upper limit for the primordial graviton mass may also be higher than $m_{gw} = 10^{-30}$ eV.

4.4 Discussions

In the massive gravity theory involving Lorentz violation, spontaneous breaking of the Lorentz invariance is induced by a convenient choice of the vacuum for the Goldstone fields. There are several mass parameters which are carefully fine-tuned relative to each other. These mass parameters are chosen in such a way that they satisfy some constraints so that the pathologies are absent. The fine-tuning relations between the mass parameters characterize certain regions in the mass parameter space so that in these regions, the Lorentz-violating gravity theory is free of pathologies like rapid instabilities and ghost modes. Hence the mass parameters cannot be chosen arbitrarily, and in these regions, the theory is described by a consistent low-energy effective theory with strong coupling scale $\Lambda \sim (mm_{pl})^{1/2}$ which implies a ghost-free scenario. In the vector sector, provided $m_2 \neq 0$, the vector field behaves similarly as in the general relativity case; hence they decay quickly after the inflationary phase and there is no propagating perturbation and no modification of gravity in this sector unless one considers the non-linear effects. In the scalar sector, the scalar field has massless limit which coincides with the GR expression; hence there is no vDVZ discontinuity. Thus, there is no modification in the vector and scalar sectors. In the tensor sector, there are perturbations h_{ij} which are transverse-traceless and consist of two components. The field equation of these perturbations is that of a spin-2 massive field, the mass being represented by the parameter m_2; hence in the tensor sector, there are two propagating degrees of freedom. The only modification therefore comes from the tensor sector in which the dispersion relation acquires a non-zero mass.

If primordial gravitons have mass, the superhorizon modes would oscillate when the mass becomes larger than the Hubble parameter, this behavior would leave observable signatures on the CMB anisotropy spectrum. For primordial gravitational waves, the upper bound on the mass of the graviton is estimated from the exponential decay of the Yukawa potential which yields $m_{gw} < 10^{-30}$ eV ($\equiv 2.418 \times 10^{-16}$ Hz) at the Compton wavelength $\lambda_g > 10^{20}$ km of the graviton [104, 114]. The lower bound has been proposed to be $m_{gw} > 10^{-29}$ cm^{-1} ($\equiv 10^{-19}$ Hz) [115]. Hence, for

our study, we analyzed the graviton mass ranging from $m_{gw} = 2.418 \times 10^{-18}$ Hz to $m_{gw} = 2.418 \times 10^{-16}$ Hz. The comparative study of the BB-mode power spectrum is carried out for these masses with the massless cases for the selected slow-roll inflation models with the joint analysis data of the BICEP2/Keck Array and Planck mission to put bounds on the potential mass. Thus it can be observed from the results that on comparison with the joint data, both the lower and upper bounds on the primordial graviton mass may be actually higher than earlier proposals. Assuming a dispersion relation for the primordial massive GWs, the mass of the primordial graviton is estimated to be $m_{gw} \approx 1.4 \times 10^{-16}$ Hz ($\equiv 5.79 \times 10^{-31}$ eV). Repetition of the present work with other inflation models do not alter the results and conclusions of the present study.

Chapter 5

Quantum and Thermal effects on Primordial Massive Gravitational Waves and BB-mode spectrum of CMB

It is assumed that the massless primordial GWs were generated due to the parametric amplification of the zero-point fluctuations in the early universe [53, 54]. Therefore, if the primordial massive gravitational waves exist, it is reasonable to believe that the primordial massive gravitational waves were also created due to the parametric amplification of the quantum fluctuations. Hence, the massive gravitational waves can also be placed in the squeezed vacuum state and the subsequent effect is also expected to reflect on the CMB anisotropy.

If the primordial gravitational waves have non-zero mass, then their small mass is expected to have observable effect on the B-mode auto-correlation spectrum of the CMB. It has been shown that gravitons with mass range 10^{-27} cm^{-1} and 10^{-26} cm^{-1} ($10^{-17}Hz \leq m_{gw} \leq 10^{-16}Hz$) can have signature on the lower multipoles of the CMB anisotropy [115]. The goal of this study is to explore the potential existence of primordial massive GWs in the squeezed vacuum state through the BB-mode correlation spectrum of the CMB for various slow-roll inflation models with the joint analysis data of the BICEP2/Keck Array and Planck missions.

5.1 BB-mode of CMB for massive GWs in squeezed vacuum state

To obtain the BB-mode angular power spectrum of the CMB for the massive primordial GWs in the squeezed vacuum state requires the computation of the tensor power spectrum for the massive GWs in the squeezed vacuum state. The tensor power spectrum for the primordial massive GWs is introduced in the previous chapter and is given by

$$P_T(k) = A_T(k_0) \left(\frac{k}{k_0}\right)^{n_T} S^2(w_o). \tag{5.1}$$

where $A_T(k_0)$ is the normalization constant, $S(w_o)$ is the enhancement factor given by eq.(4.28), k_0 is the pivot wave number for the tensor spectrum and n_T is the tensor spectral index, which depends on the effective potential of each inflation model.

The primordial massive GWs are assumed to have originated during the inflationary period due to the parametric amplification of the zero-point quantum fluctuations [55]. Hence, these waves can also be placed in the squeezed vacuum state. The power spectrum for the massive GWs in the squeezed vacuum state is obtained with the help of the result given in Chapter 3 and eq.(4.29). As mentioned, the power spectrum for the primordial massive gravitational waves differ from its massless counterpart only by the enhancement factor, thus the tensor power spectrum for the massive GWs in the squeezed vacuum state is obtained by eqs.(3.61) and (5.1) as

$$P_T(k) = A_T \left(\frac{k}{k_0}\right)^{n_T} \left[1 + 2\sinh^2 r_s + \sinh 2r_s \cos\left(\gamma + (2 - n_T)\frac{\pi}{2}\right)\right] S^2(w_o). \tag{5.2}$$

Using eq.(5.2) in eq.(3.62), the BB-mode spectrum of CMB for primordial massive GWs in the squeezed vacuum state can be obtained for various inflation models. The present study is restricted to four slow-roll inflation models only, namely the Starobinsky inflation model, the Higgs inflation model, the natural inflation model and the Coleman-Weinberg inflation model. These models are selected for the study because they are found either highly or marginally favoured by the joint analysis data of BICEP2/Keck Array at 150 GHz and Planck mission at 353 GHz. The lensed BB mode angular power spectrum of CMB for each inflation model is generated using

the CAMB code with its corresponding r, n_T and P_T values which are computed in the Chapter 3. For all the cases, the pivot wave number for tensor mode is taken as $k_0 = 0.002$ Mpc^{-1}, for scalar mode it is $k_* = 0.05$ Mpc^{-1} and the optical depth is taken as $\kappa = 0.08$.

The BB-mode power spectrum of CMB is recomputed for the massive GWs for the aforementioned slow-roll inflationary models for various values of the squeezing parameter and angle. The values of the squeezing parameter $r_s = 0.1$, 0.6 and 0.95 are used to reflect the growth in the parameter from the initial vacuum state ($r_s = 0$) upto the inflationary period ($r_s = 1$). For each inflation model, BB-mode spectrum is studied with the primordial massive GW mass ranging from $2.418 \times 10^{-18} \leq m_{gw} \leq 2.418 \times 10^{-16}$ Hz.

The obtained BB-mode spectrum for various inflationary models for the lensed effect are compared with the joint analysis data of the BICEP2/Keck Array and Planck mission as well as their massless counterparts. Note that implemented limit here is taken from Ref.[15], that is (BK x BK - α BK x P)/(1 - α) at $\alpha = \alpha_{fid} = 0.04$ is computed from the cross-spectra and auto-spectra of the combined BICEP2/Keck 150 GHz and Planck 353 GHz maps to remove the dust contribution. And BK x P indicates the cross-spectra of BICEP2/Keck maps at 150 GHz and Planck maps at 353 GHz and BK x BK indicates the BICEP2/Keck auto-spectra at 150 GHz.

On comparing results for each inflation model, it can be seen that there is oscillation in the amplitude and hence in angular power spectrum due to squeezing effect and power level increases with increase in the squeezing parameter. For models which are highly favored by the BKP data like the R2 inflation model, the Higgs inflation model and the Coleman-Weinberg inflation model, the generated spectra for the massive GWs are also found to be still well within the limit of the joint data even in the presence of squeezing effect. For the natural inflation model which is found to be marginally within the BKP data, the spectra for higher mass value ($m_{gw} > 2 \times 10^{-16}$ Hz) are found to be within the limit only at higher multipoles ($l > 100$), while the lower mass value ($m_{gw} \leq 2.418 \times 10^{-17}$ Hz) are found within the limit at $l > 160$. This matter can be explained away as due to this particular

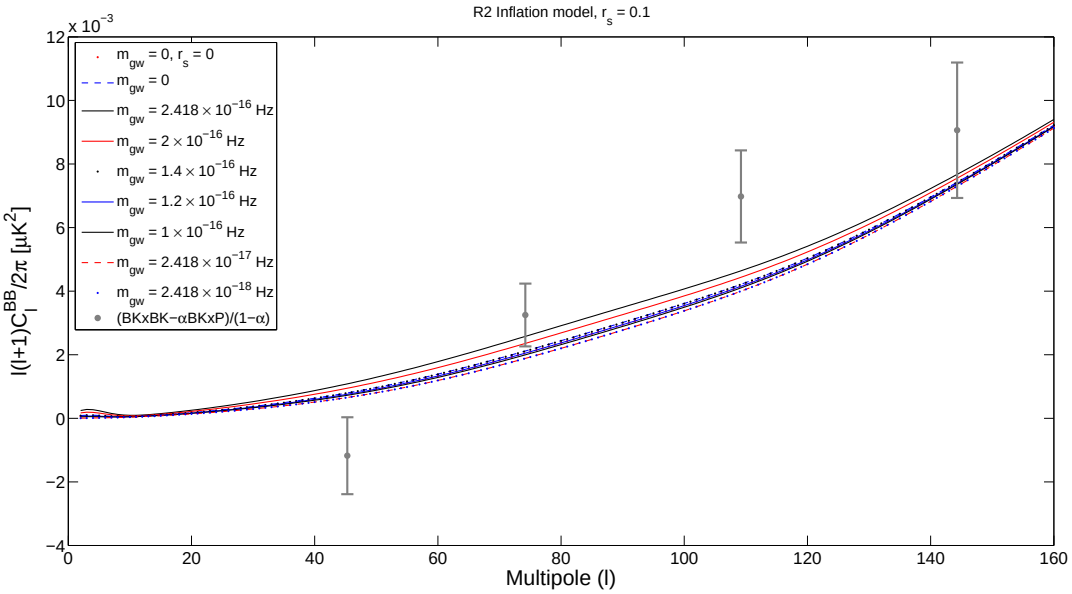

Figure 5.1: Lensed BB-mode angular spectrum of CMB for the Starobinsky inflation model ($n_T = -4.06 \times 10^{-4}$) for squeezing parameter $r_s = 0.1$ for various values of the primordial gravitational wave mass with the joint BKP data.

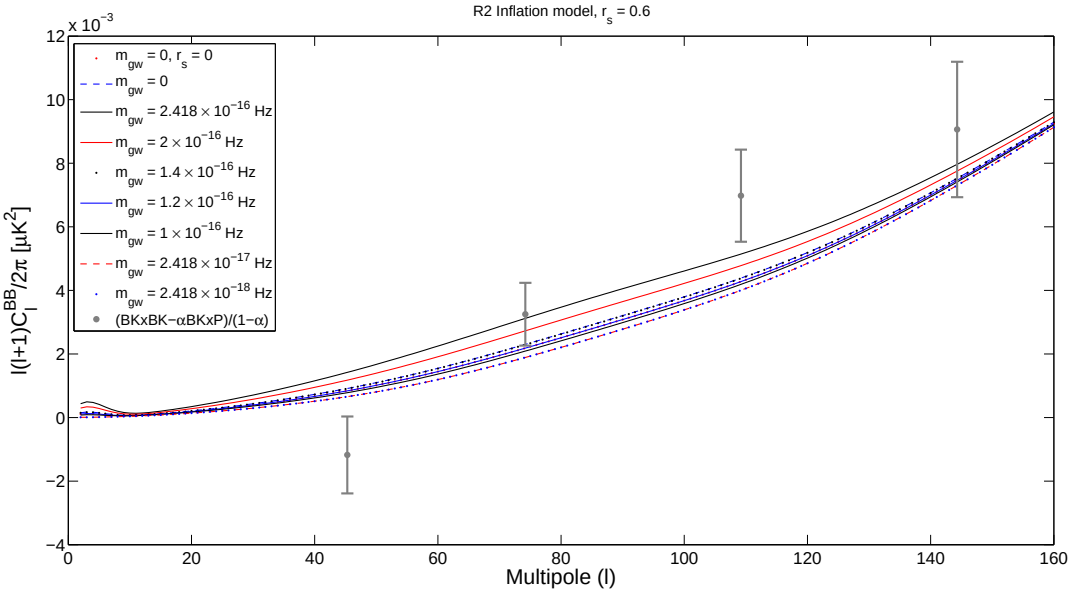

Figure 5.2: Lensed BB-mode angular spectrum of CMB for the Starobinsky inflation model ($n_T = -4.06 \times 10^{-4}$) for squeezing parameter $r_s = 0.6$ for various values of the primordial gravitational wave mass with the joint BKP data.

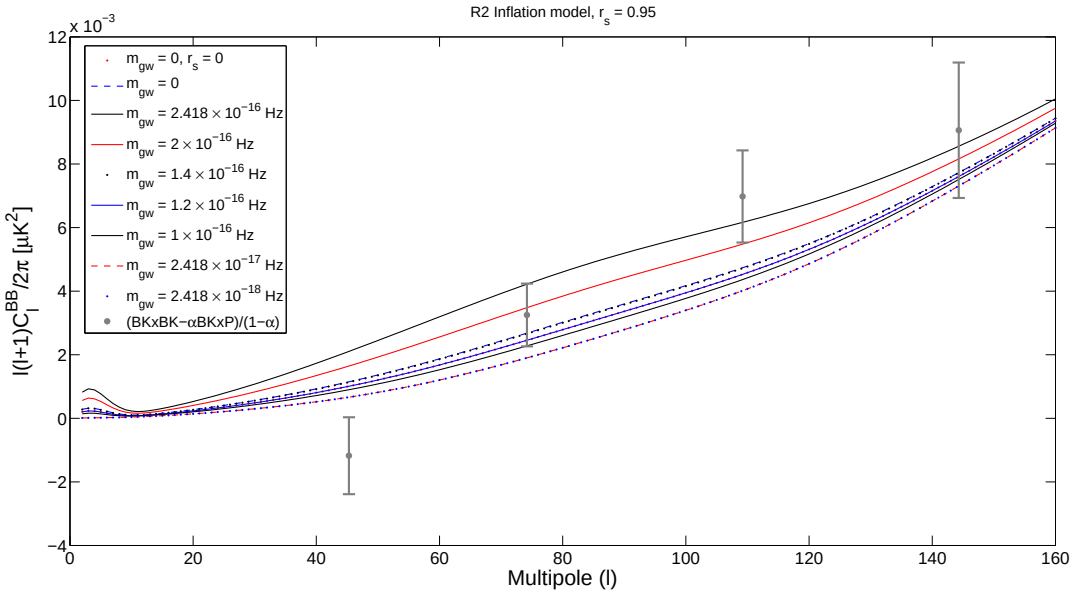

Figure 5.3: Lensed BB-mode angular spectrum of CMB for the Starobinsky (R2) inflation model ($n_T = -4.06 \times 10^{-4}$) for squeezing parameter $r_s = 0.95$ for various values of the primordial gravitational wave mass with the joint BKP data.

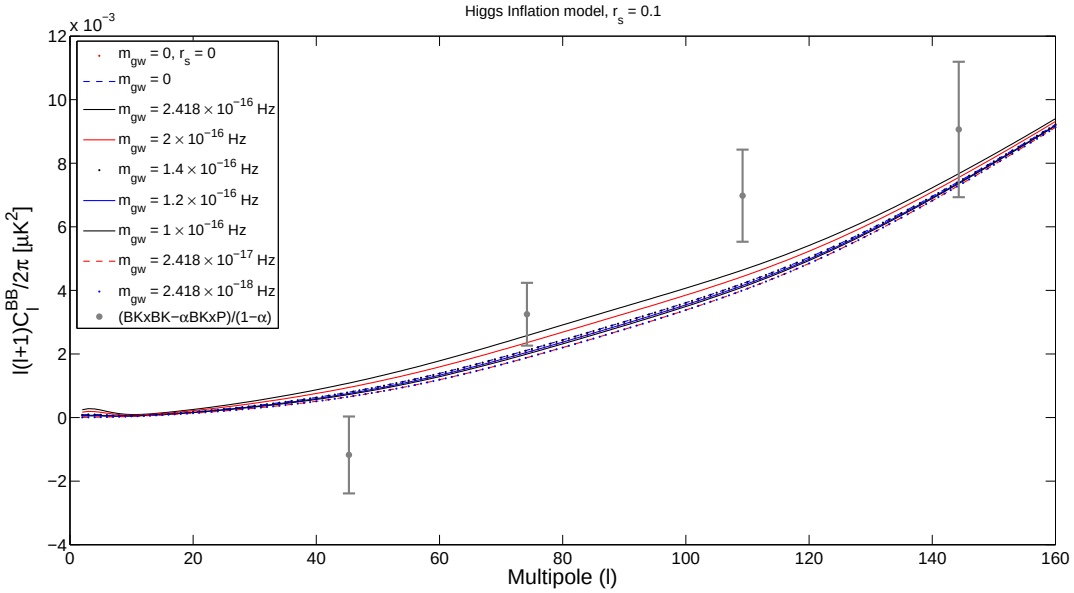

Figure 5.4: Lensed BB-mode angular spectrum of CMB for the Higgs inflation model ($n_T = -3.53 \times 10^{-4}$) for squeezing parameter $r_s = 0.1$ for various values of the primordial gravitational wave mass with the joint BKP data.

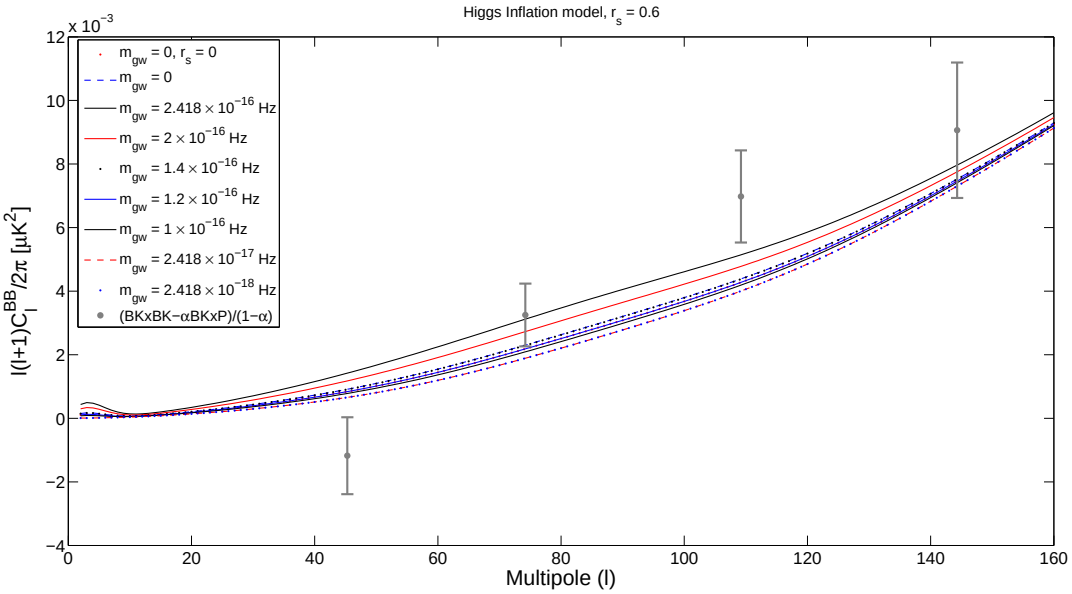

Figure 5.5: Lensed BB-mode angular spectrum of CMB for the Higgs inflation model ($n_T = -3.53 \times 10^{-4}$) for squeezing parameter $r_s = 0.6$ for various values of the primordial gravitational wave mass with the joint BKP data.

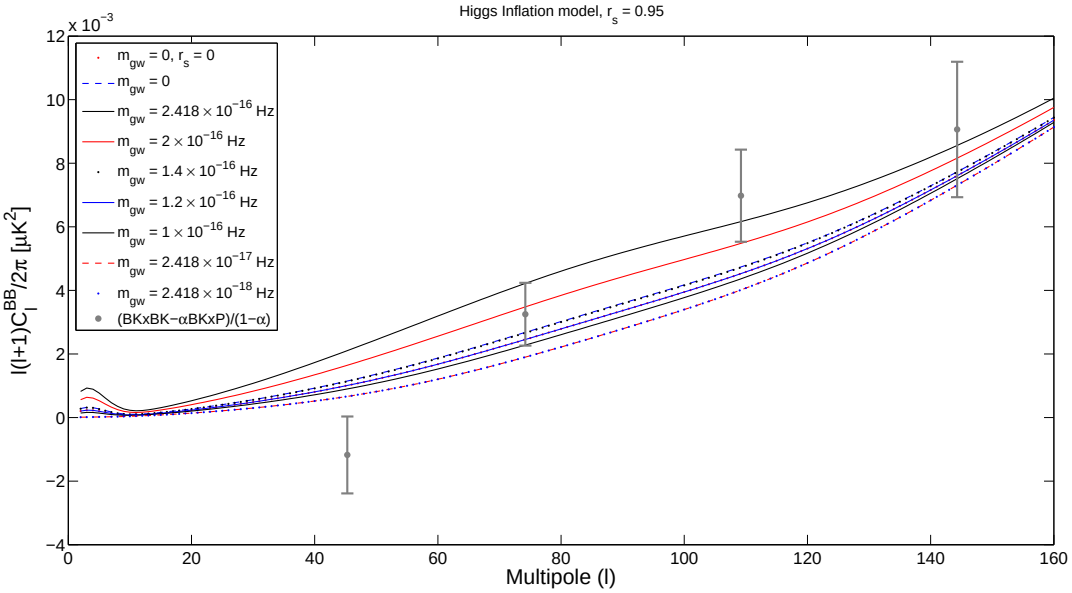

Figure 5.6: Lensed BB-mode angular spectrum of CMB for the Higgs inflation model ($n_T = -3.53 \times 10^{-4}$) for squeezing parameter $r_s = 0.95$ for various values of the primordial gravitational wave mass with the joint BKP data.

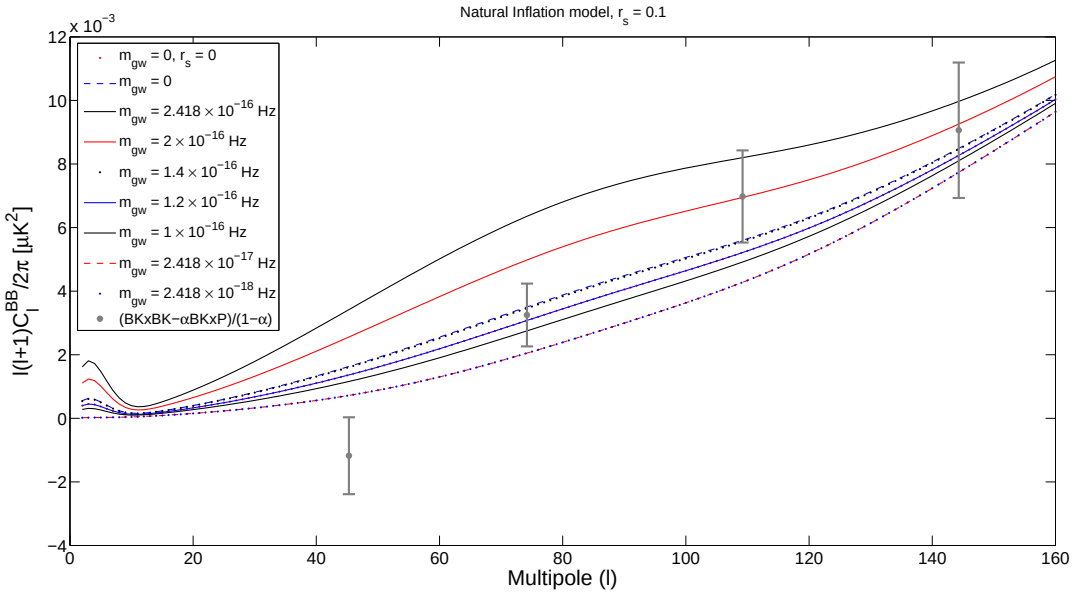

Figure 5.7: Lensed BB-mode angular spectrum of CMB for the natural inflation model ($n_T = -2.58 \times 10^{-3}$) for squeezing parameter $r_s = 0.1$ for various values of the primordial gravitational wave mass with the joint BKP data.

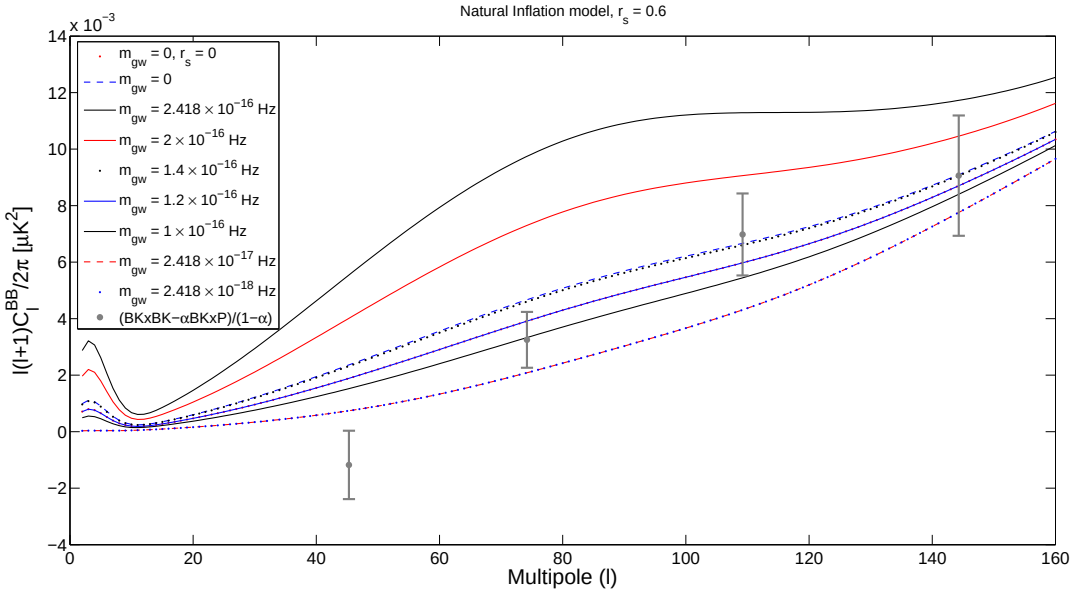

Figure 5.8: Lensed BB-mode angular spectrum of CMB for the natural inflation model ($n_T = -2.58 \times 10^{-3}$) for squeezing parameter $r_s = 0.6$ for various values of the primordial gravitational wave mass with the joint BKP data.

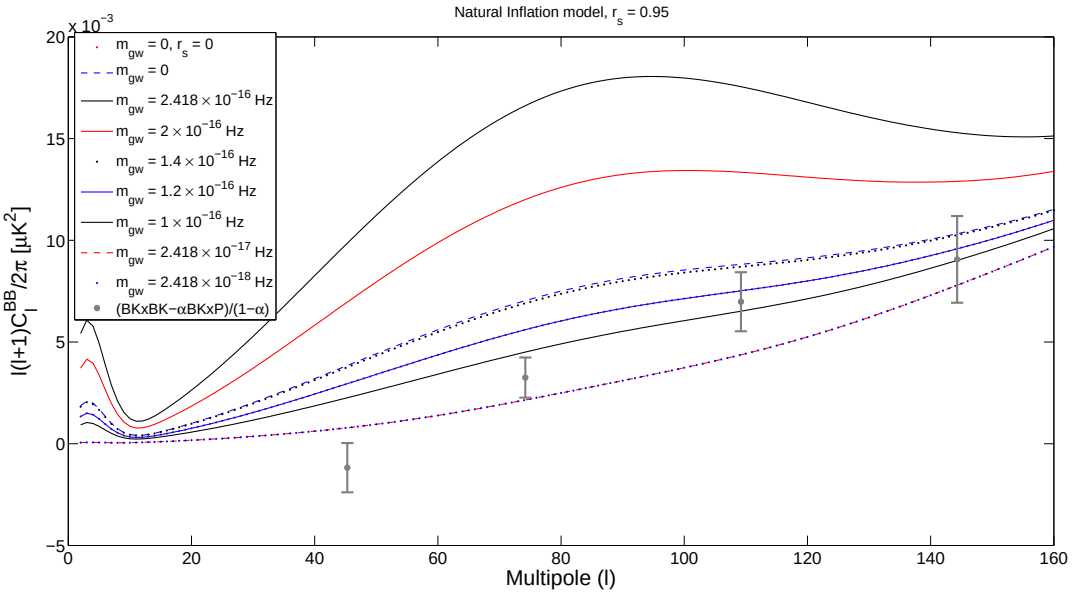

Figure 5.9: Lensed BB-mode angular spectrum of CMB for the natural inflation model($n_T = -2.58 \times 10^{-3}$) for squeezing parameter $r_s = 0.95$ for various values of the primordial gravitational wave mass with the joint BKP data.

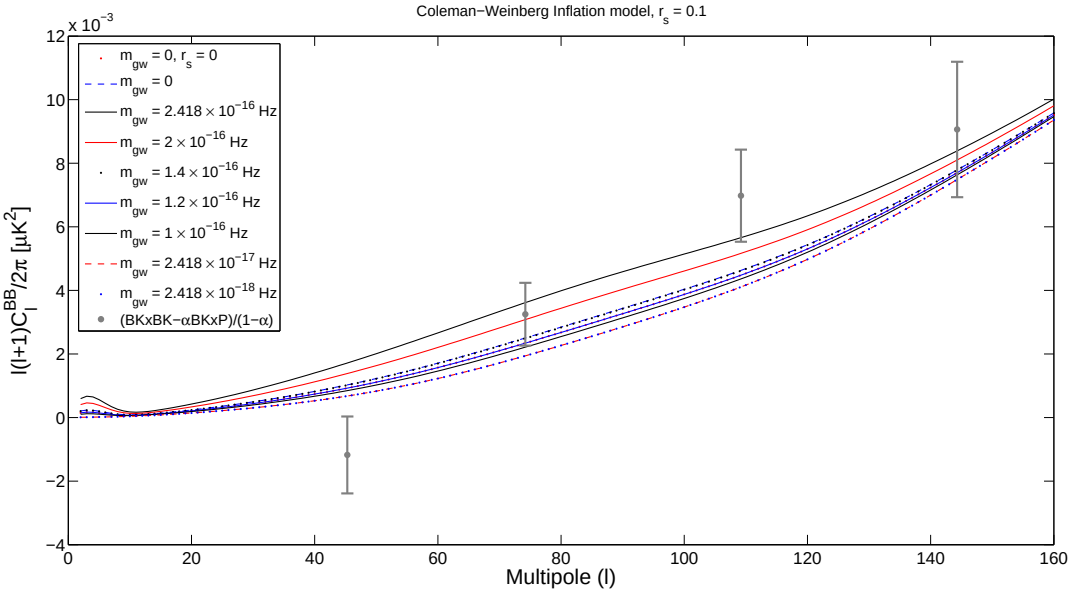

Figure 5.10: Lensed BB-mode angular spectrum of CMB for the Coleman-Weinberg inflation model ($n_T = -9.72 \times 10^{-4}$) for squeezing parameter $r_s = 0.1$ for various values of the primordial gravitational wave mass with the joint BKP data.

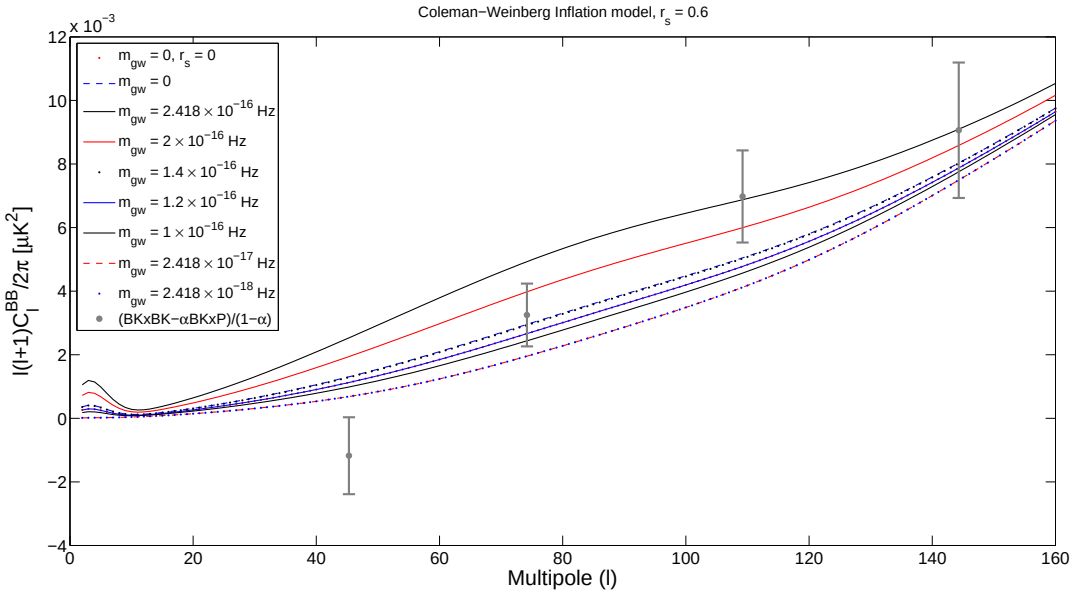

Figure 5.11: Lensed BB-mode angular spectrum of CMB for the Coleman-Weinberg inflation model ($n_T = -9.72 \times 10^{-4}$) for squeezing parameter $r_s = 0.6$ for various values of the primordial gravitational wave mass with the joint BKP data.

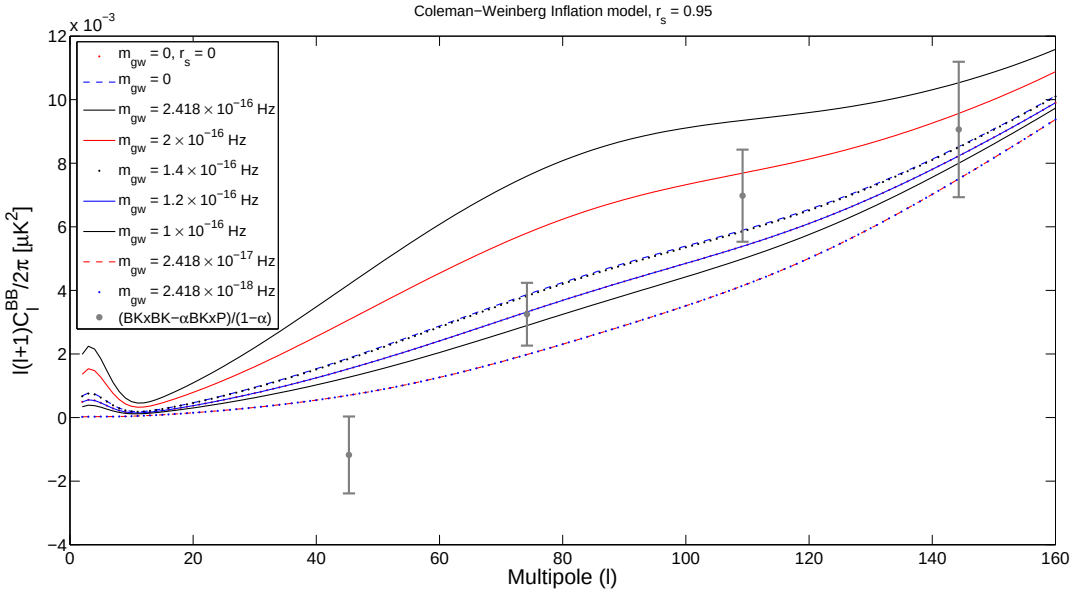

Figure 5.12: Lensed BB-mode angular spectrum of CMB for the Coleman-Weinberg inflation model ($n_T = -9.72 \times 10^{-4}$) for squeezing parameter $r_s = 0.95$ for various values of the primordial gravitational wave mass with the joint BKP data.

model being only marginally within the BKP limit. This implies that the existence of primordial massive gravitational waves in the squeezed vacuum state is not ruled out; in fact, squeezing effect may also be very helpful in constraining the mass of the primordial gravitational waves.

5.2 BB-mode of CMB for massive GWs in thermal vacuum state

The gravitons are believed to be among the thermalized particles which decoupled after the recombination and if they are indeed in the thermal state, then this feature would have some effect on B-mode spectrum of the CMB. Due to these thermalized gravitons, there would occur a process of stimulated emission into the thermal background of GWs which would amplify the tensor perturbations generated during inflation thus leading to some change in the B-mode angular spectrum of the CMB by a temperature dependent factor. Therefore, the thermal effect of the primordial massive gravitational waves can also be expected to reflect on the BB-mode power spectrum of the CMB. Moreover, if the primordial GWs exist in the squeezed vacuum state, then the thermal and squeezing effects are expected to be reflected on the BB-mode power spectrum of the CMB. Therefore it is interesting to study the combined effects of the thermal and squeezing of primordial massive gravitational waves on the BB-mode power spectrum for various slow-roll inflation models with the joint analysis data of BICEP2/Keck and Planck missions.

Since tensor power spectrum for the primordial massive GWs differ from its massless counterpart only by the enhancement factor, the power spectrum for the massive GWs in thermal state is obtained from eqs.(3.72) and (5.1) as

$$P_T(k) \;=\; A_T \left(\frac{k}{k_0}\right)^{n_T} \times \coth\left[\frac{k}{2T}\right] S^2(w_o),$$

where $A_T(k_0)$ is the normalization constant, $S(w_o)$ is the enhancement factor given by eq.(4.28), k_0 is the pivot wave number of the tensor perturbation and n_T is the tensor spectral index, which depends on the effective potential of each inflation model.

In earlier chapter the combined effect of the squeezed vacuum and thermal states on primordial massless GWs has been studied. Therefore it is interesting to study such combined effect for primordial massive GWs and its effect on the BB-mode angular spectrum of CMB. For this, the tensor power spectrum for the primordial massive GWs in the squeezed vacuum state as well as the thermal state can be written by using eqs.(3.61) and (5.3) as follows

$$\begin{aligned} P_T(k) &= A_T \left(\frac{k}{k_0}\right)^{n_T} \left[1 + 2\sinh^2 r_s + \sinh 2r_s \cos\left(\gamma + (2 - n_T)\frac{\pi}{2}\right)\right] \\ &\quad \times \coth\left[\frac{k}{2T}\right] S^2(w_o). \end{aligned} \tag{5.3}$$

Using eq.(5.3) and eq.(3.62), the BB-mode correlation spectrum can be computed for the primordial GWs in the squeezed vacuum state as well as the thermal state for various inflation models. As mentioned the study is again restricted to three slow-roll inflation models only, namely the Starobinsky inflation model, the Higgs inflation model and the Coleman-Weinberg inflation model which are found to be highly favored by the joint analysis data of BICEP2/Keck Array at 150 GHz and Planck at 353 GHz. The lensed BB mode angular power spectrum of CMB for each inflation model is generated using the CAMB code with the corresponding r, n_T and P_T values which are computed in the Chapter 3. For all the cases, the pivot wave number for tensor perturbation is taken as $k_0 = 0.002$ Mpc^{-1}, for scalar perturbation, it is $k_* = 0.05$ Mpc^{-1} and the optical depth is taken as $\kappa = 0.08$.

The BB-mode power spectrum of CMB is studied for the massive GWs for the aforementioned slow-roll inflationary models for several values of the squeezing parameters and temperature parameter. The obtained BB-mode spectrum of CMB are compared with the joint BKP data. Note that implemented limit here is taken from Ref.[15], that is (BK x BK - α BK x P)/(1 - α) at $\alpha = \alpha_{fid} = 0.04$ is computed from the cross-spectra and auto-spectra of the combined BICEP2/Keck 150 GHz and Planck 353 GHz maps to remove the dust contribution. And BK x P indicates the cross-spectra of BICEP2/Keck maps at 150 GHz and Planck maps at 353 GHz and BK x BK indicates the auto-spectra from BICEP2/Keck band at 150 GHz.

The obtained results of the BB-mode power spectrum of CMB for the primordial massive GWs in the squeezed vacuum state as well as in thermal state for the

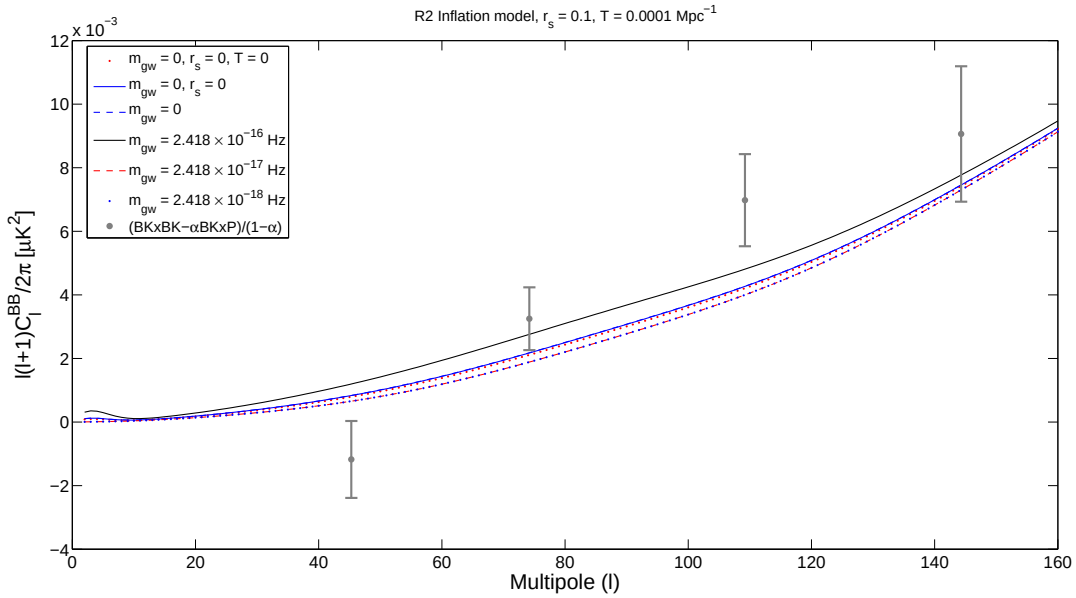

Figure 5.13: Lensed BB-mode angular spectrum of CMB for the Starobinsky inflation model with $n_T = -4.06 \times 10^{-4}$, for the squeezing parameter $r_s = 0.1$, temperature $T = 0.0001$ Mpc^{-1} and for various values of the primordial gravitational wave mass with the joint BKP data.

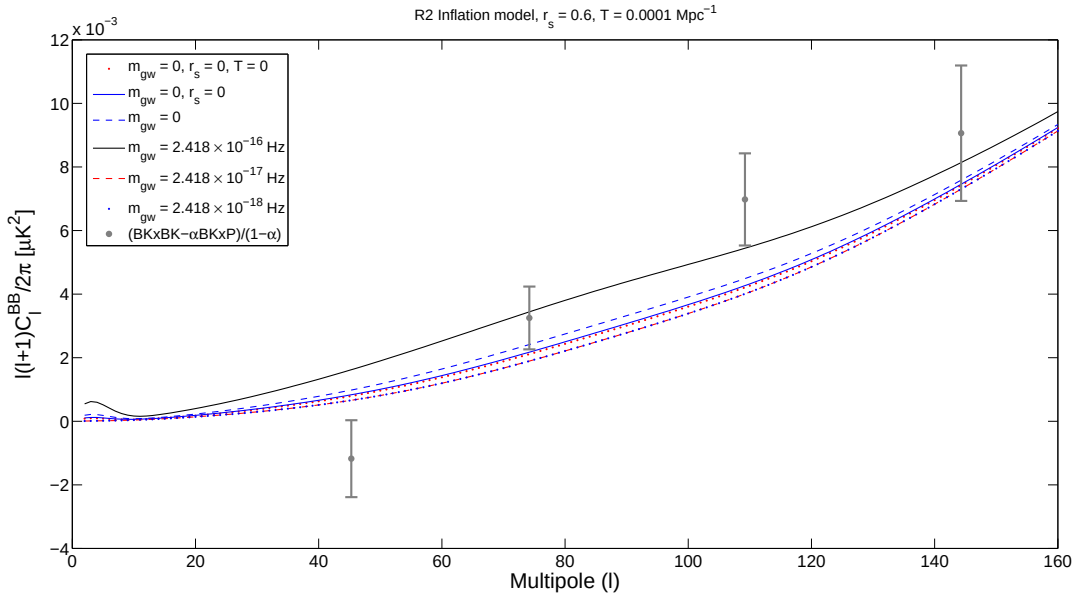

Figure 5.14: Lensed BB-mode angular spectrum of CMB for the Starobinsky inflation model with $n_T = -4.06 \times 10^{-4}$), for squeezing parameter $r_s = 0.6$, temperature $T = 0.0001$ Mpc^{-1} and for various values of the primordial gravitational wave mass with the joint BKP data.

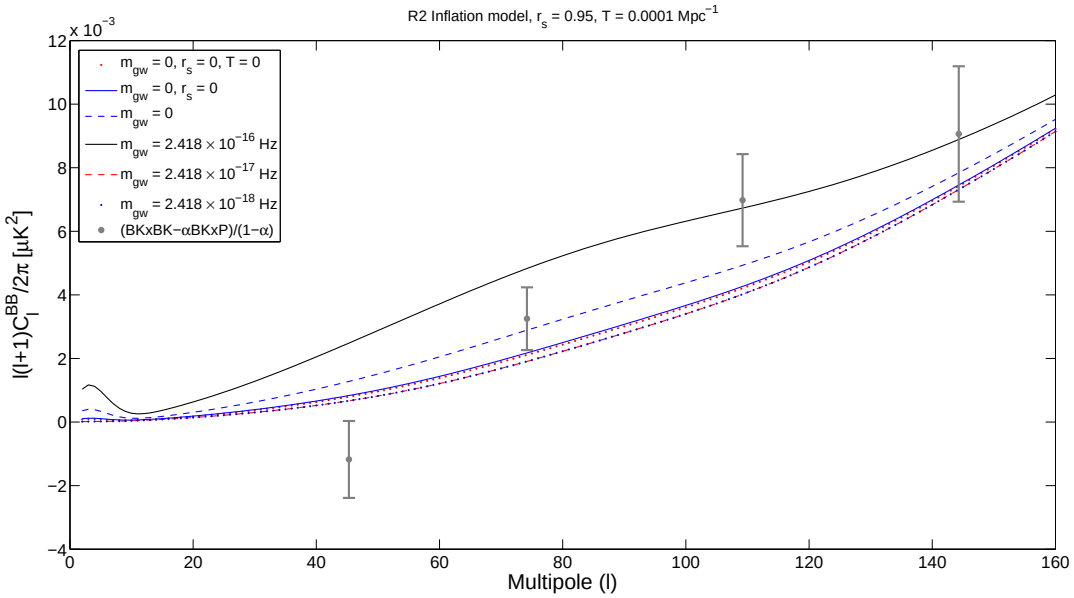

Figure 5.15: Lensed BB-mode angular spectrum of CMB for the Starobinsky inflation model with $n_T = -4.06 \times 10^{-4}$ for squeezing parameter $r_s = 0.95$, temperature $T = 0.0001$ Mpc^{-1} and for various values of the primordial gravitational wave mass with the joint BKP data.

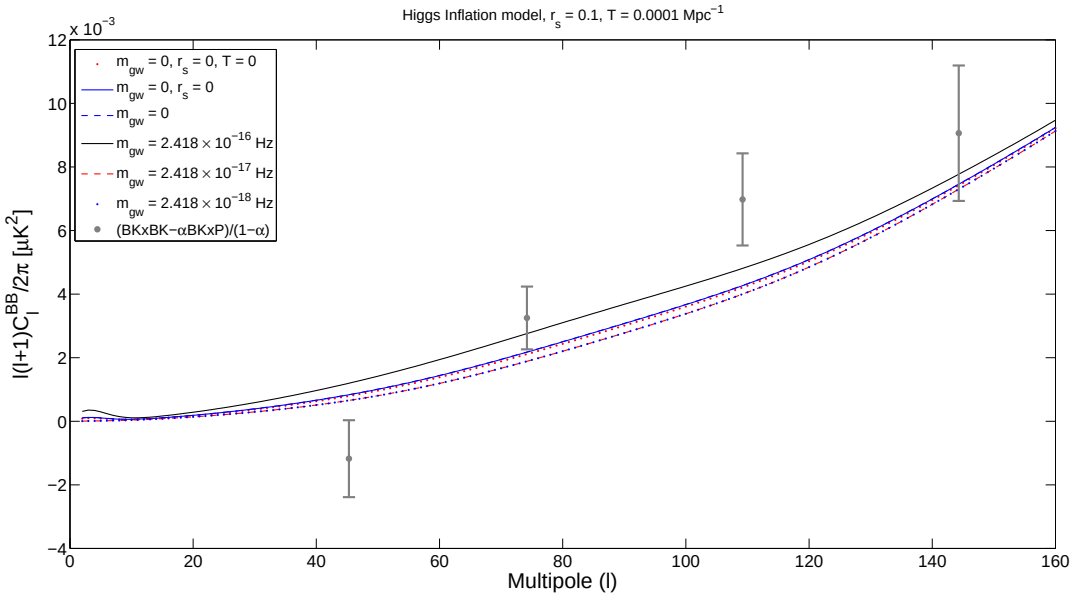

Figure 5.16: Lensed BB-mode angular spectrum of CMB for the Higgs inflation model with $n_T = -3.53 \times 10^{-4}$ for squeezing parameter $r_s = 0.1$, temperature $T = 0.0001$ Mpc^{-1} and for various values of the primordial gravitational wave mass with the joint BKP data.

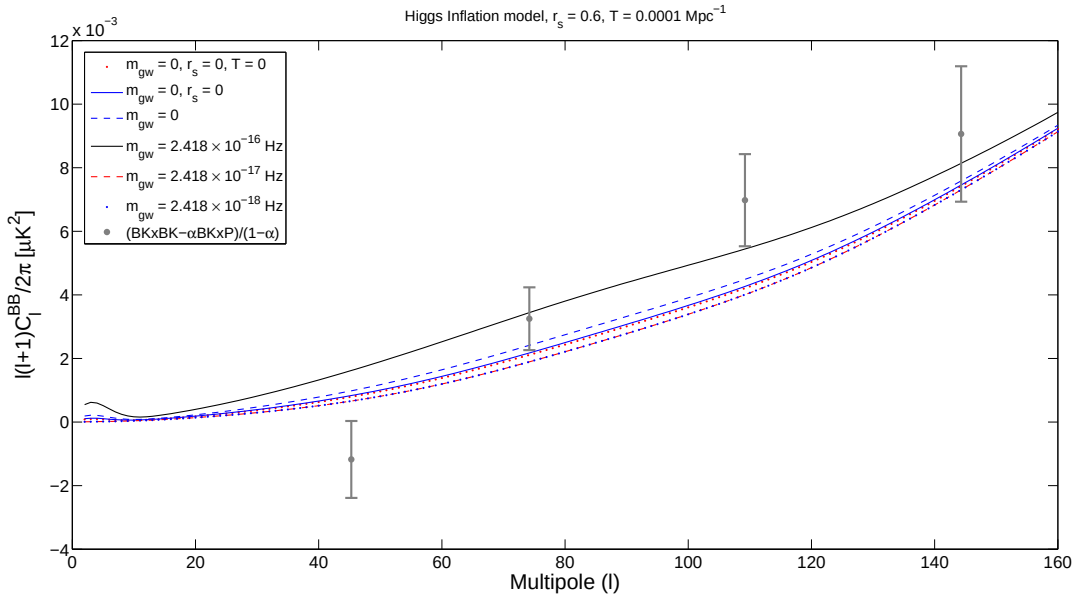

Figure 5.17: Lensed BB-mode angular spectrum of CMB for the Higgs inflation model with $n_T = -3.53 \times 10^{-4}$ for squeezing parameter $r_s = 0.6$, $T = 0.0001$ Mpc^{-1} and for various values of the primordial gravitational wave mass with the joint BKP data.

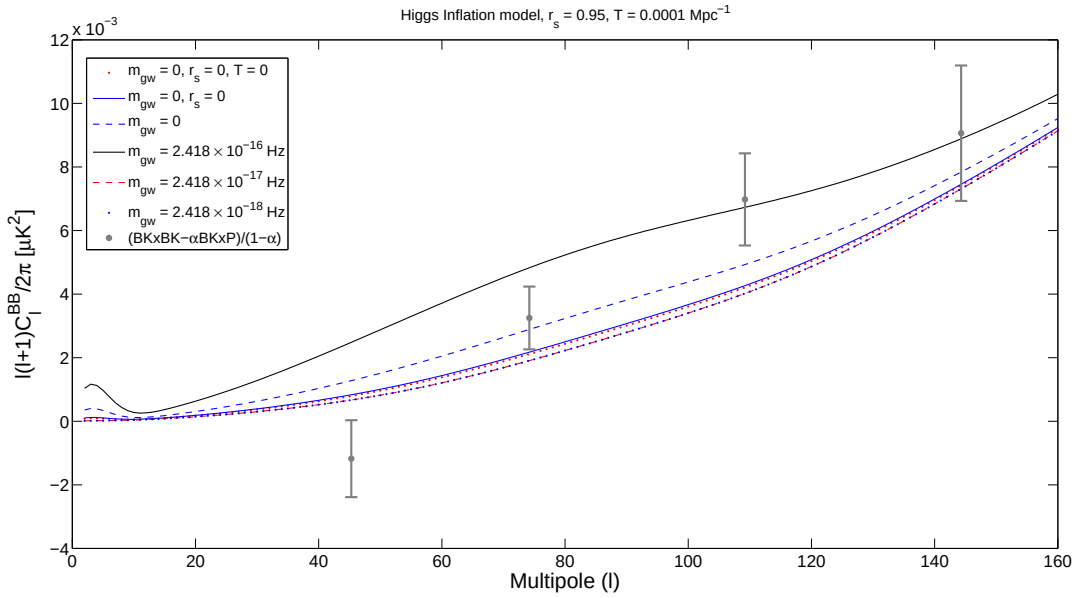

Figure 5.18: Lensed BB-mode angular spectrum of CMB for the Higgs inflation model with $n_T = -3.53 \times 10^{-4}$ for squeezing parameter $r_s = 0.95$, $T = 0.0001$ Mpc^{-1} and for various values of the primordial gravitational wave mass with the joint BKP data.

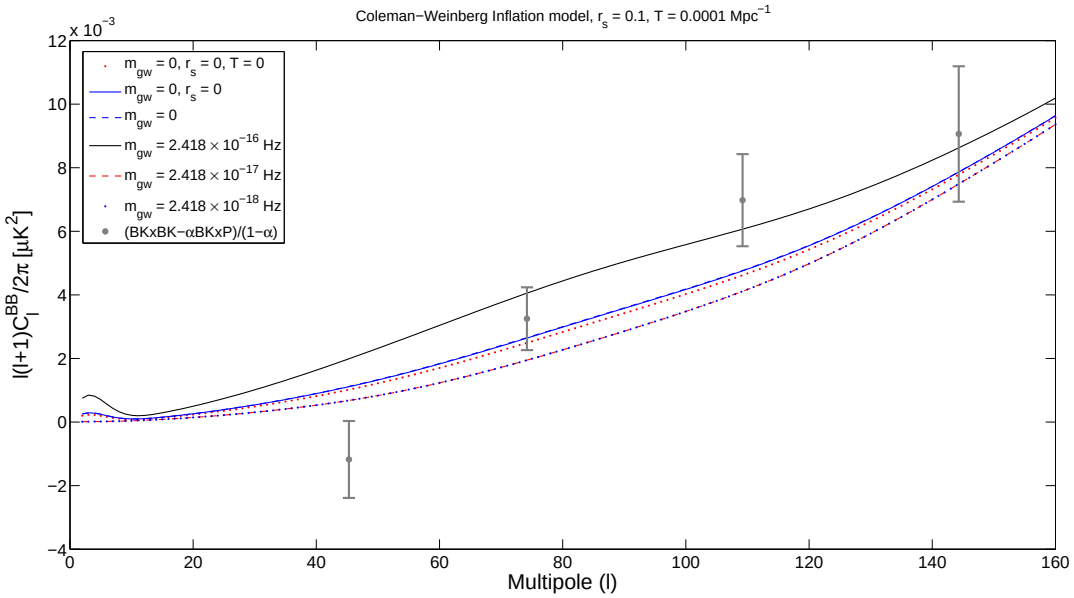

Figure 5.19: Lensed BB-mode angular spectrum of CMB for the Coleman-Weinberg inflation model with $n_T = -9.72 \times 10^{-4}$ for squeezing parameter $r_s = 0.1$, temperature $T = 0.0001$ Mpc^{-1} and for various values of the primordial gravitational wave mass with the joint BKP data.

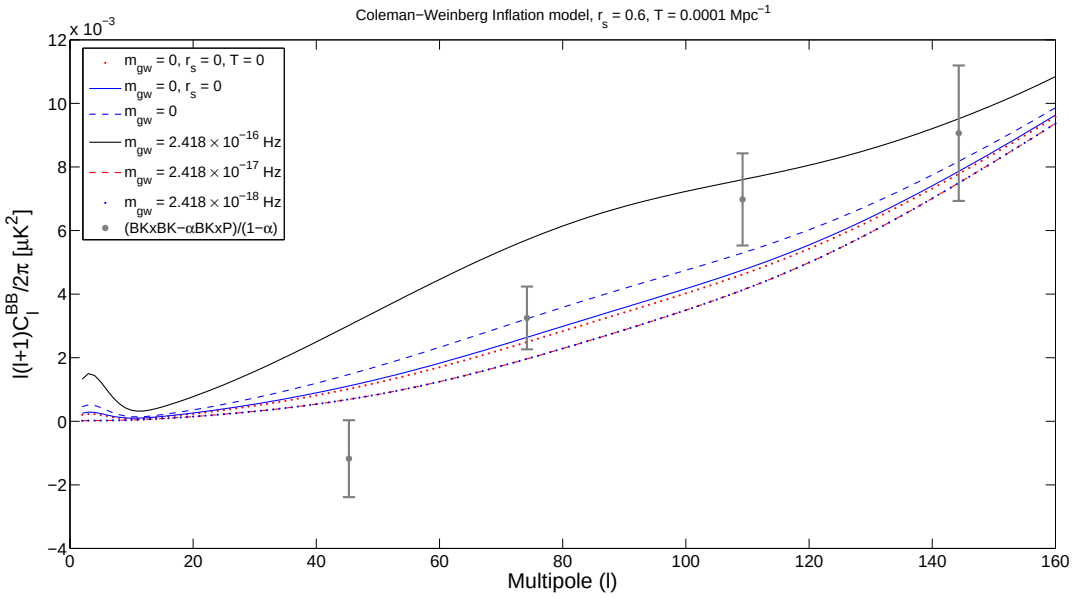

Figure 5.20: Lensed BB-mode angular spectrum of CMB for the Coleman-Weinberg inflation model with $n_T = -9.72 \times 10^{-4}$ for squeezing parameter $r_s = 0.6$, temperature $T = 0.0001$ Mpc^{-1} and for various values of the primordial gravitational wave mass with the joint BKP data.

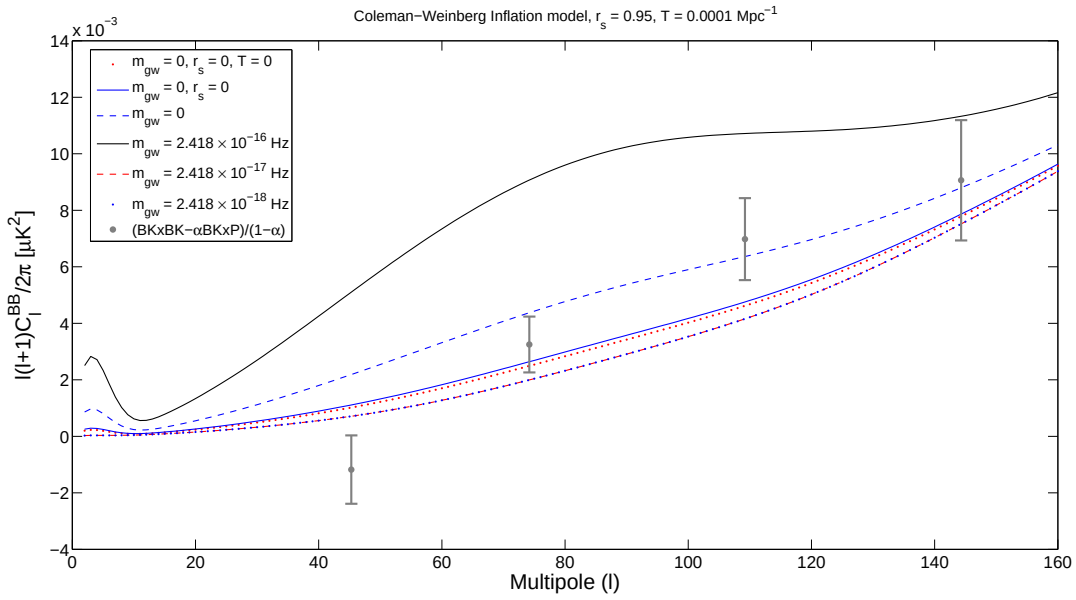

Figure 5.21: Lensed BB-mode angular spectrum of CMB for the Coleman-Weinberg inflation model with $n_T = -9.72 \times 10^{-4}$ for squeezing parameter $r_s = 0.95$, temperature $T = 0.0001$ Mpc^{-1} and for various values of the primordial gravitational wave mass with the joint BKP data.

selected slow-roll inflation models with several values of the squeezing parameter, temperature parameter and mass parameter with the joint BKP data are given in Figs.(5.13)-(5.21). The BB-mode angular power spectrum of CMB for each inflation model comprises the study for the three values of the squeezing parameter, $r_s = 0.1$, 0.6 and 0.95 and temperature parameter with various values of the mass parameter for the primordial GWs. Also the comparative study is carried out for the massless, non-thermal case and zero squeezing effect as well as the massless case with thermal effect but without squeezing with its counterparts. Note that the display unit for mass of the primordial gravitational waves m_{gw} is Hz while for temperature the unit is given as Mpc^{-1} while in the actual calculations, each mass is calculated in terms of Mpc^{-1} so that there is no conflict in the energy unit.

It is observed that there is increase in power level of the BB-mode spectrum of CMB which is more prominent for inflation models with larger tensor-to-scalar values and smaller tensor spectral index. There is further enhancement in the power spectrum due to thermal effect. However, the enhancement is very small for smaller mass values $m_{gw} = 2.418 \times 10^{-17}$ Hz and $m_{gw} = 2.418 \times 10^{-18}$ Hz. For the analysis only the large angular scales, $l \leq 160$ are considered also due to the fact that

there is contamination in the smaller angular scales of B-modes due to gravitational lensing which deflects the E-mode pattern to form the B-mode pattern. All sets of the BB-mode spectrum for each case are expected to converge at higher multipoles, enhancement due to squeezing and thermal effects are negligible at higher multipoles.

The analysis of the results of study shows that the Starobinsky inflation model ($r = 3.25 \times 10^{-3}$), the Higgs inflation model ($r = 2.83 \times 10^{-3}$) and the Coleman-Weinberg inflation model($r = 7.77 \times 10^{-3}$) are in good agreement with the joint BKP data. It has been concluded that the possibility of primordial massive gravitational waves existing in the thermal as well as squeezed vacuum states is not ruled out.

5.3 Discussions

The BB-mode angular spectrum of the CMB is studied for several slow-roll inflation models for massive GWs in the squeezed vacuum state and in the thermal vacuum state. There is oscillation in the amplitude due to the squeezing effect which leads to enhancement in the power spectrum. For models which are already in good agreement with the joint data of the BICEP2/Keck Array and Planck missions, the angular power spectrum for the squeezed vacuum state lie well within the BKP limit. Hence squeezing effect would be able to provide a good platform to further constrain the mass of the graviton. There is further enhancement in the power level of the B-mode spectrum for each inflation model for massive GWs in the thermal state for $T = 0.0001$ Mpc^{-1}, though the enhancement is very small. Thermal effect with smaller T values are negligible while larger T values like $T = 0.001$ Mpc^{-1} tend to provide over-enhancement in the B-mode spectrum thus overshooting them out of limit. This implies that if the primordial GWs indeed exist in the thermal state, with the squeezing parameters being $0 < r_s \leq 1$ in the early universe, then the temperature must be tuned to $T = 0.0001$ Mpc^{-1} to be within the BKP joint limit. The overall analysis supports the possibility of the primordial massive GWs being in the combined thermal and squeezed vacuum states. Repeating the analysis for other inflation models does not alter the results.

Chapter 6

Discussions and Conclusions

The theory of general relativity is a highly successful theory for gravity and it is important in understanding astrophysical systems and the universe. This theory relates spacetime curvature to the matter or energy which is the source for gravity through the Einstein field equations. The general theory of relativity made several predictions and are confirmed by various observational and experimental tests. An important prediction of this theory is the existence of gravitational waves. Gravitational waves can be generated by various astrophysical systems and also by the dynamics of very early universe. Gravitational wave astronomy is a developing and promising branch of observational astronomy and has the potential to unveil information on many astrophysical systems and very early universe which other observations and probes cannot yield. Gravitational waves from astrophysical sources have been detected both indirectly and directly. The gravitational waves induced by quantum fluctuations during the inflationary period are called the primordial gravitational waves. The primordial GWs have traversed the various evolutionary stages of the universe and its direct detection would be extremely difficult. However, these waves can also be realized through their imprints on the cosmic microwave background anisotropy in the form of B-mode polarization. At the same time, probes to detect the cosmologically originated gravitational waves have been going on actively and hopefully they may be detected in the near future.

The primordial GWs were generated during the inflation by a mechanism known as parametric amplification of zero point quantum fluctuations. Therefore the pri-

mordial GWs can be placed in the squeezed vacuum state, a well known state in the quantum optics. Also, the primordial GWs after the decoupling may remain in a thermal state after the recombination. Therefore, it is believed that due to these thermalized gravitons, there would occur a process of stimulated emission into the thermal background of GWs which would amplify the primordial tensor perturbations. Both these features are expected to have observable effects on the BB-mode angular spectrum of the CMB.

The inflationary scenario is introduced to resolve several problems associated with the standard model of cosmology according to which the universe expanded exponentially in its very early stage of evolution. There are many inflationary models proposed and all these models agree that inflation seeded the structure formation in the universe that we observe today. There are inflationary models based on single scalar field as well as multiple scalar fields. Almost all inflation models with single scalar field predict Gaussian distribution of density perturbations observable in the CMB anisotropy while multiple scalar field inflation models predict a detectable amount of non-Gaussianity in the distribution of the CMB anisotropy. The recent measurement results of Planck mission found that primordial non-Gaussianity is small and negligible which tends to favor single field inflation models. However, the recent observations of the CMB indicate large-scale anomalies in the fluctuations of CMB wherein a hemispherical asymmetry exists across the CMB sky. This was first hinted by WMAP and confirmed by Planck. It is suggested that multiple scalar field inflation could lead to such results while single field inflation models cannot do so without violating the homogeneity and isotropy of the universe on large scales. Therefore these results indicate that the issue of validating the single or multi field inflation models needs an alternative study rather than the Gaussianity test alone.

The general relativity theory predicts that the GWs travel with the speed of light which implies that graviton is massless. However, there are several theories concerning massive gravity aimed to endow the graviton with non-zero mass, which aim to explain the current acceleration of the universe rather than invoking the dark energy. There are also several attempts to constrain the graviton mass from observational and theoretical approaches. If the gravitons do have mass, correspondingly

the massive primordial gravitational waves are expected to have an observable effect on the B-mode spectrum of CMB. Hence the mass of the primordial gravitational waves can have bounds coming from the cosmological consideration.

Therefore the present thesis studies the aforementioned issues with BB-mode correlation spectrum of CMB by considering the primordial massless as well as massive GWs in the squeezed vacuum state and thermal vacuum state for several slow-roll inflation models with the joint analysis data of the BICEP2/Keck Array and Planck collaborations.

It is observed that there is enhancement in the power spectrum due to the squeezing effect for each inflation model. This effect increases with increase in the squeezing parameter. It is observed that the enhancement is greater for inflation models with larger tensor-to-scalar-ratio. This would also provide a platform to constrain the inflation models. The results are compared with the joint data from the BICEP2/Keck and Planck collaboration. It is found that of the models analyzed in the present study, the hybrid inflation model, the general Coleman-Weinberg inflation model, the inverse monomial inflation model, the Higgs inflation model and the R2 inflation model are highly favorable while the natural inflation model, the radiatively corrected quadratic chaotic inflation model and the loop inflation model are marginally within the data limit and are marginally favorable. The quadratic chaotic inflation model, the quartic chaotic inflation model and the new inflation model are out of limit and hence, they are ruled out at present.

There are many models of massive gravity; the primordial massive gravitational waves studied in this thesis is based on the Lorentz-violating massive gravity theory where the graviton acquires mass when the Lorentz invariance is spontaneously broken around a flat spacetime. This theory is free of pathologies which usually plaque the massive gravity theories. The analysis of the BB-mode spectrum for the primordial massive GWs is carried out for the R2 inflation model, the arctan inflation model, the Higgs inflation model, inverse monomial inflation model, the loop inflation model and the hybrid inflation model. The results of the BB-mode angular spectrum for these models and also their massless counterparts are compared

with the joint BICEP2/Keck and Planck data. From the analysis of the results with the current BICEP2/Keck and Planck limit for B-modes, it is found that the upper and lower graviton mass bounds tend to be higher than the current proposals.

The potential existence of massive primordial GWs in the squeezed vacuum state and in the thermal state or the combined thermal-squeezed vacuum state is explored with several slow-roll inflation models. The resulting BB-mode spectrum for these models with the corresponding effects are compared with the BICEP2/Keck and Planck collaboration data. Among the studied four inflation models, the R2 inflation model, the Higgs inflation model, the natural inflation model and the Coleman-Weinberg inflation model, only the R2 inflation model, the Higgs inflation model and the Coleman-Weinberg inflation model are highly favored by the current data. It can be observed that the oscillation due to the squeezing effect enhances the power level of the B-mode angular power spectrum of CMB. This implies the prospect of primordial massive GWs existing in the squeezed vacuum state and that the squeezing effect can help in further constraining the graviton mass. It is also observed that there is small increase in power level when the primordial massive GWs are placed in the thermal-squeezed vacuum state when the temperature is $T = 0.0001$ Mpc^{-1} such that the B-mode spectrum for each model still lies well within the BICEP2/Keck and Planck limit. This concludes that the potential existence of primordial massive GWs in the squeezed vacuum state or thermal state or their combined state is not ruled out completely.

We conclude our current work with the prospect of primordial gravitational waves, both massless and massive, existing in the squeezed vacuum state and also in the thermal state or its combined feature. The primordial GWs being in the squeezed vacuum state can help in constraining the inflation models and also the mass of the primordial graviton. The direct detection of GWs from black hole mergers by LIGO in 2015 indicates only the classical nature of gravitational waves. Further, this experiment is unable to detect individual gravitons. However, further studies are going on currently and more insights and results are expected to come in the near future. Since primordial gravitational waves were generated quantum mechanically, they are strongly expected to have quantum nature. However, further

discussions on this prospect is beyond the scope of the present work and hopefully, future detection of primordial gravitational waves or their signature would verify these claims.

Appendices

Appendix A

Linearized Einstein field equations

The gravitational wave equation can be obtained from the linearized Einstein field equations where the metric is assumed to differ slightly from the Minkowski metric and can be written as,

$$g_{\alpha\beta} = \eta_{\alpha\beta} + h_{\alpha\beta}, \tag{A.1}$$

where $\eta_{\alpha\beta}$ is the Minkowski metric and $|h_{\alpha\beta}| \ll 1$ is the perturbation.

In the linearized limit, the Einstein tensor becomes,

$$G_{\alpha\beta} = \frac{1}{2}(h_{\beta}{}^{\gamma}{}_{,\alpha\gamma} + h_{\alpha\gamma}{}^{,\gamma}{}_{\beta} - \Box h_{\alpha\beta} - h_{,\alpha\beta} - h^{\gamma\delta}{}_{,\gamma\delta}\eta_{\alpha\beta} + \eta_{\alpha\beta}\Box h), \tag{A.2}$$

where $h \equiv h^{\alpha}{}_{\alpha}$, and $\Box = \partial^{\alpha}\partial_{\alpha} = -\partial_t^2 + \nabla^2$ is the d'Alembertian operator, and the linearized gravity is described by the linearized Einstein equation,

$$h_{\beta}{}^{\gamma}{}_{,\alpha\gamma} + h_{\alpha\gamma}{}^{,\gamma}{}_{\beta} - \Box h_{\alpha\beta} - h_{,\alpha\beta} - h^{\gamma\delta}{}_{,\gamma\delta}\eta_{\alpha\beta} + \eta_{\alpha\beta}\Box h = 16\pi T_{\alpha\beta}. \tag{A.3}$$

The metric perturbation in eq.(A.3) can be written in terms of trace-reversed perturbation variable as,

$$\bar{h}_{\alpha\beta} = h_{\alpha\beta} - \frac{1}{2}h\eta_{\alpha\beta}, \tag{A.4}$$

where $h_{\alpha\beta}$ and $\bar{h}_{\alpha\beta}$ contain the same information. Using eq.(A.4) in eq.(A.3) leads to,

$$\bar{h}_{\beta}{}^{\gamma}{}_{,\alpha\gamma} + \bar{h}_{\alpha\gamma}{}^{,\gamma}{}_{\beta} - \Box\bar{h}_{\alpha\beta} - \bar{h}^{\gamma\delta}{}_{,\gamma\delta}\eta_{\alpha\beta} = 16\pi T_{\alpha\beta}. \tag{A.5}$$

Under the Lorentz gauge,

$$\bar{h}^{\alpha\gamma}{}_{,\gamma} = 0, \tag{A.6}$$

the linearized Einstein field equation becomes,

$$\Box\bar{h}_{\alpha\beta} = -16\pi T_{\alpha\beta}. \tag{A.7}$$

In the free space, the linearized Einstein equation takes the form,

$$\Box\bar{h}_{\alpha\beta} = 0. \tag{A.8}$$

Thus the metric perturbations travel in free space with the speed of light.

In the free space, the linearized Einstein equation is a system of 10 scalar wave equations and has plane wave solution of the form,

$$\bar{h}_{\alpha\beta} = A_{\alpha\beta}e^{ik_\gamma x^\gamma} = A_{\alpha\beta}e^{ik_i x^i}e^{-iwt}, \tag{A.9}$$

where $A_{\alpha\beta}$ is a constant rank-2 symmetric tensor which represents the amplitude of the wave, k_α denotes the wave vector and the dispersion relation is $w = k^0 = -k_0$, and $\Box = \partial_\gamma\partial^\gamma = (ik_\gamma)(ik^\gamma) = -k_\gamma k^\gamma$.

Hence, one has a solution if $k_\gamma k^\gamma = 0$ or if $w^2 = (k_1)^2 + (k_2)^2 + (k_3)^2$. Thus, from the dispersion relation, all perturbations are expected to have both phase and group velocities equal to the speed of light. The Lorentz gauge condition eq.(A.6) leads to the transverse condition,

$$A^{\alpha\gamma}k_\gamma = 0. \tag{A.10}$$

This condition removes 4 degrees of freedom in $A_{\alpha\beta}$, leaving only 6 degrees of freedom. One may introduce a gauge transformation $\xi = iB^\alpha e^{ik_\gamma x^\gamma}$ and for transverse Lorentz gauge condition to be conserved, $\Box\xi = 0$. Thus, the metric perturbation transforms as,

$$\bar{h}_{\alpha\beta} \to \bar{h}_{\alpha\beta} - \xi_{\alpha,\beta} - \xi_{\beta,\alpha} + \xi^\gamma{}_{,\gamma}\eta_{\alpha\beta}, \tag{A.11}$$

such that one gets the transformation in the polarization tensor,

$$A_{\alpha\beta} \to A_{\alpha\beta} + k_\alpha B_\beta + k_\beta B_\alpha - k_\gamma\zeta^\gamma\eta_{\alpha\beta}, \tag{A.12}$$

which has an invertible 4×4 matrix which fixes the gauge such that the gauge transformation cannot eliminate the waves, hence these waves are real. One has

the freedom to choose the coordinate system such that the polarization tensor is traceless,

$$\begin{aligned} A^{\gamma}{}_{\gamma} &= 0, \\ A_{0i} &= A_{i0} = 0. \end{aligned} \tag{A.13}$$

The choice of the gauge in eq.(A.10) and eq.(A.13) is called the transverse-traceless gauge. Due to this gauge freedom, the number of the independent components of $A_{\alpha\beta}$ is reduced to 2 in the transverse-traceless gauge. Expanding eq.(A.10), the $\alpha = 0$ component yields,

$$-wA^{00} + k_i w^{0i} = 0, \tag{A.14}$$

and the spatial components of the same equation give

$$\varepsilon_{ij} k_j = 0. \tag{A.15}$$

Thus, from eq.(A.13), for $w \neq 0$, we get $A^{00} = 0$ and $A_{ii} = A^{\gamma}{}_{\gamma} + \varepsilon^{00} = 0$. This implies that the polarization tensor $A_{\alpha\beta}$ is purely spatial and transverse-traceless.

Consider a wave propagating in a direction, then using the transverse traceless conditions, the metric perturbation can be written in terms of the polarization tensor using eq.(A.9) as,

$$h_{\alpha\beta} = \begin{bmatrix} 0 & 0 & 0 & 0 \\ 0 & h_+ & h_\times & 0 \\ 0 & h_\times & -h_+ & 0 \\ 0 & 0 & 0 & 0 \end{bmatrix} e^{i(k_i x^i - wt)}, \tag{A.16}$$

where the gravitational wave amplitude can be written as,

$$A_{\alpha\beta} = \varepsilon^{+}_{\alpha\beta} h_+ + \varepsilon^{\times}_{\alpha\beta} h_\times, \tag{A.17}$$

and the two polarization states can be expressed using eq.(1.45) and eq.(A.16) as,

$$\varepsilon^{+}_{\alpha\beta} = \begin{bmatrix} 0 & 0 & 0 & 0 \\ 0 & 1 & 0 & 0 \\ 0 & 0 & -1 & 0 \\ 0 & 0 & 0 & 0 \end{bmatrix}, \tag{A.18}$$

$$\varepsilon^{\times}_{\alpha\beta} = \begin{bmatrix} 0 & 0 & 0 & 0 \\ 0 & 0 & 1 & 0 \\ 0 & 1 & 0 & 0 \\ 0 & 0 & 0 & 0 \end{bmatrix}. \tag{A.19}$$

Due to the gravitational wave being a rank-2 tensor, the rotation angle between the two independent states of polarization is 45°.

Appendix B

Graviton mass parameter

Action for the Lorentz-violating massive gravity about a flat FLRW spacetime is given by eq.(4.1) where the mass term originates from the second term. In terms of the tensor, scalar and vector fields, the quadratic Lagrangian in eq.(4.5) can be written as,

$$\begin{aligned} L_m &= m_{pl}^2\Big[-\frac{1}{4}m_2^2h_{ij}^2-\frac{1}{2}m_2^2(\partial_iF_j)^2+m_0^2\varphi^2+\frac{1}{2}m_1^2(\partial_iB)^2 \\ &\quad +(m_3^2-m_2^2)(\partial_i^2E)^2-2(3m_3^2-m_2^2)\psi\partial_i^2E+3(3m_3^2-m_2^2)\psi^2 \\ &\quad +2m_4^2\varphi\partial_i^2E-6m_4^2\varphi\psi\Big]. \end{aligned} \tag{B.1}$$

Considering the eq.(4.2) and eq.(4.6), for a particular case where the equation of state parameter $w=-(3\gamma)^{-1}$ so that $\rho_\phi=-3\gamma p_\phi$, the mass parameters follow the relations,

$$\begin{aligned} m_0^2 &= 3\gamma\left(m_4^2-\frac{m_1^2}{2}\right), \\ m_1^2 &= 2(3\gamma-1)p_\phi, \\ m_4^2 &= \gamma(3m_3^2-m_2^2). \end{aligned} \tag{B.2}$$

For the cases $m_0\neq 0$ and $m_1\neq 0$ and $m_4\neq 0$, there are two scalar degrees of freedom at the linear level about the flat spacetime, one of these degrees of freedom introduces a ghost mode. Hence absence of ghost demands either $m_0=0$ or $m_1=0$ or both $m_2=m_3$ and $m_4=0$.

When $m_0 = 0$, the scalar field φ acts as the Lagrangian multiplier which leads to the constraint,

$$2\partial_i\psi = m_4^2(3\psi - \partial_i E).$$

Thus ψ remains as the only remaining dynamical scalar field and the tensor perturbation h_{00} enters the action linearly. This property sufficiently ensures the ghost-free scenario.

The parameter m_1 is responsible for turning on a kinetic term for the scalar modes. When $m_1 = 0$, the scalar field B acts as Lagrangian multiplier leading to the constraint for propagating modes as $\psi = 0$. Applying this into the action, it can be obtained that there are no propagating modes in the scalar sector. This property is same in the vector sector. Thus the only propagating modes under this condition are the tensor modes. Thus, the model is free of scalar degrees of freedom about the Minkowski at the linear level, thus there is no vDVZ discontinuity.

In the last condition, $m_2 = m_3$ and $m_4 = 0$, the field E enters the action linearly leading to the corresponding field equation,

$$2\ddot{\psi} + (3m_3^2 - m_2^2)\psi) = 0.$$

This implies the absence of high frequency propagating modes.

When the parameter $m_2^2 \geq 0$, there is no rapid instabilities in the model. This mass parameter represents the mass of the graviton and is represented in the main body of the thesis as m_{gw}.

Hence there are some regions in the mass parameter space where the Lorentz-violating theory of massive gravity is free of ghosts and other pathologies in the linearized theory about the Minkowski spacetime.

Appendix C

Cosmological Perturbations for Massive gravitational waves

The massive gravity action on a flat FLRW background is given by eq.(4.1). Parametrization of cosmological perturbations to the metric is given in eq.(1.38). The Goldstone fields are set to their vacuum values given in eq.(4.3) and their perturbations can be parametrized as,

$$\begin{aligned} \tilde{\Phi}_0 &= \Phi_0 + \Lambda^2\lambda_0, \\ \tilde{\Phi}_i &= \Phi_i + \Lambda^2(\lambda_i + \nabla_i\lambda), \end{aligned} \tag{C.1}$$

where λ_0 is scalar field and λ_i is the vector field.

Ordinary matter perturbation can be parametrized as,

$$\delta T^m_{\alpha\beta} = (\delta\rho_m + \delta p_m)U_\alpha U_\beta - g_{\alpha\beta}\delta p_m - p_m\delta g_{\alpha\beta} + (\rho_m p_m)(U_\beta\delta U_\alpha + U_\alpha\delta U_\beta), \tag{C.2}$$

where ρ_m and p_m are related by the equation of state of matter, and the perturbation for the 4-velocity can be given in terms of the scalar and vector fields by,

$$\begin{aligned} \delta U_0 &= a\varphi, \\ \delta U_i &= a(\varrho_i + \partial_i\varrho). \end{aligned} \tag{C.3}$$

In the tensor sector, only the transverse-traceless perturbations h_{ij} consisting of two components are present. The equation for the massive tensor perturbations can be given by,

$$h^{(m)\prime\prime}_{ij}(\tau) + 2Hh^{(m)\prime}_{ij}(\tau) + k^2h^{(m)}_{ij}(\tau) + a^2m_2^2h^{(m)}_{ij}(\tau) = 0. \tag{C.4}$$

Under infinitesimal coordinate transformation $\tilde{x}^i = x^i + \varpi^i$, the vector fields are invariant, i.e.,

$$\vartheta_i = Q_i + F_i', \tag{C.5}$$

$$\sigma_i = \lambda_i - F_i. \tag{C.6}$$

The gauge-invariant vector fields are then described by,

$$\nabla^2\vartheta_i - 2a^2\rho_m m_{pl}^{-2}(1+w)\varrho_i = 0, \tag{C.7}$$

$$\vartheta_i' + 2H\vartheta_i - a^2 m_2^2\sigma_i = 0, \tag{C.8}$$

$$m_2^2\nabla^2\sigma_i = 0, \tag{C.9}$$

where w is the equation of state parameter which appears in the ordinary matter state as $p_m = w\rho_m$. eq.(C.7) allows for ϱ_i to be described in terms of ϑ_i, while eq.(C.9) implies $\sigma_i = 0$. This leaves eq.(C.8) as the only non-trivial equation thus, ϑ remains the only relevant vector whose amplitude decays as a^{-2}. These are evaluated under the condition that $m_2 \neq 0$. Thus vector perturbations behave as in the general relativity case, the decay process after the inflationary process is too fast so that they do not leave any signature on the CMB anisotropy spectrum.

In the scalar sector, the only trace of the Goldstone field are the two energy densities: $\rho_\Lambda = -\Lambda^4 F/2$ which behaves like a cosmological constant and $\rho_\phi = -3\gamma\Lambda^4 Z F_Z$ which corresponds to matter with the equation of state parameter $w = -(3\gamma)^{-1}$, where γ is a constant free parameter, and $\frac{\partial F}{\partial Z^{ij}} = F_Z\delta_{ij}$.

Considering a homogeneous and isotropic ordinary matter, the Friedmann equation and the field equation for the Goldstone scalar ϕ^0 can be written as,

$$H^2 = \frac{a^2}{3m_{pl}^2}(\rho_m + \rho_\phi + \rho_\Lambda), \tag{C.10}$$

$$0 = \partial_0(a^{3-1/\gamma}Z^{1-1/2\gamma}F_Z). \tag{C.11}$$

From the given energy densities, the Friedmann equation reduces to the standard one. Thus the only trace of the Goldstone scalars are the contributions from the energy densities.

The growth of the perturbations in the scalar sector depends on γ. When $-1 \leq \gamma < 0$, the growth of the perturbations is slower than that of the ordinary GR ones, hence the latter dominates. For $\gamma = 1$, the contributions to the perturbations cancel out so that only the perturbations in the GR case remain. For $\gamma \geq 1$, the normal perturbations (GR case) dominate at matter dominated epoch. Hence in these cases, the scalar perturbations behave as in the GR case and the model remains consistent with the structure formation.

Bibliography

[1] S. Dodelson, *Modern Cosmology*, (Elsevier, 2006).

[2] J.B. Hartle, *Gravity: An Introduction to Einstein's General Relativity*, (Pearson Education India, 2003).

[3] R.A. Hulse and J.H. Taylor, *Astrophys. J.* **195** (1975) L51.

[4] M. Burgay *et.al.*, *Nature* **426** (2003) 531.

[5] B.P. Abbott *et.al.*, *Phys. Rev. Lett.* **116** (2016) 061102.

[6] B.P. Abbott *et.al.*, *Astrophys. J.* **818** (2016) L22.

[7] B.P. Abbott *et.al.*, *Phys. Rev. Lett.* **116** (2016) 241103.

[8] B.P. Abbott *et.al.*, *Phys. Rev. Lett.* **118** (2017) 221101.

[9] E.M. Leitch *et.al.*, *Nature* **420** (2002) 763.

[10] J.M. Kovac *et.al.*, *Nature* **420** (2002) 772.

[11] D. Hanson *et.al.*, *Phys. Rev. Lett.* **111** (2013) 141301.

[12] Planck Collaboration, *Astron. Astrophys.* **594** (2016) A1.

[13] Planck Collaboration, *Astron. Astrophys.* **594** (2016) A11.

[14] Keck Array and BICEP2 Collaborations, *Astrophys. J.* **811** (2015) 126.

[15] P.A.R. Ade *et.al.*, *Phys. Rev. Lett.* **114** (2015) 101301.

[16] R. Keisler *et.al.*, arXiv:1503.02315v1 (2015).

[17] R.H. Brandenberger, arXiv:hep-ph/9910410v1 (1999).

[18] A.A. Starobinsky, *Phys. Lett. B* **91** (1980) 99.

[19] A.H. Guth, *Phys. Rev. D* **23** (1981) 347.

[20] M. Giovannini, *A Primer on the Physics of the Cosmic Microwave Background*, (World Scientific Publishing Company, 2008).

[21] R.A. Alpher and R.C. Herman, *Phys. Rev.* **74** (1948) 1737.

[22] G. Gamow, *Phys. Rev.* **74** (1948) 505.

[23] G. Gamow, *Nature* **162** (1948) 680.

[24] R.H. Dicke *et.al.*, *Phys. Rev.* **70** (1946) 340.

[25] A.G. Doroshkevich and I.D. Novikov, *Sov. Phys. Dok.* **9** (1964) 111.

[26] A.A. Penzias and R.W. Wilson, *Astrophys. J.* **142** (1965) 419.

[27] G.F. Smoot *et.al.*, *Astrophys. J. Lett.* **396** (1992) 1.

[28] C.L. Bennett *et.al.*, *Astrophys. J. Suppl.* **148** (2003) 1.

[29] C.L. Bennett *et.al.*, *Astrophys. J. Suppl.* **208** (2013) 20.

[30] T.J. Pearson *et.al.*, *Astrophys. J.* **591** (2003) 556.

[31] A.C.S. Readhead *et.al.*, *Astrophys. J.* **609** (2004) 498.

[32] M.C. Runyan *et.al.*, *New Astron. Rev.* **47** (2003) 915.

[33] C.L. Kuo *et.al.*, *Astrophys. J.* **600** (2004) 32.

[34] K. Grainge *et.al.*, *Mon. Not. R. Astron. Soc.* **341** (2003) L23.

[35] A.C. Taylor *et.al.*, *Mon. Not. R. Astron. Soc.* **341** (2003) 1066.

[36] S. Masi *et.al.*, *Prog. Part. Nucl. Phys.* **48** (2002) 243.

[37] B.P. Crill *et.al.*, *Astrophys. J. Suppl.* **148** (2003) 527.

[38] M. Kamionkowski, *Nucl. Phys. Proc. Suppl.* **70** (1999) 529.

[39] M. Kamionkowski, A. Kosowski and A. Stebbins, *Phys. Rev. Lett.* **78** (1997) 2058.

[40] M. Zaldariagga and U. Seljak, *Phys. Rev. D* **55** (1997) 1830.

[41] W. Hu, arXiv:0802.3688v1 [astro-ph] (2008).

[42] K. Subramanian, *Curr. Sci.* **88** (2005) 1068.

[43] W. Hu, *Annals. Phys.* **303** (2003) 203.

[44] R.K. Sachs and A.M. Wolfe, *Astrophys. J.* **147** (1967) 73.

[45] M. Kamionkowski, A. Kosowski and A. Stebbins, *Phys. Rev. D* **55** (1997) 7368.

[46] P. Cabella and M. Kamionkowski, arXiv:astro-ph/0403392v2 (2005).

[47] D. Baskaran, L.P. Grishchuk and A.G. Polnarev, *Phys. Rev. D* **74** (2006) 083008.

[48] U. Seljak and M. Zaldariagga, *Phys. Rev. Lett.* **78** (1997) 2054.

[49] M. Kamionkowski and E.D. Kovetz, *Ann. Rev. Astron. Astrophys.* **54** (2016) 227.

[50] A. Lewis and A. Challinor, *Phys. Rep.* **429** (2006) 1.

[51] J. Martin, C. Ringeval and V. Vennin, arXiv:1303.3787v3 [astro-ph.CO] (2013).

[52] Planck Collaboration, *Astron. Astrophys.* **571** (2014) A22.

[53] L.P. Grishchuk, *Class. Quant. Grav.* **10** (1993) 2449.

[54] L.P. Grishchuk, *Sov. Phys. JETP* **40** (1975) 409.

[55] L.P. Grishchuk, *Lect. Notes Phys.* **562** (2001) 167.

[56] L.P. Grishchuk and Y.V. Sidorov, *Class. Quant. Grav.* **6** (1989) L161.

[57] J. Martin, C. Ringeval, R. Trotta and V. Vennin, arXiv:1312.3529v3 [astro-ph.CO] (2014).

[58] J. Martin, arXiv:1502.05733v1 [astro-ph.CO] (2015).

[59] Planck Collaboration, *Astron. Astrophys.* **571** (2014) A24.

[60] E.L. Erickceck, M. Kamionkowski and S.M. Carroll, *Phys. Rev. D* **78** (2008) 123520.

[61] G. Barenboim and W.I. Park, arXiv:1509.07132 [astro-ph.CO] (2015).

[62] A.D. Linde, *Phys. Lett. B* **129** (1983) 177.

[63] S. Coleman and E. Weinberg, *Phys. Rev. D* **7** (1973) 1888.

[64] A.H. Guth and S.Y. Pi, *Phys. Rev. Lett.* **49** (1982) 1110.

[65] A.D. Linde, *Phys. Lett. B* **114** (1982) 431.

[66] M.S. Turner, M.J. White and J.E. Lidsey, *Phys. Rev. D* **48**, (1993) 4613.

[67] G. Huey and J.E. Lidsey, *Phys. Lett. B* **514** (2001) 217.

[68] B. Ratra and P.J.E. Peebles, *Phys. Rev. D* **37** (1988) 3406.

[69] P.J.E. Peebles and B. Ratra, *Astrophys. J* **325** (1988) L17.

[70] F. Takahasi, arXiv:1505.07950v1[hep-ph] (2015).

[71] M. Drees and E. Erfani, *JCAP* **2012** (2012) 035.

[72] M. Drees and E. Erfani, arXiv:1205.4012 [astro-ph.CO] (2012).

[73] K. Freese, J.A. Frieman and A.V. Olinto, *Phys. Rev. Lett.* **65** (1990) 3233.

[74] F.C. Adams, J.R. Bond, *et.al.*, *Phys. Rev. D* **47** (1993) 426.

[75] V.N. Senoguz and Q. Shafi, *Phys. Lett. B* **668** (2008) 6.

[76] P. Binetruy and G. Dvali, *Phys. Lett. B* **388** (1996) 241.

[77] E. Halyo, *Phys. Lett. B* **387** (1996) 43.

[78] D. Dvali, *Phys. Lett. B* **387** (1996) 471.

[79] A.D. Linde, *Phys. Rev. D* **49** (1994) 748.

[80] J. Garcia-Bellido and A.D. Linde, *Phys. Rev. D* **57** (1998) 6075.

[81] B.L. Schumaker, *Phys. Rep.* **135** (1986) 317.

[82] L.P. Grishchuk, arXiv:gr-qc/9903079v1 (1999).

[83] K. Bhattacharya, S. Mohanty and A. Nautiyal, *Phys. Rev. Lett.* **97** (2006) 251301.

[84] S. Koh, S.P. Kim and D.J. Song, *JHEP* **2004** (2004) 060.

[85] H. Umezawa, H. Matsumoto and M. Tachiki, *Thermo field dynamics and condensed states* (North-Holland Publishing Company, Amsterdam, 1982).

[86] W. Zhao, D. Baskaran and P. Coles, *Phys. Lett. B* **680** (2009) 411.

[87] M. Fierz and W. Pauli, *Proc. Roy. Soc. Lond.* **A173** (1939) 211.

[88] S.L. Dubovsky, P.G. Tinyakov and I.I. Tkachev, *Phys. Rev. Lett.* **94** (2005) 181102.

[89] K. Hinterbichler, arXiv:1105.3735v2 [hep-th] (2011).

[90] D.G. Boulware and S. Deser, *Phys. Rev. D* **6** (1972) 6.

[91] H. van Dam and M. Veltman, *Nucl. Phys.* **B22** (1970) 397.

[92] V.I. Zakharov, *ZhETF Pis. Red.* **12** (1970) 447.

[93] A. I. Vainshtein, *Phys. Lett. B* **22** (1972) 393.

[94] C. de Rham, G. Gabadadze, A. J. Tolley, *Phys. Rev. Lett.* **106** (2011) 231101.

[95] C. de Rham, arXiv:1401.4173v2 [hep-th] (2014).

[96] S.F. Hassan, R.A. Rosen, *Phys. Rev. Lett.* **108** (2002) 041101.

[97] A.E. Gumrukcuoglu, C. Lin and S. Mukohyama, *JCAP* **1111** (2011) 030.

[98] A.E. Gumrukcuoglu, C. Lin and S. Mukohyama, *JCAP* **1203** (2012) 006.

[99] A.E. Gumrukcuoglu, C. Lin and S. Mukohyama, *Phys. Lett. B* **717** (2012) 295.

[100] A. De Felice and S. Mukohyama, *Phys. Lett. B* **752** (2015) 302.

[101] A. De Felice and S. Mukohyama, *JCAP* **1604** (2015) 028.

[102] N.A. Hamed *et.al.*, *JHEP* **0405** (2004) 074.

[103] V. Rubakov, arXiv:hep-th/0407104v1 (2004).

[104] S. L. Dubovsky, *JHEP* **0410** (2004) 076.

[105] A.S. Goldhaber and M.M. Nieto, *Phys. Rev. D* **9** (1974) 1119.

[106] C. Talmadge *et.al.*, *Phys. Rev. Lett.* **61** (1988) 1159.

[107] C.M. Will, arXiv:gr-qc/9709011v1 (1997).

[108] S.S. Gershtein, A.A. Logunov, and M.A. Mestvirishvili, arXiv:hep-th/9711147v1 (1997).

[109] L.S. Finn and P.J. Sutton, *Phys. Rev. D* **65** (2002) 044022.

[110] A. Cooray and N. Seto, *Phys. Rev. D* **69** (2004) 103502.

[111] D. Valev, *Aerospace Res. Bulg.* **22** (2008) 68.

[112] C. de Rham *et.al.*, arXiv:1606.08462v1 [astro-ph.CO] (2016).

[113] M. Fasiello and A.J. Tolley, *JCAP* **1211** (2012) 035.

[114] S. Dubovsky, R. Flauger, A. Starobinsky and I. Tkachev, *Phys. Rev. D* **81** (2010) 023523.

[115] D. Bessada and O.D. Miranda, *JCAP* **0908** (2009) 033.

[116] A.F. Ali and S. Das, *Int. J. Mod. Phys. D* **25** (2016) 1644001.

[117] D. Bessada and O.D. Miranda, *Class. Quant. Grav.* **26** (2009) 045005.

[118] M.V. Bebronne and P.G. Tinyakov, *Phys. Rev. D* **76** (2007) 084011.

[119] A.E. Gumrukcuoglu *et.al.*, *Class. Quant. Grav.* **29** (2012) 235026.

Eur. Phys. J. C (2016) 76:240
DOI 10.1140/epjc/s10052-016-4029-5

THE EUROPEAN PHYSICAL JOURNAL C

Regular Article - Theoretical Physics

Slow-roll inflation and BB-mode angular power spectrum of CMB

N. Malsawmtluangi[a], **P. K. Suresh**[b]

School of Physics, University of Hyderabad, P. O. Central University, Hyderabad 500046, India

Received: 13 December 2015 / Accepted: 15 March 2016 / Published online: 29 April 2016

Abstract The BB-mode correlation angular power spectrum of CMB is obtained by considering the primordial gravitational waves in the squeezed vacuum state for various inflationary models and results are compared with the joint analysis of the BICEP2/Keck Array and Planck 353 GHz data. The present results may constrain several models of inflation.

1 Introduction

Cosmic inflation is the most widely known scenario proposed for resolving several problems associated with the standard model of cosmology [1,2]. A number of inflationary models have been proposed over several decades [1–8]. The recent observations on the cosmic microwave background (CMB) anisotropy data may constrain many of the inflationary models [9–13]. It is believed that inflation seeded the formation of the large scale structures in the universe. Inflation also predicts a nearly scale invariant spectrum for the scalar and tensor perturbations which occurred in the early universe. The tensor perturbations of cosmological origin are known as primordial gravitational waves (GWs).

It is believed that the primordial gravitational waves have left an imprint on the cosmic microwave background. The primordial GWs can be studied with the aid of CMB anisotropy and polarization. The CMB is polarized in the early universe due to the Thomson scattering. The density (scalar) fluctuations generate the E-mode polarization of the CMB, while the gravitational waves generate both E-mode and B-mode polarizations [14–17]. The primordial gravitational waves are a unique source of B-mode of CMB and its detection will help in understanding the inflation as well as the primordial gravitational waves itself.

The gravitational waves were generated during the inflation period due to the zero-point quantum oscillations [18]. An initial vacuum state (no graviton) can evolve into a multiparticle quantum state known as the squeezed vacuum state [19], which is a well-known state in the context of quantum optics [20–22]. The primordial gravitational waves are believed to exist in the squeezed vacuum state [23–25]. The primordial gravitational waves are placed in the squeezed vacuum state and its effect on the BB-mode correlation angular power spectrum of CMB is studied with WMAP data [26]. Recently, it is shown that the BB-mode angular power spectrum gets enhanced at its lower multipoles by considering the primordial gravitational waves in thermal state [27]. These studies show that the primordial gravitational waves may exhibit both the squeezing and the thermal features and hence it is worthwhile to examine their combined effects on the BB-mode correlation angular power spectrum in light of the recent joint BICEP2/Keck Array and Planck data.

The aim of the present work is to study effect of primordial gravitational waves in the squeezed vacuum state on the BB-mode correlation angular power spectrum of CMB for various slow-roll inflationary models. Thus the obtained BB-mode correlation angular power spectrum of CMB for the squeezed vacuum as well as the joint effect of squeezing and thermal cases are compared with the joint BICEP2/Keck Array and Planck data.

2 Tensor power spectrum in squeezed state

The perturbed metric for a flat Friedmann–Lemaître–Robertson–Walker universe can be written as

$$\mathrm{d}s^2 = R^2(\tau)[-\mathrm{d}\tau^2 + (\delta_{ij} + h_{ij})\mathrm{d}x^i\mathrm{d}x^j], \tag{1}$$

where δ_{ij} is the flat space metric and h_{ij} is the tensor perturbation, $|h_{ij}| \ll \delta_{ij}$, $\partial_i h^{ij} = 0$, $\delta^{ij}h_{ij} = 0$, and $\mathrm{d}\tau = \frac{\mathrm{d}r}{R}$ is the conformal time.

In quantum theory, the field $h_{ij}(\mathbf{x}, \tau)$ can be written in the Fourier mode as

[a] e-mail: tei.naulak@uohyd.ac.in
[b] e-mail: pkssp@uohyd.ernet.in

N Malsawmtluangi <tei.naulak@uohyd.ac.in>

Your paper "Slow-roll inflation and the BB-mode correlation spectrum of the Cosmic Microwave Background"

1 message

Douglas Singleton <dougs@mail.fresnostate.edu> Sun, Jul 16, 2017 at 7:48 PM
To: N Malsawmtluangi <tei.naulak@uohyd.ac.in>
Cc: "Nicolini, Piero" <nicolini@th.physik.uni-frankfurt.de>, "lake, matt" <matt.lake@gmail.com>, "portable, shingo" <shingo.portable@gmail.com>, "Dzhunushaliev, Vladimir" <v.dzhunushaliev@gmail.com>

Dear Dr. Malsawmtluangi,

Your paper "Slow-roll inflation and the BB-mode correlation spectrum of the Cosmic Microwave Background" has been accepted for publication as part of the Proceeding for the symposium IF-YITP-GR+HEP+COSMO-VI. The issue of the IoP proceedings should be published in the next 1-2 months. Let us know if you have any questions/comments.

Congratulations on behalf of myself and the other editors (Dr. Piero Nicolini, Dr. Matthew Lake, Dr. Shingo Takeuchi. Dr. Vladimir Dzhunushaliev)

Douglas Singleton, Professor
Physics Department, California State University, Fresno
Fresno, CA 93740
559-278-2523

Inflation and BB mode angular spectrum of CMB

ORIGINALITY REPORT

%18	%2	%17	%1
SIMILARITY INDEX	INTERNET SOURCES	PUBLICATIONS	STUDENT PAPERS

PRIMARY SOURCES

1	Malsawmtluangi, N., and P. K. Suresh. "Slow-roll inflation and BB-mode angular power spectrum of CMB", The European Physical Journal C, 2016. Publication	%8
2	Takeo Moroi. "Relaxing constraints on inflation models with curvaton", Physical Review D, 07/2005 Publication	%1
3	GHAYOUR, BASEM, and P. K. SURESH. "B MODE CORRELATION ENHANCEMENT OF CMB FROM THERMAL SQUEEZED VACUUM STATE", International Journal of Modern Physics D, 2013. Publication	<%1
4	cph-theory.persiangig.com Internet Source	<%1
5	arxiv.org Internet Source	<%1

Submitted to Queen Mary and Westfield

This is to certify that the thesis entitled "**Inflation and BB-mode angular spectrum of CMB**", submitted by my research student Ms. N. Malsawmtluangi, Regn. No. 12PHPH15 of School of Physics, has been screened by the Turnitin software at the Indira Gandhi Memorial Library (IGML), University of Hyderabad. This software shows 18% similarity index out of which 8% came from the candidate's research article (where she is the first author) directly related to this thesis.

From the detailed similarity index report, it is obvious that the remaining 10% of the similarity index is due to the similarity coming from the frequent use of well-known standard terms such as gravitational waves, inflation model, BB mode angular (power) spectrum, cosmic microwave background, E-modes, B-modes, joint analysis of BICEP2/Keck Array (at 150 GHz) and Planck (at 353 GHz), squeezed vacuum state, general relativity, the big bang, energy-momentum tensor, two-point correlation function, tensor-to-scalar ratio, tensor spectral index, to name a few, and names of observatories and experiments like Cosmic Background Explorer, Cosmic Background Imager, Arcminute Cosmology Bolometer Array Receiver, Very Small Array and so on. The software also detected similarity on some equations and Greek letters used for notations. It should be noted that use of such terms and equations cannot be avoided.

Prof. P.K. Suresh
Thesis Supervisor
School of Physics
University of Hyderabad